Violation of the fluctuation–dissipation theorem in glassy systems: basic notions and the numerical evidence

2003 J. Phys. A: Math. Gen. 36 R181

(http://iopscience.iop.org/0305-4470/36/21/201)

INSTITUTE OF PHYSICS PUBLISHING JOURNAL OF PHYSICS A: MATHEMATICAL AND GENERAL

J. Phys. A: Math. Gen. **36** (2003) R181–R290 PII: S0305-4470(03)33121-X

TOPICAL REVIEW

Violation of the fluctuation–dissipation theorem in glassy systems: basic notions and the numerical evidence

A Crisanti[1] **and F Ritort**[2]

[1] Dipartimento di Fisica, Università di Roma 'La Sapienza', INFM Sezione di Roma I and SMC, Ple Aldo Moro 2, 00185 Roma, Italy
[2] Departament de Física Fonamental, Facultat de Física, Universitat de Barcelona, Diagonal 647, 08028 Barcelona, Spain

E-mail: andrea.crisanti@phys.uniroma1.it and ritort@ffn.ub.es

Received 2 January 2003, in final form 25 March 2003
Published 13 May 2003
Online at stacks.iop.org/JPhysA/36/R181

Abstract

This review reports on the research done during past years on violations of the fluctuation–dissipation theorem (FDT) in glassy systems. It is focused on the existence of a quasi-fluctuation–dissipation theorem (QFDT) in glassy systems and the current supporting knowledge gained from numerical simulation studies. It covers a broad range of non-stationary aging and stationary driven systems such as structural glasses, spin glasses, coarsening systems, ferromagnetic models at criticality, trap models, models with entropy barriers, kinetically constrained models, sheared systems and granular media. The review is divided into four main parts: (1) an introductory section explaining basic notions related to the existence of the FDT in equilibrium and its possible extension to the glassy regime (QFDT), (2) a description of the basic analytical tools and results derived in the framework of some exactly solvable models, (3) a detailed report of the current evidence in favour of the QFDT and (4) a brief digression on the experimental evidence in its favour. This review is intended for inexpert readers who want to learn about the basic notions and concepts related to the existence of the QFDT as well as for the more expert readers who may be interested in more specific results.

PACS numbers: 64.40.−i, 64.60.Cn, 75.10.Nr

Contents

Nomenclature

1RSB	One-step replica symmetry breaking
BG	Backgammon
BTM	Bouchaud trap model
EA	Edwards–Anderson model

FD	Fluctuation–dissipation
FDR	Fluctuation–dissipation ratio
FDT	Fluctuation–dissipation theorem
FILG	Frustrated Ising lattice gas
IRF	Integrated response function
IS	Inherent structure
LJ	Lennard-Jones
ME	Master equation
MF	Mean-field
MCT	Mode-coupling theory
OSC	Oscillator
QFDT	Quasi-fluctuation–dissipation theorem
REM	Random energy model
RFIM	Random field Ising model
ROM	Random orthogonal model
RSB	Replica symmetry breaking
SK	Sherrington–Kirkpatrick
TAP	Thouless–Anderson–Palmer
T_c	Mode-coupling critical temperature, dynamical critical temperature
T_{eff}	Effective temperature
T_g	Glass transition temperature
T_K	Kauzmann temperature
T_{RSB}	Static transition temperature in replica calculations
TRM	Thermoremanent magnetization
TTI	Time translation invariance
ZFC	Zero field cooled

1. Introduction

The search for a general theory of non-equilibrium processes has been a primary goal in modern statistical physics. Despite many efforts in this direction, we have a limited understanding of the basic principles behind non-equilibrium theories. Compared with ensemble equilibrium theory, a general principle such as the equal probability Boltzmann principle (that forms the basis of equilibrium statistical mechanics and provides a statistical foundation of thermodynamics) is still lacking. During the last century, the field of non-equilibrium phenomena has grown in two directions: (1) by developing new statistical models as an inspiring source of fruitful new concepts and ideas and (2) by establishing partial links among different, apparently disconnected, non-equilibrium phenomena.

Although much progress has been made in the first direction, the second one remains less unexplored. While a general principle governing non-equilibrium systems probably does not exist, substantial progress could be made following the second route in the search for basic principles governing a restricted category or class of systems. The applications of such basic principles may be very important because *a priori* many different systems can fall into the same category. Hence the interest in the research on the existence of such restricted formulations.

During the past years it has become increasingly clear that *glassy systems* may constitute one of these large categories where their physical behaviour can be rationalized within a restricted formulation. Glassy systems are rather common in nature and many systems such as structural glasses, spin glasses, disordered and granular materials or proteins present what is called *glassy behaviour*. This means a dramatic slowing down of relaxational processes

when some control parameters are varied. A typical signature of glassy behaviour is a *power law* or *stretched exponential* behaviour of correlation functions, as opposed to exponential decay. As the characteristic relaxation time may change by several orders of magnitude it can easily exceed the observation time. As a consequence the system *ages*: the observed static and dynamic properties depend on the *age* of the system defined as the time since the system was prepared (also called *waiting time*). For this reason, this residual very slow non-equilibrium phenomenon is commonly known as *aging*.

Aging systems include a large variety of materials. In fact, nearly all physical systems, within an appropriate set of conditions and observed during a specific time window, display glassy properties. The origin of glassy behaviour, however, can vary from system to system. The most important class of glassy systems (which include window glasses) are glass forming liquids where glassy behaviour is due to the appearance, as some external parameter is changed, of a long-lived complex pattern of interacting bonds between their microscopic constituents which strongly inhibits relaxation towards equilibrium. Aging follows from the very slow motion of such a complex pattern of interacting bonds which induces a slow change of the atomic structure of the liquid. For this reason glass forming liquids are usually called *structural glasses*. Our current understanding of the slow glassy relaxation dynamics is greatly limited by the lack of a general non-equilibrium theory that accounts for these phenomena.

Glasses can be generated by the fast cooling of a liquid. Upon cooling from high temperatures down to the melting transition temperature T_{M}, sometimes crystallization does not occur and the liquid continues its way down in temperature beyond T_{M} by following a line (called the supercooled liquid line) which is the continuation of the liquid line. As the liquid line is thermodynamically stable only above T_{M}, the supercooled liquid line is metastable with locally equilibrated properties, so its lifetime can be extremely large. As cooling proceeds it is observed that the supercooled liquid falls out of equilibrium (i.e. departs from the supercooled liquid line), below a temperature $T^*(r)$ which depends on the cooling rate r. The state reached below $T^*(r)$ is called a glass and the corresponding relaxational regime is indistinctly termed as *aging* or *glassy*. For small values of r a sharp transition is observed at $T^*(r)$, usually referred to as structural arrest, where the heat capacity jumps down, indicating the freezing of degrees of freedom. In contrast to the supercooled state, the glass state is of non-equilibrium nature and $T^*(r)$ is observed to decrease with r. As $T^*(r)$ depends on the cooling rate, no equilibrium phase transition occurs at that temperature. This means that the liquid will eventually equilibrate back to the supercooled state. The equilibration process may take an extremely long time (even for temperatures only a few degrees below T^*) being inaccessible from any practical point of view. Under some conditions the equilibration time can be larger than the age of the universe! In these conditions the glass state is the only *observable* state.

Long equilibration times imply that the glass state is characterized by very low energy dissipation rates, also called entropy production. This may give the false impression that the glass is in a stationary state. For instance, a piece of silica glass at room temperature looks pretty stable, indeed its optical, electrical and mechanical properties appear constant in time. However, a more careful examination reveals that the physical properties are constant only if observed on timescales much smaller than the time elapsed since the glass was prepared or formed. Beyond that timescale, the physical properties change revealing that the glass is aging.

Although aging was identified a long time ago in the study of polymers [1] it has received renewed interest in connection with the study of spin-glasses. Measurements of the magnetization in spin glasses have shown that aging is a general property of the low-temperature spin-glass phase. There are several types of spin-glass materials, the most common ones are metallic spin glasses. These are random diluted magnetic systems where

glassy behaviour arises from the disordered pattern of exchange interactions, rather than being self-generated as in structural glasses. Indeed random dilution generates exchange interactions with random competing signs, the system is then frustrated since a finite fraction of bonds cannot be satisfied. Aging is a consequence of the slow evolution of the pattern of satisfied bonds which becomes strongly inhibited as the temperature is lowered.

Another class of systems with glassy properties are *driven systems* which, under certain conditions, reach a stationary state characterized by non-Gibbsian probability distributions. After applying a time-dependent perturbation of frequency $\omega > 1/t_{\rm eq}$, upon an initially equilibrated system of relaxation time $t_{\rm eq}$, a new stationary state is reached which for many aspects is similar to the aging state of the relaxational system of age $\sim 1/\omega$.

Another important aspect of glassy systems that has received considerable attention for a long time [2] is the idea of the existence of an effective temperature (sometimes also called fictive temperature) describing the non-equilibrium properties of the glassy state. During the last decades, it has emerged that a possible way to rationalize the existence of an effective temperature is by measuring violations of the fluctuation–dissipation theorem (FDT). In glassy systems, a new modified relation between correlations and responses that goes under the name of quasi-FDT (QFDT) provides a description of the dynamics in the glassy state by quantifying the violations of the FDT. In this new theorem the effective temperature plays the role of the temperature of the bath. Related to the concept of the effective temperature is the idea of the existence of a heat flow from the glass to the thermal bath put in contact with the system. As the glass has an effective temperature higher than that of the bath, the heat flows from the glass to the bath. However, the energy dissipation rate from the glass towards the bath is extremely low (hardly measurable) and, in general, this flow can also be understood in terms of an effective very low thermal conductivity. The reader should be aware that using QFDT is only one among other possible ways of introducing an effective temperature for the description of the glassy state. In general, other definitions which use a generalization of different equilibrium relations to the non-equilibrium regime are possible. This gives rise to the problem of the equivalence of all possible definitions. We shall not discuss this point in this review and we will stick to the QFDT definition of an effective temperature.

This review will concentrate on the existence of a QFDT, its physical meaning, in what conditions it can emerge and the numerical evidence reported in favour of its validity. This is a rapidly growing area of research which is attracting new condensed matter and statistical physicists. We will report here the most important results obtained up until the summer of the year 2002. Although we have tried to cover most of the published work some contributions may have been overlooked. We apologize in advance to those colleagues. Although some of the results reviewed here are currently well understood many others still lack a full comprehension so it is no exaggeration to say that some of the ideas and suggestions described in this review could be modified in the future to adapt to the forthcoming theoretical, numerical or experimental evidence. Most of the results reported here deal with relaxational aging systems (as compared to driven systems) since these are those that have mostly attracted the attention of the researchers in the field. However, future developments in this exciting area of research might compensate this original unbalance as driven systems appear more amenable to experimental research than aging systems. Moreover, in this review we shall only consider the FDT in its classical version. Although most of the ideas can be extended to the quantum regime, to our knowledge there are neither numerical nor experimental works challenging FDT violations in the quantum aging regime. Therefore we shall not address them, the interested reader is referred to a recent review [3].

Many textbooks and article reviews can be useful to complement the contents of this review. Basic reviews on the glass transition since the mid 1980's until now can be found

in [4–7]. Other accounts dealing with aspects of the glass transition include thermodynamic theories of the glass transition [8, 9], mode-coupling theory (MCT) [10, 11] and numerical simulations [12]. For spin glasses a good selection of review articles can be found in [13]. A clear discussion of mode-coupling approximations in the context of disordered systems can be found in [14]. A recent discussion of several aspects concerning FDT violations can be found also in a recent review on kinetically constrained models [15]. Finally, a thorough compendium of analytical methods for glassy dynamics has been recently collected in [3] and a review of granular systems in [16]. Proceeding articles covering several aspects of glasses and spin glasses can be found in [17, 18] and for kinetically constrained models in [19].

The contents of this review have been written with two kinds of readers in mind: inexpert and expert. Those inexpert readers who want to understand the most basic ideas as well as the interest of investigating FDT violations must read sections 2, 3 and 4. These sections have been written at an introductory level, so expert readers who know about the subject may start reading directly from section 5. However, a careful reading of section 4 is recommended to those readers who want to have a more physically appealing description of the possible origin of FDT violations. Section 5 deals with some of the thermodynamic consequences of FDT violations. Sections 6 and 7 constitute the core of the review. Section 6 describes our knowledge of FDT violations gathered from several exactly solvable models where many aspects of their non-equilibrium behaviour can be understood by analytical means. Section 7 covers all evidence collected in the past years in favour of the existence of a QFDT in glassy systems. Many of the model systems described in this section correspond to realistic as well as model systems for which analytical solutions are hardly known. The expert reader who wants to grasp the state of the art concerning these questions will be mainly interested in these two sections. Finally, a brief account of some experimental results on FDT violations is described in section 8. Section 9 presents some conclusions.

2. Basic definitions and concepts

In this section, we recall some concepts of equilibrium theory which will be needed later for the description of the glassy state.

2.1. The microcanonical and canonical ensembles

The foundations of equilibrium statistical mechanics rely on the maximum entropy postulate and the Boltzmann equal probability hypothesis. An introduction to the basic postulates can be found in the classical books on statistical mechanics; rather excellent are those by Ma [20] and Callen [21]. Good discussions also come from information theory, see for example the book of Beck and Schloegel [22].

In what follows we shall denote by $\mathcal{C}$ a generic system configuration in the phase space. The phase space can be either continuous or discrete depending on the particular system. For example, for a system of N particles $\mathcal{C}$ are the positions and momenta in a continuous $6N$-dimensional space, while for a system of $N\frac{1}{2}$-spins $\mathcal{C}$ is a point in a discrete N-dimensional space with 2^N points. The system evolves in time following a dynamical rule which generally speaking is a rule that for each configuration $\mathcal{C}$ associates a new configuration $\mathcal{C}'$. The set of configurations which can be visited given a dynamical rule, defines the region of motion in the phase space. Let Γ be the volume of the region of motion allowed by the invariant quantities. The basic assumption of statistical mechanics asserts that the entropy is the logarithm of Γ. This makes the entropy computable without having to solve the dynamics. If we assume that

the system is described by an energy function $E(\mathcal{C})$ then the motion is confined to a region in phase space of constant energy. The calculation of entropy is then reduced to

$$S(E) = \ln \sum_{\mathcal{C}} \delta(E - E(\mathcal{C})) \tag{1}$$

where in the case of continuous variables the sum must be read as an integral. This equation defines the *microcanonical ensemble*. Since all allowed states are included $S(E)$ is clearly a maximum over all possible regions of constant energy E into which the phase space can be divided.

Let us consider now an observable $A(\mathcal{C})$ which we will assume to be neither a constant of motion nor a univocal function of the energy E. We also assume that $A(\mathcal{C})$ is extensive, i.e., it is proportional to the system size (volume or the number of constituents). We can then divide the phase space according to the value of $A(\mathcal{C})$ and, defining the degeneration $\Omega(E, A)$ of the partition as the total number of configurations $\mathcal{C}$ of energy E and observable value A,

$$\Omega(E, A) = \sum_{\mathcal{C}} \delta(E - E(\mathcal{C}))\delta(A - A(\mathcal{C})) \tag{2}$$

introduce the entropy in analogy with (1):

$$S(E, A) = \ln \Omega(E, A). \tag{3}$$

Using the integral representation of delta functions $\Omega(E, A)$ can be rewritten as

$$\begin{aligned}\Omega(E, A) &= \int_{-\infty}^{\infty} \frac{\mathrm{d}\alpha_1\, \mathrm{d}\alpha_2}{(2\pi)^2} \exp(\mathrm{i}\alpha_1 E + \mathrm{i}\alpha_2 A) \sum_{\mathcal{C}} \exp[-\mathrm{i}\alpha_1 E(C) - \mathrm{i}\alpha_2 A(C)] \\ &= \int_{-\infty}^{\infty} \frac{\mathrm{d}\alpha_1\, \mathrm{d}\alpha_2}{(2\pi)^2} \exp[\mathcal{S}(E, A, \alpha_1, \alpha_2)] \end{aligned} \tag{4}$$

where the function $\mathcal{S}(E, A, \alpha_1, \alpha_2)$ is given by

$$\mathcal{S}(E, A, \alpha_1, \alpha_2) = \mathrm{i}\alpha_1 E + \mathrm{i}\alpha_2 A + \ln \mathcal{Z}(\alpha_1, \alpha_2) \tag{5}$$

and $\mathcal{Z}(\alpha_1, \alpha_2)$ is the *partition function* given by

$$\mathcal{Z}(\alpha_1, \alpha_2) = \sum_{\mathcal{C}} \exp[-\mathrm{i}\alpha_1 E(\mathcal{C}) - \mathrm{i}\alpha_2 A(\mathcal{C})]. \tag{6}$$

Since both energy and the observable are extensive quantities the sum in (6) is dominated, in the limit of large system size, by the largest contribution, and $\mathcal{Z}$ is exponentially large in the system size. The function $\mathcal{S}(E, A, \alpha_1, \alpha_2)$ is then an extensive quantity and, in that limit, the integrations can be done selecting the dominant contribution using the saddle point method,

$$\frac{\partial \mathcal{S}(E, A, \alpha_1, \alpha_2)}{\partial \alpha_1} = \frac{\partial \mathcal{S}(E, A, \alpha_1, \alpha_2)}{\partial \alpha_2} = 0 \tag{7}$$

which leads to the saddle point equations

$$E = \frac{1}{\mathcal{Z}(\alpha_1, \alpha_2)} \sum_{\mathcal{C}} E(\mathcal{C}) \exp[-\mathrm{i}\alpha_1 E(\mathcal{C}) - \mathrm{i}\alpha_2 A(\mathcal{C})] \equiv \langle E \rangle \tag{8}$$

$$A = \frac{1}{\mathcal{Z}(\alpha_1, \alpha_2)} \sum_{\mathcal{C}} A(\mathcal{C}) \exp[-\mathrm{i}\alpha_1 E(\mathcal{C}) - \mathrm{i}\alpha_2 A(\mathcal{C})] \equiv \langle A \rangle. \tag{9}$$

Reality of $\Omega(E, A)$ implies that the solution $\alpha_1^*(E, A)$, $\alpha_2^*(E, A)$ of the saddle point equations must be pure imaginary: $\alpha_1^* = -\mathrm{i}\beta$, $\alpha_2^* = -\mathrm{i}\mu$ with β and μ real numbers. The entropy (3) is given by the value of $\mathcal{S}(E, A, \alpha_1, \alpha_2)$ evaluated at the saddle point:

$$S(E, A) = \mathcal{S}(E, A, -\mathrm{i}\beta, -\mathrm{i}\mu) = \beta E + \mu A + \ln \mathcal{Z}(\beta, \mu). \tag{10}$$

We can now ask the following question. What is the best choice of the value of $A(\mathcal{C})$ for which S attains its maximum? Stationarity of $\mathcal{S}$ with respect to α_1 and α_2 at the saddle point implies

$$\frac{\partial S(E, A)}{\partial E} = \beta \tag{11}$$

$$\frac{\partial S(E, A)}{\partial A} = \mu \tag{12}$$

so that the maximum entropy assumption requires $\mu = 0$, i.e., the entropy $S(E, A)$ must be stationary with respect to variations of A. For any energy E the best choice of A is then

$$A = \langle A \rangle = \frac{1}{\mathcal{Z}(\beta)} \sum_{\mathcal{C}} A(\mathcal{C}) \exp[-\beta E(\mathcal{C})] \tag{13}$$

where

$$\mathcal{Z}(\beta) = \sum_{\mathcal{C}} \exp[-\beta E(\mathcal{C})] = \exp[-\beta F(\beta)]. \tag{14}$$

The value of the entropy is

$$S(E) = \beta E + \ln \mathcal{Z}(\beta) \tag{15}$$

and is independent of A as required from stationarity. Finally, from (11) it follows that β^{-1} can be identified with the temperature T of equilibrium thermodynamics, while insertion of (14) into (15) yields the thermodynamic relation $F(\beta) = E(T) - TS(E)$ identifying $F(\beta)$ with the Helmholtz free energy. Equations (11), (13), (14) and (15) define the *canonical ensemble*.

Different to the microcanonical ensemble, the measure of the canonical ensemble is not restricted on states of constant energy. All possible states $\mathcal{C}$ enter but with a weight proportional to $\exp[-\beta E(\mathcal{C})]$. For a given temperature, however, only states with energy $E = \langle E \rangle$ given by (13) for $A(\mathcal{C}) = E(\mathcal{C})$ (see (8)) significantly contribute to the measure. The temperature can be seen as a *Lagrange multiplier* used to fix the value of the energy. Conversely, each value of E in equilibrium selects a temperature T through (11).

2.2. *Einstein fluctuation theory*

A key contribution in the development of equilibrium statistical mechanics is the statistical theory of fluctuations developed by Einstein [21]. In the previous section we have seen that in equilibrium the value of any observable $A(\mathcal{C})$ is given by (13), which for the purpose of this section will be denoted by $A_{\rm eq}$. The equilibrium value corresponds to the most probable value of $A(\mathcal{C})$, i.e., to the value of $A(\mathcal{C})$ which has the overwhelming probability of being seen in equilibrium. The same considerations apply to the energy $E(\mathcal{C})$ in the canonical ensemble.

We may then ask what is the probability of observing a value of $A(\mathcal{C})$ different from the equilibrium value. This probability is simply proportional to the number of configurations with $A(\mathcal{C}) = A$ which from (3) is

$$P(\delta A) \propto \Omega(E_{\rm eq}, A = A_{\rm eq} + \delta A) \propto \exp[S(E_{\rm eq}, A_{\rm eq} + \delta A)] \tag{16}$$

where following our notation $E_{\rm eq}$ is equilibrium energy. For small values of the fluctuations δA the exponent can be expanded and using stationarity of the entropy with respect to variation of A we get

$$S(E_{\rm eq}, A) = S(E_{\rm eq}, A_{\rm eq}) + \frac{(\delta A)^2}{2} \left(\frac{\partial^2 S}{\partial A^2} \right)_{A=A_{\rm eq}} + O(\delta A)^3. \tag{17}$$

If $A_{\rm eq}$ is a maximum, then a necessary condition is

$$\left(\frac{\partial^2 S}{\partial A^2}\right)_{A=A_{\rm eq}} = -\frac{1}{T\chi_A} < 0. \tag{18}$$

From (16) we finally obtain

$$P(\delta A) = \frac{1}{\sqrt{2\pi T\chi_A}} \exp\left[-\frac{(\delta A)^2}{2T\chi_A}\right]. \tag{19}$$

As χ_A is an extensive quantity only subextensive fluctuations $\delta A \sim \sqrt{V}$, where V is the system size, have finite probability in equilibrium. This justifies the most probable character of the equilibrium the value $A_{\rm eq}$.

The quantity χ_A is called *susceptibility*, and from (19) is related to fluctuations of A through

$$T\chi_A = \langle A^2\rangle - \langle A\rangle^2. \tag{20}$$

This relation is the simplest form of the static fluctuation–dissipation theorem (FDT) which relates the magnitude of thermal fluctuations with the response of the system to a (small) perturbation.

Suppose we add a constant perturbation $-\epsilon A(\mathcal{C})$ to the energy $E(\mathcal{C})$. Then in the new equilibrium the value $\langle A\rangle_\epsilon$ of A is (see (13))

$$\langle A\rangle_\epsilon = \frac{\sum_{\mathcal{C}} A(\mathcal{C}) \exp[-\beta E(\mathcal{C}) + \beta\epsilon A(\mathcal{C})]}{\sum_{\mathcal{C}} \exp[-\beta E(\mathcal{C}) + \beta\epsilon A(\mathcal{C})]}. \tag{21}$$

The susceptibility χ_A is defined as the variation of $\langle A\rangle$ induced by a small perturbation

$$\chi_A = \left.\frac{\partial\langle A\rangle_\epsilon}{\partial\epsilon}\right|_{\epsilon=0} \tag{22}$$

and hence measures the response of the system to the perturbation. Inserting (21) into (22) a straightforward calculation leads to (20).

The FDT formula (20) is a non-trivial result, since it relates different physical processes: the susceptibility describes an extensive $O(V)$ variation of the observable A while the rhs of (20) describes subextensive $O(\sqrt{V})$ thermal fluctuations. This fact is at the basis of the Onsager regression principle discussed in the next section.

2.3. The Onsager regression principle: a simple derivation of the fluctuation–dissipation theorem (FDT)

Onsager proposed [23, 24] a simple derivation of FDT for time-dependent perturbations. The derivation bypasses the more cumbersome analytical developments using linear response theory formalism, the Fokker–Planck equation or the generalized master equation approach.

Onsager derivation is based on the following *regression principle*: if a system initially in an equilibrium state 1 is driven by an external perturbation to a different equilibrium state 2, then the evolution of the system from state 1 towards state 2 in the presence of the perturbation can be treated as a spontaneous equilibrium fluctuation (in the presence of the perturbation) from the (now) non-equilibrium state 1 to the (now) equilibrium state 2.

Suppose that the system is initially in equilibrium with a thermal bath at temperature T, then the probability distribution of system configuration $\mathcal{C}$ in state 1 is given by the canonical ensemble (13):

$$P_0(\mathcal{C}) = \frac{\exp[-\beta E(\mathcal{C})]}{\sum_{\mathcal{C}} \exp[-\beta E(\mathcal{C})]}. \tag{23}$$

The subscript '0' indicates that the system is unperturbed.

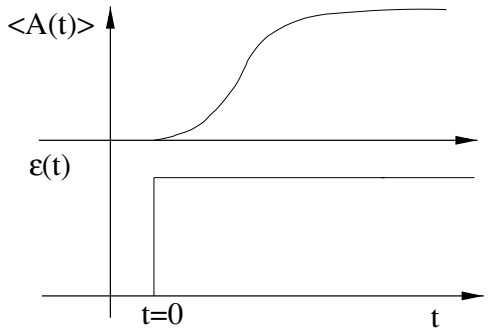

Figure 1. Perturbation $\epsilon(t)$ and typical evolution curve for $\langle A(t)\rangle_\epsilon$.

At time $t = 0$ a constant perturbation coupled to the observable $B(\mathcal{C})$ is applied to the system changing its energy into

$$E_\epsilon(\mathcal{C}) = E(\mathcal{C}) - \epsilon(t)B(\mathcal{C}) \tag{24}$$

where $\epsilon(t) = \epsilon$ if $t > 0$, and zero otherwise. The effect of the perturbation can be monitored by looking at the evolution of the expectation value $\langle A(t)\rangle_\epsilon$ of an observable $A(\mathcal{C})$, not necessarily equal to $B(\mathcal{C})$, from the equilibrium value in state 1 $\langle A(t = 0)\rangle_\epsilon = \langle A\rangle_0$ towards the new equilibrium value in state 2. The shape of $\epsilon(t)$ and a typical evolution of $\langle A(t)\rangle_\epsilon$ are shown in figure 1.

The expectation value of $\langle A(t)\rangle_\epsilon$ is given by the average over all possible dynamical paths originating from initial configurations weighted with the probability distribution (23),

$$\langle A(t)\rangle_\epsilon = \sum_{\mathcal{C},\mathcal{C}_0} A(\mathcal{C})\, P_\epsilon(\mathcal{C}, t|\mathcal{C}_0, 0)\, P_0(\mathcal{C}_0) \tag{25}$$

where $P_\epsilon(\mathcal{C}, t|\mathcal{C}_0, 0)$ is the conditional probability for the evolution from the configuration $\mathcal{C}_0$ at time $t = 0$ to the configuration $\mathcal{C}$ at time t. If $\epsilon = 0$ the expectation value becomes time independent since the initial state is in equilibrium and $P_0(\mathcal{C}, t|\mathcal{C}_0, 0)$ describes spontaneous equilibrium fluctuations.

The Onsager regression principle asserts that the conditional probabilities after having applied the perturbation are equal to those of spontaneous equilibrium fluctuations in state 2. Hence since the state 2 is still described by the canonical ensemble (23), but with the energy (24) now including the perturbation term, then

$$P_\epsilon(\mathcal{C}, t|\mathcal{C}_0, 0) = P_0(\mathcal{C}, t|\mathcal{C}_0, 0) \exp\{\beta\epsilon[B(\mathcal{C}) - B(\mathcal{C}_0)]\} \tag{26}$$

where the rhs of this equation is just the product of the spontaneous equilibrium fluctuation conditional probabilities $P_0(\mathcal{C}, t|\mathcal{C}_0, 0)$ in state 1 corrected by the presence of the perturbation term $\epsilon B(\mathcal{C})$.[3] Inserting (26) into (25) and expanding the exponential up to linear order we get

$$\begin{aligned}\langle A(t)\rangle_\epsilon - \langle A\rangle_0 &= \beta\epsilon \sum_{\mathcal{C},\mathcal{C}_0} A(\mathcal{C})[B(\mathcal{C}) - B(\mathcal{C}_0)]P_0(\mathcal{C}_0) \\ &= \beta\epsilon[\langle A(t)B(t)\rangle_0 - \langle A(t)B(0)\rangle_0].\end{aligned} \tag{27}$$

[3] Relation (26) is only valid for $\mathcal{C}_0 \neq \mathcal{C}$. Indeed, the normalization condition of conditional probabilities $\sum_{\mathcal{C}} P_\epsilon(\mathcal{C}, t|\mathcal{C}_0, 0) = 1$ implies that $P_\epsilon(\mathcal{C}, t|\mathcal{C}, 0) \neq P_0(\mathcal{C}, t|\mathcal{C}, 0)$ so relation (26) does not hold for $\mathcal{C}_0 = \mathcal{C}$. The difference between both probabilities $P_\epsilon(\mathcal{C}, t|\mathcal{C}, 0)$, $P_0(\mathcal{C}, t|\mathcal{C}, 0)$ does not matter as the transition $\mathcal{C} \to \mathcal{C}$ does not contribute to the response function in (27).

If we define the correlation function and time-dependent susceptibility as

$$C_{A,B}(t,s) = \langle A(t)B(s)\rangle_0 \tag{28}$$

$$\chi_{A,B}(t) = \lim_{\epsilon\to 0}\frac{\langle A(t)\rangle_\epsilon - \langle A\rangle_0}{\epsilon} \tag{29}$$

then from (27) we get the integrated form of the FDT relation

$$\chi_{A,B}(t) = \beta[C_{A,B}(t,t) - C_{A,B}(t,0)]. \tag{30}$$

The static form of the FDT (20) is easily obtained from (30) by taking $A = B$ and the limit $t \to \infty$. In this case $\chi_{A,A}(t) \to \chi_A$ (cf (22)) and $C_{AA}(t,t) = \langle A^2\rangle_0$ while $C_{AA}(t,0) \to \langle A\rangle_0^2$ as correlations factorize for infinitely separated times.

Sometimes the FDT relation is written in a differential form by considering the two-times response or retarded Green function,

$$R_{A,B}(t,s) = \frac{\delta\langle A(t)\rangle}{\delta\epsilon(s)} \qquad t > s \tag{31}$$

which gives the response to an impulsive perturbation $\epsilon(s)$ acting at time s. Causality imposes that the response function $R_{A,B}(t,s)$ is zero for $t < s$: perturbations cannot propagate backwards in time. The susceptibility $\chi_{A,B}(t)$ is the integral of the response function $R_{A,B}(t,s)$ then, using (30),

$$\begin{aligned}\int_0^t R_{A,B}(t,s)\,\mathrm{d}s &= \chi_{A,B}(t)\\ &= \beta[C_{A,B}(0) - C_{A,B}(t)]\\ &= \beta\int_0^t \frac{\partial}{\partial s}C_{A,B}(t,s)\,\mathrm{d}s.\end{aligned} \tag{32}$$

The last equality, and the arbitrarity of time t, implies that

$$R_{A,B}(t,s) = \beta\frac{\partial}{\partial s}C_{A,B}(t,s)\theta(t-s). \tag{33}$$

This is the differential form of the FDT relation.

3. The master equation approach

In this section, we introduce the master equation for the dynamical evolution of a generic system and show how the FDT arises within this approach. Besides the previous derivation in section 2.3, many other derivations of the FDT exist. We give a few collections of references where these are presented. Derivations can be classified in two families: deterministic or stochastic. Deterministic approaches are linear response theory [25], operator formalism for master equations [26] and quantum statistical mechanics [27]. Stochastic approaches are the Langevin and Fokker–Planck equations [28]. Here we present a stochastic derivation which is convenient for the purpose of the present review.

3.1. The master equation (ME)

Any dynamical law describing the evolution of a system is a rule which for each system configuration $\mathcal{C}$ associates a new configuration $\mathcal{C}'$. The time is just a label for bookkeeping the sequence so generated. Therefore, to simplify the presentation and the notation we shall

consider the time as an integer variable giving the equivalent expressions for the continuous limit when needed. This picture also has the advantage of being more closely related to numerical simulations since all numerical methods use discrete time schemes.

The dynamics can be encoded into the *conditional* or *transition* probability $W(\mathcal{C}, t|\mathcal{C}', t-1)$ of going from configuration $\mathcal{C}'$ at time $t-1$ to configuration $\mathcal{C}$ at time t. Indeed if $P(\mathcal{C}, t)$ denotes the probability that the system at time t is in the configuration $\mathcal{C}$, then from the Bayes theorem it follows that

$$P(\mathcal{C}, t) = \sum_{\mathcal{C}'} W(\mathcal{C}, t|\mathcal{C}', t-1) P(\mathcal{C}', t-1) \tag{34}$$

and the $W(\mathcal{C}, t|\mathcal{C}', t-1)$ together with the initial condition $P(\mathcal{C}, 0)$ fully define the dynamical evolution of the system in the phase space. Equation (34) is an identity valid for all processes and is the first of a hierarchy of equations for joint probabilities. Only if the process is Markovian, i.e., only if the conditional probability is determined entirely by the knowledge of the most recent past, can the hierarchy then be closed. Equation (34) and probability conservation at all times $\left(\sum_{\mathcal{C}'} P(\mathcal{C}', t) = 1\right)$ imply that $W(\mathcal{C}, t|\mathcal{C}', t-1)$ must satisfy the normalization condition

$$\sum_{\mathcal{C}'} W(\mathcal{C}', t|\mathcal{C}, t-1) = 1 \qquad \text{for all } \mathcal{C} \text{ and } t. \tag{35}$$

In the continuous time limit (34) is not well defined. To have an expression valid in this limit one then considers the variation of $P(\mathcal{C}, t)$ between two successive times which, using the normalization condition (35), reads

$$P(\mathcal{C}, t+1) - P(\mathcal{C}, t) = \sum_{\mathcal{C}'} W(\mathcal{C}, t+1|\mathcal{C}', t) P(\mathcal{C}', t) - \sum_{\mathcal{C}'} W(\mathcal{C}', t+1|\mathcal{C}, t) P(\mathcal{C}, t). \tag{36}$$

Dividing both sides of this equality for the time increment Δt and taking it to zero, we get the *master equation* (ME)

$$\frac{\partial P(\mathcal{C}, t)}{\partial t} = \sum_{\mathcal{C}'} W(\mathcal{C}|\mathcal{C}'; t) P(\mathcal{C}', t) - \sum_{\mathcal{C}'} W(\mathcal{C}'|\mathcal{C}; t) P(\mathcal{C}, t) \tag{37}$$

where $W(\mathcal{C}'|\mathcal{C}; t) = \lim_{\Delta t \to 0} W(\mathcal{C}, t + \Delta t|\mathcal{C}', t)/\Delta t$ is called the *transition rate* and gives the transition probability per unit of time. Solving the ME is often an extremely difficult and unaffordable task, even in the Markovian case.

Loosely speaking, the transition probability $W(\mathcal{C}, t|\mathcal{C}', t-1)$ can be seen as a transition rate for a unit time interval ($\Delta t = 1$), thus in what follows we shall not make a distinction between transition probabilities and transition rates and shall call them generically transition rates using for both the notation $W(\mathcal{C}'|\mathcal{C}; t)$. Which one is appropriate will be clear from the context.

Transition rates depend on the specific dynamical rules and hence by the Hamiltonian and eventual constraints (holonomic or non-holonomic). Let the system under consideration be described by an Hamiltonian which can depend on time through a set of time-dependent external parameters λ_t^j. For instance, λ_t may denote an time-dependent external pressure applied to a liquid or a time varying electric or magnetic field applied in a dielectric or a magnetic medium. We shall denote the set of these parameters by the vector $\boldsymbol{\lambda}_t$ and the Hamiltonian by $\mathcal{H}_{\boldsymbol{\lambda}_t}(\mathcal{C})$ to indicate the time dependence through $\boldsymbol{\lambda}_t$. Accordingly we shall also denote $W(\mathcal{C}|\mathcal{C}', t)$ by $W_{\boldsymbol{\lambda}_t}(\mathcal{C}|\mathcal{C}')$. If the Hamiltonian is time independent either $\boldsymbol{\lambda}_t$ or just the subindex t will be dropped, depending on the context.

Regardless of their form the transition rates must satisfy the following requirements:

- *Non-negativeness and normalization.* The $W_{\boldsymbol{\lambda}_t}(\mathcal{C}|\mathcal{C}';t)$ are probabilities so they must be non-negative and satisfy the normalization condition (35).
- *Ergodicity.* Transition rates must be such that starting from any configuration any other configuration of a finite system can be visited in a finite time. For continuous variables the condition is stated by considering an arbitrary finite phase space region around a given point ('neighbourhood').
- *Detailed balance.* If the $\boldsymbol{\lambda}$ are time independent the equilibrium distribution $P^{\mathrm{eq}}_{\boldsymbol{\lambda}}(\mathcal{C})$ is the stationary solution of the ME (37). A sufficient condition for this is that the transition rates be time independent and

$$\frac{W_{\boldsymbol{\lambda}}(\mathcal{C}'|\mathcal{C})}{W_{\boldsymbol{\lambda}}(\mathcal{C}|\mathcal{C}')} = \frac{P^{\mathrm{eq}}_{\boldsymbol{\lambda}}(\mathcal{C}')}{P^{\mathrm{eq}}_{\boldsymbol{\lambda}}(\mathcal{C})}. \tag{38}$$

  This condition receives the name of *detailed balance*. Different equilibrium ensembles are thus encoded into the different forms of transition rates. The Perron–Frobenius theorem assures [29] that this condition, together with non-negativeness, normalization and ergodicity guarantees that the equilibrium distribution in a finite system is reached in a finite time.
- *Causality.* This is an important assumption for the time-dependent transition rates and means that future is only determined by the past, i.e., a perturbation applied at a given time can only propagate forwards in time and not backwards. The consequence of this is that the transition rates must depend only on the values of $\boldsymbol{\lambda}_t$ taken at the *lowest* time t.

For arbitrary time-dependent $\boldsymbol{\lambda}_t$ the stationary solution of ME will, in general, also depend on time. In this case, however, the previous conditions, and in particular the detailed balance condition, are not enough to determine the stationary state which in general will not be Gibbsian, i.e., not described by the Boltzmann–Gibbs distribution. Only when $\boldsymbol{\lambda}_t$ can be treated as small perturbations can some predictions be obtained from the linear response theory.

3.2. Correlations, responses and the FDT

Consider two arbitrary observables $A(\mathcal{C}), B(\mathcal{C})$ which for simplicity are assumed time independent. These can be either local or global quantities defined over a microscopic or macroscopic region respectively. For instance, in a liquid an observable could be the local density at a point or the total mass of a given macroscopic region. In systems with discrete variables such as magnetic systems, it can be a spin of a given magnetic atom or the magnetization of a macroscopic part of the system.

The two-times correlation function $C_{A,B}(t,s)$ between $A(t)$ and $B(s)$ is defined as the average $\langle A(t)B(s)\rangle$ over all possible dynamical paths from time 0 to time t and all possible initial conditions weighted by the probability distribution $P(\mathcal{C},0)$,

$$C_{A,B}(t,s) = \langle A(t)B(s)\rangle = \sum_{\mathcal{C},\mathcal{C}'} A(\mathcal{C}')P(\mathcal{C}',t|\mathcal{C},s)B(\mathcal{C})P(\mathcal{C},s) \tag{39}$$

where $P(\mathcal{C}',t|\mathcal{C},s)$ is the conditional probability to evolve from $\mathcal{C}$ at time s to $\mathcal{C}'$ at later time t. Unless otherwise stated, in what follows we shall adopt the convention that $t \geqslant s$.

To simplify the notation, we switch to discrete (integer) time variable so that a dynamical path from time 0 to time t is given by a sequence of t configurations $\{\mathcal{C}_0, \mathcal{C}_1, \ldots, \mathcal{C}_t\}$, along

which $\boldsymbol{\lambda}$ takes the sequence of values $\{\boldsymbol{\lambda}_0, \boldsymbol{\lambda}_1, \ldots, \boldsymbol{\lambda}_t\}$. In this case, using (34), the correlation can be easily rewritten in terms of transition rates as

$$C_{A,B}(t,s) = \sum_{\mathcal{C}_s,\ldots,\mathcal{C}_t} A(\mathcal{C}_t)\left[\prod_{k=s}^{t-1} W_{\boldsymbol{\lambda}_k}(\mathcal{C}_{k+1}|\mathcal{C}_k)\right] B(\mathcal{C}_s)P(\mathcal{C}_s,s) \tag{40}$$

where we have used the short-hand notation $W_{\boldsymbol{\lambda}_k}(\mathcal{C}_{k+1}|\mathcal{C}_k) \equiv W_{\boldsymbol{\lambda}_k}(\mathcal{C}_{k+1}|\mathcal{C}_k;k)$.

In equilibrium, correlations satisfy the time translational invariance (TTI) property: $C_{A,B}(t,s) = C_{A,B}(t-s)$. Indeed in this case $P(\mathcal{C}_s,s)$ is replaced by $P^{\rm eq}(\mathcal{C}_s)$ and the transition rates satisfy the detailed balance condition (38):

$$W_{\boldsymbol{\lambda}}(\mathcal{C}_{k+1}|\mathcal{C}_k) = W_{\boldsymbol{\lambda}}(\mathcal{C}_k|\mathcal{C}_{k+1})\frac{P^{\rm eq}_{\boldsymbol{\lambda}}(\mathcal{C}_{k+1})}{P^{\rm eq}_{\boldsymbol{\lambda}}(\mathcal{C}_k)}. \tag{41}$$

Inserting this relation into (40) the factors $P^{\rm eq}(\mathcal{C}_k)$ in the numerator and denominator of the product cancel one by one and, exchanging the indices $t \leftrightarrow s$, we obtain

$$\begin{aligned} C_{A,B}(t,s) &= \sum_{\mathcal{C}_s,\ldots,\mathcal{C}_t} A(\mathcal{C}_t)P^{\rm eq}_{\boldsymbol{\lambda}}(\mathcal{C}_t)\left[\prod_{k=s}^{t-1} W_{\boldsymbol{\lambda}}(\mathcal{C}_{k+1}|\mathcal{C}_k)\right] B(\mathcal{C}_s) \\ &= (t \leftrightarrow s) \\ &= \sum_{\mathcal{C}_t,\ldots,\mathcal{C}_s} B(\mathcal{C}_t)\left[\prod_{k=t}^{s-1} W_{\boldsymbol{\lambda}}(\mathcal{C}_k|\mathcal{C}_{k+1})\right] A(\mathcal{C}_s)P^{\rm eq}_{\boldsymbol{\lambda}}(\mathcal{C}_s) \\ &= \langle B(t)A(s)\rangle \\ &= C_{B,A}(t,s) \end{aligned} \tag{42}$$

which implies that $C_{A,B}(t,s) = C_{A,B}(t-s)$.

The correlation function $C_{A,B}(t,s)$ is a measure of how the system loses memory of its past history and hence decays for large time separations. To measure how a system responds to external perturbations one introduces the response functions. Similar to correlations, responses also tend to decay with time because the effect of the perturbation is progressively forgotten in a thermal environment. However, there is an important difference between correlations and responses: causality. While two observables can be correlated forwards or backwards in time, a perturbation cannot propagate backwards in time and the response of the system for times before the perturbation is applied must be zero. Nevertheless, despite this difference, response and correlations can be treated on equal footing by employing a supersymmetric formalism. The interested reader can find more details, e.g., in the classical book by Zinn-Justin [28].

To study the response of the system to an external perturbation, we assume that at time s an impulsive perturbation of small intensity ϵ is applied to the observable $B(\mathcal{C})$ and measure the variation of the average value of an observable $A(\mathcal{C})$ at later times. The response function $R_{A,B}(t,s)$ is defined in the limit of vanishing perturbation strength as

$$R_{A,B}(t,s) = \lim_{\epsilon\to 0}\frac{\langle A(t)\rangle_{\epsilon_s} - \langle A(t)\rangle_0}{\epsilon} \qquad t > s \tag{43}$$

with

$$\langle A(t)\rangle_{\epsilon_s} = \sum_{\mathcal{C}} A(\mathcal{C})P_{\epsilon_s}(\mathcal{C},t) \tag{44}$$

$$\langle A(t)\rangle_0 = \sum_{\mathcal{C}} A(\mathcal{C})P_0(\mathcal{C},t) \tag{45}$$

where $P_{\epsilon_s}(\mathcal{C}, t)$ and $P_0(\mathcal{C}, t)$ are the probabilities that the system is in the configuration $\mathcal{C}$ at time $t > s$ in the perturbed and unperturbed cases, respectively. If the system is described by the unperturbed Hamiltonian $\mathcal{H}_0(\mathcal{C})$, then in presence of the perturbation the Hamiltonian becomes

$$\mathcal{H}_{\epsilon_s}(\mathcal{C}) = \mathcal{H}_0(\mathcal{C}) - \delta_{t,s}\epsilon B(\mathcal{C}). \tag{46}$$

By using (34) and the fact that the Hamiltonians only differ at time s when the impulse is applied, the probabilities $P_{\epsilon_s}(\mathcal{C}, t)$ and $P_0(\mathcal{C}, t)$ can be written as

$$P_{\epsilon_s}(\mathcal{C}_t, t) = \sum_{\mathcal{C}_s,\ldots,\mathcal{C}_{t-1}} \left[\prod_{k=s+1}^{t-1} W_0(\mathcal{C}_{k+1}|\mathcal{C}_k)\right] W_\epsilon(\mathcal{C}_{s+1}|C_s) P_0(\mathcal{C}_s, s) \tag{47}$$

$$P_0(\mathcal{C}_t, t) = \sum_{\mathcal{C}_s,\ldots,\mathcal{C}_{t-1}} \left[\prod_{k=s+1}^{t-1} W_0(\mathcal{C}_{k+1}|\mathcal{C}_k)\right] W_0(\mathcal{C}_{s+1}|C_s) P_0(\mathcal{C}_s, s) \tag{48}$$

where $W_{0,\epsilon}$ denotes the transition rates in the unperturbed/perturbed case, and we have used the short-hand notation $W(\mathcal{C}_{k+1}|\mathcal{C}_k) \equiv W(\mathcal{C}_{k+1}|\mathcal{C}_k; k)$.

Because we are interested in the $\epsilon \to 0$ limit the transition rates in the perturbed and unperturbed cases can be related by expanding the detailed balance condition (38) for the perturbed state around $\epsilon = 0$ up to the first order in ϵ,

$$\begin{aligned}\frac{W_\epsilon(\mathcal{C}'|\mathcal{C})}{W_\epsilon(\mathcal{C}|\mathcal{C}')} &= \frac{P_\epsilon^{\mathrm{eq}}(\mathcal{C}')}{P_\epsilon^{\mathrm{eq}}(\mathcal{C})} \\ &= \frac{W_0(\mathcal{C}'|\mathcal{C})}{W_0(\mathcal{C}|\mathcal{C}')}\left\{1 + \epsilon\,\frac{\partial}{\partial\epsilon}\ln\left[P_\epsilon^{\mathrm{eq}}(\mathcal{C}')\big/P_\epsilon^{\mathrm{eq}}(\mathcal{C})\right]\Big|_{\epsilon=0} + \mathcal{O}(\epsilon^2)\right\}\end{aligned} \tag{49}$$

where $P_\epsilon^{\mathrm{eq}}(\mathcal{C})$ is the equilibrium probability distribution in the perturbed state[4]. In general we can write

$$\log\left[P_\epsilon^{\mathrm{eq}}(\mathcal{C})\right] = \log\left[P_0^{\mathrm{eq}}(\mathcal{C})\right] + \phi_0 - \phi_\epsilon + \beta\epsilon B(\mathcal{C}) \tag{50}$$

where ϕ denotes the corresponding thermodynamic potential. For instance, in the canonical ensemble it corresponds to minus the Helmholtz free energy F while in the grandcanonical ensemble it corresponds to the grandcanonical potential given by the pressure times the volume.

Using (49) we finally obtain, to the leading order in ϵ,

$$W_\epsilon(\mathcal{C}'|\mathcal{C}) - W_0(\mathcal{C}'|\mathcal{C}) = \left[\frac{W_\epsilon(\mathcal{C}|\mathcal{C}')}{W_0(\mathcal{C}|\mathcal{C}')} - 1\right] W_0(\mathcal{C}'|\mathcal{C}) + \epsilon\frac{\partial}{\partial\epsilon}\ln\left[P_\epsilon^{\mathrm{eq}}(\mathcal{C}')\big/P_\epsilon^{\mathrm{eq}}(\mathcal{C})\right]\Big|_{\epsilon=0} W_0(\mathcal{C}'|\mathcal{C}). \tag{51}$$

The physical meaning of the two terms appearing in this expression is different. The first term, absent in the Onsager postulate (26), accounts for the variation due to the change in the transition rates and does not directly depend upon the particular form of the equilibrium

[4] An observation concerning (49) and its relation with the Onsager postulate (26) is important. Ideally, in order to demonstrate FDT, one would like to have a relation similar to (26) relating the unperturbed and the perturbed rates rather than a relation between the forward and backward rates as given in (49). However, such a relation does not exist as it depends upon the type of dynamics through the particular form of the transition rules. For instance, by considering rates of the type $W_\lambda(\mathcal{C}'|\mathcal{C}) \propto P_\lambda^{\mathrm{eq}}(\mathcal{C}')$, i.e. depending only upon the final configuration, one finds that (26) automatically holds. However, such rates cannot be used to derive the FDT (33), (55) as they lead to the trivial identity $0 = 0$ because any impulse does not affect dynamics at later times $R(t, s) = 0$ and there are no time correlations. In other words, the Onsager postulate extended to the non-equilibrium regime generates violation terms different from those obtained in the present approach (for instance the term $R^{(1)}$ in the rhs of (59)).

distribution. The second term depends directly on the equilibrium distribution. This distinction is important since they give different contributions to the response. For the response function (43) to be well defined the difference $\langle A(t)\rangle_\epsilon - \langle A(t)\rangle_0$ must be at least linear in ϵ. This requirement is at the roots of the applicability of linear response theory and implies that both terms in (51) must be at least linear in ϵ. Concerning the first term, it is required that the difference $W_\epsilon(\mathcal{C}|\mathcal{C}')/W_0(\mathcal{C}|\mathcal{C}') - 1$ be linear in ϵ, so the transition rates must change linearly with ϵ when the system is perturbed. This means that, during the dynamics, and after applying the perturbation, one cannot switch arbitrarily from one class of dynamics to another class of dynamics in a random fashion. To better illustrate what this means let us consider a Monte Carlo stochastic dynamics. There are different possible algorithms or transition rules which fulfil detailed balance (e.g. Metropolis, heat-bath, Glauber). One could imagine switching randomly from one algorithm to another one while doing the dynamics. Nothing forbids this quite *artificial* choice. But, when measuring the response function, it is required that the same time sequence of algorithms must be used for the unperturbed and perturbed dynamical evolutions. Usually, the same algorithm is chosen in a given simulation so one does not care about this subtlety. For the second term, we require that $(\partial/\partial\epsilon)\ln\left[P_\epsilon^{\rm eq}(\mathcal{C}')\big/P_\epsilon^{\rm eq}(\mathcal{C})\right]\big|_{\epsilon=0}$ be finite. Inspection of (50) reveals that this holds if the observable $B(C)$ does not jump discontinuously when the perturbation is switched on. This condition requires that the system is not at a first order transition point. This situation is encountered, for instance, by perturbing the Ising model at zero temperature with a uniform magnetic field.

Inserting (51) into (43) the response function decomposes into two parts,

$$R_{A,B}(t,s) = R^{(1)}_{A,B}(t,s) + R^{(2)}_{A,B}(t,s) \tag{52}$$

where

$$R^{(1)}_{A,B}(t,s) = \lim_{\epsilon\to 0}\frac{1}{\epsilon}\sum_{\mathcal{C}_s,\ldots,\mathcal{C}_t} A(\mathcal{C}_t)\left[\prod_{k=s+1}^{t-1} W_0(\mathcal{C}_{k+1}|\mathcal{C}_k)\right]\left[\frac{W_\epsilon(\mathcal{C}_s|\mathcal{C}_{s+1})}{W_0(\mathcal{C}_s|\mathcal{C}_{s+1})} - 1\right] W_0(\mathcal{C}_{s+1}|\mathcal{C}_s)\,P_0(\mathcal{C}_s,s) \tag{53}$$

$$R^{(2)}_{A,B}(t,s) = \sum_{\mathcal{C}_s,\ldots,\mathcal{C}_t} A(\mathcal{C}_t)\left[\prod_{k=s+1}^{t-1} W_0(\mathcal{C}_{k+1}|\mathcal{C}_k)\right] \times \frac{\partial}{\partial\epsilon}\ln\left[P_\epsilon^{\rm eq}(\mathcal{C}')\big/P_\epsilon^{\rm eq}(\mathcal{C})\right]\Big|_{\epsilon=0} W_0(\mathcal{C}_{s+1}|\mathcal{C}_s)\,P_0(\mathcal{C}_s,s). \tag{54}$$

Inserting (50) for the second term we get

$$R^{(2)}_{A,B}(t,s) = \left\langle A(t)\,\frac{\partial \ln P_\epsilon^{\rm eq}(\mathcal{C}_{s+1})}{\partial\epsilon}\Big|_{\epsilon=0}\right\rangle_0 - \left\langle A(t)\,\frac{\partial \ln P_\epsilon^{\rm eq}(\mathcal{C}_s)}{\partial\epsilon}\Big|_{\epsilon=0}\right\rangle_0 \tag{55}$$

which using (50) becomes

$$R^{(2)}_{A,B}(t,s) = \beta\langle A(t)B(s+1)\rangle_0 - \beta\langle A(t)B(s)\rangle_0. \tag{56}$$

In the limit of continuous time $R^{(2)}$ in (56) must be replaced by

$$R^{(2)}_{A,B}(t,s) = \beta\frac{\partial}{\partial s}\langle A(t)B(s)\rangle_0. \tag{57}$$

The first term $R^{(1)}$ cannot be expressed in a simple form. Only in equilibrium it is possible to show that it vanishes. To prove it requires the following steps: first use the identity

$$\prod_{k=s+1}^{t-1} W_0(\mathcal{C}_{k+1}|\mathcal{C}_k) = \left[\prod_{k=s+1}^{t-1} W_0(\mathcal{C}_k|\mathcal{C}_{k+1})\right]\frac{P_0^{\rm eq}(\mathcal{C}_t)}{P_0^{\rm eq}(\mathcal{C}_{s+1})} \tag{58}$$

and then the normalization (35). Collecting all terms we finally obtain for the response function

$$R_{A,B}(t,s) = R^{(1)}_{A,B}(t,s) + \beta \frac{\partial}{\partial s}\langle A(t)B(s)\rangle_0. \tag{59}$$

In equilibrium, besides $R^{(1)} = 0$, the correlation function satisfies TTI, so from (59) we get the equilibrium FDT

$$R^{\rm eq}_{A,B}(t-s) = \beta \frac{\partial}{\partial s} C^{\rm eq}_{A,B}(t-s) = -\beta \frac{\partial}{\partial t} C^{\rm eq}_{A,B}(t-s) \qquad t > s. \tag{60}$$

The term $R^{(1)}$ may also vanish in the non-equilibrium state if the first term in (51) vanishes faster than linearly with ϵ for $\epsilon \to 0$. In this case (59) reduces to the usual FDT relation (33):

$$R_{A,B}(t,s) = \beta\theta(t-s)\frac{\partial}{\partial s} C_{A,B}(t,s). \tag{61}$$

Therefore, the lowest time s has a special role in the relation (59) between correlations and responses. This is not a surprise since the relation has been obtained by assuming causality which privileges the lowest time. In equilibrium, the role of the lowest time disappears because the system is TTI.

3.3. The component master equation

Let us now divide the phase space into different non-overlapping subsets $\mathcal{R}$ that can be called regions, phases, components or domains. In what follows, if not stated otherwise, we shall use the term *component*. Later in section 4.2 we will see that the reduction of the phase space by a suitable partitioning can be relevant for the study of the non-equilibrium regime in glassy systems and in particular for the understanding of the FDT relations. For the moment, however, we do not attach any physical meaning to such a partitioning, and assume it to be completely arbitrary, postponing the identification of a suitable partitioning scheme for glassy systems to section 4.5.

For each partition of the phase space the probability $\mathcal{P}(\mathcal{R},t)$ that the system is in the component $\mathcal{R}$ at time t is given by

$$\mathcal{P}(\mathcal{R},t) = \sum_{\mathcal{C}\in\mathcal{R}} P(\mathcal{C},t) \tag{62}$$

$$\sum_{\mathcal{R}} \mathcal{P}(\mathcal{R},t) = 1 \tag{63}$$

where the normalization condition (63) follows from normalization of $P(\mathcal{C},t)$ and the non-overlapping assumption on $\mathcal{R}$. The probability distribution $\mathcal{P}(\mathcal{R},t)$ obeys the master equation obtained by projecting the (microscopic) master equation (37) over the component space. The Markovian character of the dynamics is preserved under projection. Summing (37) over all configurations $\mathcal{C}$ belonging to a given component $\mathcal{R}$ we get the *component* master equation,

$$\frac{\partial \mathcal{P}(\mathcal{R},t)}{\partial t} = \sum_{\mathcal{R}'} \mathcal{W}(\mathcal{R}|\mathcal{R}';t)\mathcal{P}(\mathcal{R}',t) - \sum_{\mathcal{R}'} \mathcal{W}(\mathcal{R}'|\mathcal{R};t)\mathcal{P}(\mathcal{R},t) \tag{64}$$

where $\mathcal{W}(\mathcal{R}'|\mathcal{R};t)$ are the component transition rates which in terms of the original transition rates $W(\mathcal{C}'|\mathcal{C};t)$ read

$$\mathcal{W}(\mathcal{R}'|\mathcal{R};t) = \frac{\sum_{\mathcal{C}'\in\mathcal{R}',\mathcal{C}\in\mathcal{R}} W(\mathcal{C}'|\mathcal{C},t)P(\mathcal{C},t)}{\mathcal{P}(\mathcal{R},t)}. \tag{65}$$

The component transition rates satisfy the same normalization conditions as W. For example, in the case of discrete time we have (cf (35))

$$\sum_{\mathcal{R}'} \mathcal{W}(\mathcal{R}', t|\mathcal{R}, t-1) = 1 \qquad \text{for all } \mathcal{R} \text{ and } t. \tag{66}$$

However, there is an important difference between the (microscopic) master equation (37) and component master equation (64): the transition rates (65) are time dependent even in time-independent Hamiltonians since they are computed with the run-time configuration probability distribution function $P(\mathcal{C}, t)$. A direct consequence of this is that, while the properties of non-negativeness, normalization, ergodicity and causality discussed in section 3.1 for W do apply to $\mathcal{W}$, the detailed balance is not valid anymore in the component space. Indeed from (65) it follows that

$$\frac{\mathcal{W}(\mathcal{R}'|\mathcal{R}; t)}{\mathcal{W}(\mathcal{R}|\mathcal{R}'; t)} = \frac{\sum_{\mathcal{C}\in\mathcal{R},\mathcal{C}'\in\mathcal{R}'} W(\mathcal{C}'|\mathcal{C})P(\mathcal{C}, t)}{\sum_{\mathcal{C}\in\mathcal{R},\mathcal{C}'\in\mathcal{R}'} W(\mathcal{C}|\mathcal{C}')P(\mathcal{C}', t)} \times \frac{\mathcal{P}(\mathcal{R}', t)}{\mathcal{P}(\mathcal{R}, t)}. \tag{67}$$

The detailed balance condition is recovered, however, at equilibrium where $\mathcal{W}$, according to (65), becomes time independent,

$$\mathcal{W}^{\mathrm{eq}}(\mathcal{R}'|\mathcal{R}) = \frac{\sum_{\mathcal{C}\in\mathcal{R},\mathcal{C}'\in\mathcal{R}'} W(\mathcal{C}'|\mathcal{C})P^{\mathrm{eq}}(\mathcal{C})}{\mathcal{P}^{\mathrm{eq}}(\mathcal{R})} \tag{68}$$

where $\mathcal{P}^{\mathrm{eq}}(\mathcal{R})$ denotes the equilibrium probability distribution function in the component space associated through (62) with the phase space equilibrium probability distribution function $\mathcal{P}^{\mathrm{eq}}(\mathcal{C})$. Using the detailed balance condition (38) we obtain

$$\frac{\mathcal{W}^{\mathrm{eq}}(\mathcal{R}'|\mathcal{R})}{\mathcal{W}^{\mathrm{eq}}(\mathcal{R}|\mathcal{R}')} = \frac{\mathcal{P}^{\mathrm{eq}}(\mathcal{R}')}{\mathcal{P}^{\mathrm{eq}}(\mathcal{R})} \tag{69}$$

which is the detailed balance condition in the component space.

In conclusion, in the component space the rates $\mathcal{W}$ satisfy the same set of conditions as the rates W except for the detailed balance condition which in the component space only holds at equilibrium. In general, rates $\mathcal{W}$ do not satisfy detailed balance so the FDT derived in the previous sections for the microscopic master equation will not be valid in the component space. They are, however, valid in equilibrium so, for example, after an appropriate redefinition of correlations and responses the equilibrium fluctuation–dissipation theorem (60) still holds in the component space.

4. FDT extensions to the non-equilibrium regime

In this section, we discuss how to extend the previous ideas to the non-equilibrium glassy regime. After a brief introduction of aging (intended for the non-specialist) we discuss how to derive a free-energy master equation by introducing the configurational entropy and the notion of the effective temperature. We then discuss how to extend the FDT beyond equilibrium by introducing the fluctuation–dissipation ratio and the quasi-FDT. This requires the notion of neutral observables. Finally, a possible partitioning scheme is presented.

4.1. An intermezzo on aging

In this section, we discuss one of the main signatures of the non-equilibrium regime of glassy systems, i.e. the existence of aging and the quantifying of FDT violations through a modified FDT in terms of a set of effective temperatures. This discussion is intended for the inexpert reader who wants to have a glance at the key aspects of glassy systems before entering the

more detailed exposition. Therefore, the level of this discussion is highly introductory and the expert reader can move directly to the next section.

In relaxational glassy systems the two basic properties of correlations and response, time translational invariance (TTI) (42) and the FDT (60), no longer hold. In particular, TTI is observed to be violated in the following way: both correlations and responses decay slower as the system gets older, i.e. the system is aging. This fact stems from several experimental observations in polymers and deformable materials [1], structural glasses [30] and spin glasses [13]. In driven systems the situation appears less complicated as TTI holds and only the FDT is violated. Some of the aspects described below carry over also to driven systems, however for sake of clarity we will stick in what follows to the case of aging systems.

Experimentally, aging is manifest through the measurement of the so-called integrated response function (IRF) or time-dependent susceptibility described in section 4.3. In aging systems, the weak long-term memory makes response functions $R(t, s)$ hardly measurable as they asymptotically decay to zero, instead it is easier to measure the cumulative response or time-dependent susceptibility $\chi(t, s) = \int_s^t R(t, t')\,\mathrm{d}t'$ (defined after perturbing the system at the waiting time s, often denoted as t_w) which in general are finite: in dielectric measurements of glasses the IRF corresponds to the polarizability of the sample after cutting or applying an electric field; in magnetic systems it corresponds to the thermoremanent or zero field cooled susceptibility; in mechanical systems aging is observed by measuring the deformation of the sample after applying a tensile load. All these measurements reveal that $\chi(t, s)$ is well approximated by the sum of two contributions,

$$\chi(t, s) = \chi_{\mathrm{st}}(t - s) + \chi_{\mathrm{ag}}(t, s) \tag{70}$$

where the first contribution $\chi_{\mathrm{st}}(t - s)$ stands for a stationary part that asymptotically decays to a finite value or plateau and $\chi_{\mathrm{ag}}(t, s)$ is the aging part that is well approximated by the scaling relation,

$$\chi_{\mathrm{ag}}(t, s) = \hat{\chi}\left(\frac{t}{s}\right). \tag{71}$$

This scaling behaviour, that is obtained within many solvable models, is known as full aging or simple t/s scaling[5]. However, deviations from full aging have been reported in many experiments suggesting that this simple scaling behaviour does not fully account for the experimental data. In particular, spin-glass measurements clearly favour a subaging scenario where $\hat{\chi}$ has as scaling argument the variable $\frac{t}{s^\delta}$ with $\delta < 1$ (we note, however, that experiments report values around 0.95, i.e. very close to 1). The physical origin of these deviations is still unknown. For both correlation and response functions similar decompositions as in (70), (71) are expected to be valid but replacing χ by C or R (however, for the aging part of the response there is an additional factor $1/t$ multiplying $R_{\mathrm{ag}}(t, s)$) . Correlations and responses are difficult to experimentally access. In theoretical or numerical simulation studies, the calculation of correlation functions is always preferred. Typical curves for the susceptibilities or correlations are depicted in figure 2. Within the full aging scenario (71) it is usually shown that, in the asymptotic limit where both s and t are large, the FDT (60) is violated depending on the ratio $(t - s)/s$. If $(t - s)/s \ll 1$, $C(t, s) \simeq C_{\mathrm{st}}(t - s)$ and FDT holds,

$$\frac{\partial C_{\mathrm{st}}(t - s)}{\partial s} = T R_{\mathrm{st}}(t - s). \tag{72}$$

However, in the other case $(t - s)/s \geqslant 1$, then $C(t, s) \simeq C_{\mathrm{ag}}(t, s)$ and the FDT (60) is violated according to the new relation,

$$\frac{\partial C_{\mathrm{ag}}(t, s)}{\partial s} = T_{\mathrm{eff}}(s) R_{\mathrm{ag}}(t, s) \tag{73}$$

[5] A coarsening system also deviates from the simple form (71) in favour of $\chi_{\mathrm{ag}}(t, s) = s^{-a}\hat{\chi}(t/s)$ with $a \geqslant 0$.

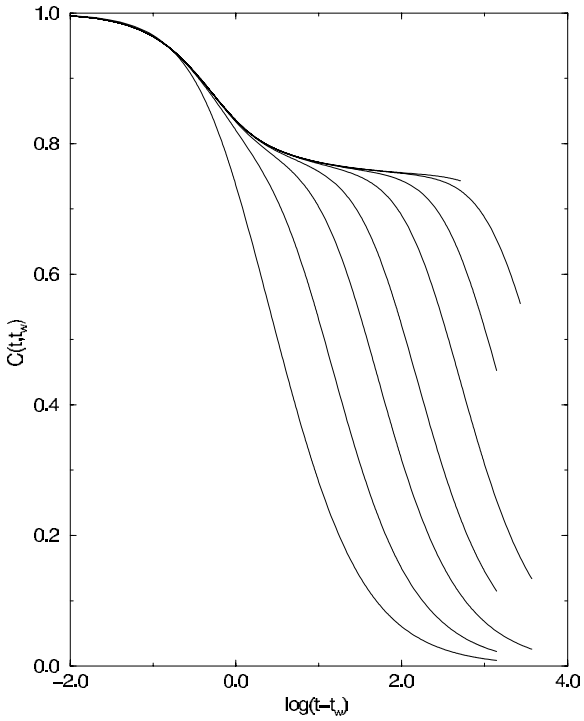

Figure 2. Typical shape of a two-times correlation function $C(t, t_w)$ (the same would be valid for the integrated susceptibility $\chi(t, t_w)$), plotted as a function of $t - t_w$ (in log scale) with system age t_w increasing from left to right. The decomposition (70) shows the two separate time sectors: in the first fast part of the relaxation $C(t, t_w) \simeq C_{\rm st}(t-t_w)$ is independent of s and obeys TTI while the slow second part $C_{\rm ag}(t - t_w)$ decays from the plateau on a timescale growing with t_w. This figure has been taken from a lattice gas coarsening model [31] with properly normalized correlations at equal times $C(t, t) = 1$.

where $T_{\rm eff}(s)$ is a new parameter that enters the new relation playing the role of an effective temperature. The particular way in which the FDT is violated suggests calling the new relation (73) a quasi-fluctuation–dissipation theorem (QFDT). Although other possible terms have been used to refer to the modified FDT, here we will adhere to the term QFDT, as this is the one originally introduced by Horner [32] that expresses the idea of partial equilibration among a subset of degrees of freedom.

Aging carries the associated decomposition of time into time sectors. In the previous example of full aging (71) there are two time sectors depending on the ratio $(t - s)/s$ as described in (72), (73). However, as we have already mentioned, deviations from the full aging behaviour are expected to be present in general. In those cases, the stationary result (72) for the short-time sector still holds but (73) is replaced by the more general relation,

$$\frac{\partial C_{\rm ag}(t, s)}{\partial s} = T_{\rm eff}(C_{\rm ag}(t, s))R_{\rm ag}(t, s) \tag{74}$$

where the new effective temperature $T_{\rm eff}(C_{\rm ag}(t, s)) \equiv T_{\rm eff}(C(t, s))$, since $C \equiv C_{\rm ag}$ when $(t - s)/s \sim O(1)$, and depends on both times only through the value of C. In this case, the aging part develops time sectors defined as those values of t, s where $t/s \sim O(1)$ [33, 34]. Each sector is then labelled by the value of the correlation function $C(t, s)$ and many effective temperatures arise in the description of the non-equilibrium regime, the QFDT (74) quantifying

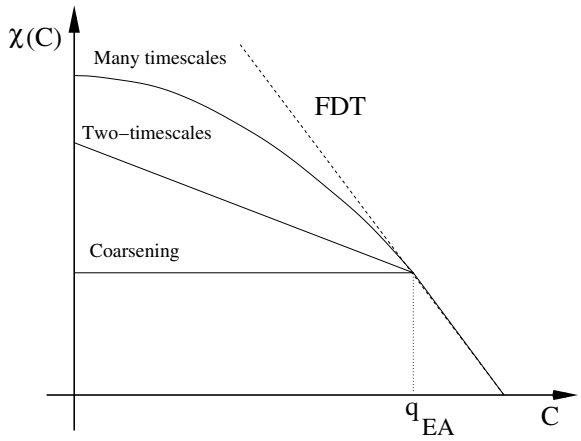

Figure 3. FD plots for the three possible scenarios. From bottom to top: (1) RS models or coarsening systems with two timescales and two temperatures (one identical to the bath, the other infinite), (2) one-step RSB models with two timescales and two temperatures (one identical to the bath, the other finite but higher than that of the bath), (3) full RSB models with many timescales and temperatures. For $C > q_{\rm EA}$ (the Edwards–Anderson parameter), i.e., the stationary regime, all models satisfy FDT (the dashed line).

FDT violations within each sector. Glassy systems are often classified into three different groups according to the dependence of $T_{\rm eff}(C)$. For coarsening systems $T_{\rm eff}(C)$ only takes two values: T and infinity for the stationary and aging regimes respectively[6]. For structural glasses $T_{\rm eff}(C)$ also takes two values: T and $T_{\rm eff}(s) > T$ for the stationary and aging regimes respectively. These are often referred to as two-timescale systems. Finally, for spin-glass systems $T_{\rm eff}(C)$ takes a continuous spectrum of values extending from a lower bound $T^* > T$ up to infinity. These are known as many-timescale systems. All these three limit cases correspond to a well-known static low-temperature description in the framework of spin-glass theory [35] in terms of replica symmetry breaking (RSB): coarsening systems are those where replica symmetry (RS) is unbroken, structural-glass systems correspond to one step of RSB while spin-glass systems correspond to full RSB. As a particular example of one-step systems there are some models (such as entropy barrier models, see section 6.5) that display glassy behaviour only at zero temperature. The stationary regime is then absent in these models and their non-equilibrium dynamics is characterized by a single effective temperature, the bath temperature being zero. Throughout this review, we will often refer to them as one-timescale models. The three possible scenarios are depicted in figure 3 (see section 4.3 for a more detailed exposition). The experimental challenge of these ideas remains one of the most awaited results.

4.2. The unbiased component ensemble and the master free-energy equation

One of the key ideas behind the existence of a quasi-fluctuation–dissipation theorem (QFDT) in aging systems is the emergence of a non-equilibrium ensemble in the asymptotic long-time regime of the relaxation process. A related non-equilibrium ensemble could also emerge in driven stationary systems. Although the nature of this ensemble is yet to be understood we

[6] We note however that in some special cases coarsening systems can display more complex behaviour of $T_{\rm eff}(C)$, see sections 6.6 and 7.3 and the discussion in section 13.1 in [3].

can anticipate some of its main properties. Some of these ideas have already been presented [36]. Here we present more elaborated work.

In a description of glassy phenomena where the system is kept in contact with a thermal bath at temperature T the energy is not constant and equipartition does not necessarily hold. Therefore this ensemble is neither microcanonical nor canonical but of a more complicated nature.

The possible existence of a non-equilibrium ensemble traces back to Palmer [37] who introduced the *unbiased component ensemble* to characterize the equilibrium sampling of phase space components. Let us consider a given partition of phase space into components (see section 3.3) and let us define the free energy $F(\mathcal{R})$ of a given component $\mathcal{R}$ by

$$F(\mathcal{R}) = -T \log \left(\sum_{\mathcal{C} \in \mathcal{R}} \exp(-\beta \mathcal{H}(\mathcal{C})) \right). \tag{75}$$

It is possible to extend this idea to the non-equilibrium regime by assuming an equal probability hypothesis: different components with identical free energy $F(\mathcal{R})$ do have the same probability,

$$\mathcal{P}(\mathcal{R}, t) = \mathbf{P}(F(\mathcal{R}), t). \tag{76}$$

In what follows, we will use the letter $\mathcal{F}$ (as opposed to $F(\mathcal{R})$) to denote component free energies defined in (75) after dropping the explicit argument $\mathcal{R}$. The existence of the unbiased ensemble is tantamount to the appearance of a new measure based on free energy rather than on energy. Contrary to Palmer [37] (who assumes an equilibrium probability distribution for $\mathbf{P}(\mathcal{F}, t)$, see (87) below) the probability distribution $\mathbf{P}(\mathcal{F}, t)$ is unknown, time dependent and must be found as a solution of a master equation (ME) as follows. To derive the free-energy ME we define the probability density

$$\mathbf{P}(\mathcal{F}, t) = \sum_{\mathcal{R}} \mathcal{P}(\mathcal{R}, t) \delta(\mathcal{F} - F(\mathcal{R})) = \mathcal{P}(\mathcal{F}, t) \Omega(\mathcal{F}, T) \tag{77}$$

where we have used (76) and the definition

$$\Omega(\mathcal{F}, T) = \sum_{\mathcal{R}} \delta(\mathcal{F} - F(\mathcal{R})) \tag{78}$$

and we have introduced explicitly the temperature dependence in Ω to stress the temperature dependence of the free energy (75). Although consistency requires adding the T dependence also to $\mathcal{F}$ here we drop this dependence in order to lighten the notation. Equation (77) describes the probability for the system to be in a component of free energy $\mathcal{F}$ at time t. We have indicated it in bold to distinguish it from the probability $\mathcal{P}(\mathcal{R}, t)$. Summing (64) over components having identical free energy $\mathcal{F}$ we get

$$\frac{\partial \mathbf{P}(\mathcal{F}, t)}{\partial t} = \sum_{\mathcal{F}'} \mathbf{P}(\mathcal{F}', t) Z_t(\mathcal{F}|\mathcal{F}') - \sum_{\mathcal{F}'} \mathbf{P}(\mathcal{F}, \mathbf{t}) Z_t(\mathcal{F}'|\mathcal{F}) \tag{79}$$

with the conditioned probabilities Z_t defined by

$$Z_t(\mathcal{F}|\mathcal{F}') = \frac{1}{\mathbf{P}(\mathcal{F}', t)} \sum_{\mathcal{R}, \mathcal{R}'} \mathcal{W}(\mathcal{R}|\mathcal{R}'; t) \delta(\mathcal{F}(\mathcal{R}) - \mathcal{F}) \delta(\mathcal{F}'(\mathcal{R}') - \mathcal{F}') P(\mathcal{R}', t) \tag{80}$$

where the $\mathcal{W}$ have already been defined in (67). Note that both $\mathcal{W}$ and Z_t are time-dependent rates. Again, as for the transition probabilities (65), the new rates $Z_t(\mathcal{F}|\mathcal{F}')$ do not satisfy detailed balance but satisfy the other requirements (non-negativeness, ergodicity and causality). Expression (80) is exact but intractable. As we are postulating the existence of the unbiased component ensemble (76), consistency in the component master equation (64) implies that

the rate $\mathcal{W}(\mathcal{R}, \mathcal{R}'; t)$ is a time-dependent function of the initial and final components, only through the value of their free energies $\mathcal{F}(\mathcal{R}')$, $\mathcal{F}(\mathcal{R})$,

$$\mathcal{W}(\mathcal{R}, \mathcal{R}'; t) = \mathcal{W}_t(\mathcal{F}(\mathcal{R}), \mathcal{F}(\mathcal{R}')). \tag{81}$$

The transition rates (80) can be further simplified,

$$Z_t(\mathcal{F}|\mathcal{F}') = \mathcal{W}_t(\mathcal{F}|\mathcal{F}')\Omega(\mathcal{F}, T). \tag{82}$$

The quantity $\Omega(\mathcal{F}, T)$ is exponentially large with the volume of the system and defines what we will denote as the configurational entropy or complexity $S_c(\mathcal{F}, T)$,[7]

$$\Omega(\mathcal{F}, T) = \exp(S_c(\mathcal{F}, T)). \tag{83}$$

Therefore, all the information on the master equation (79) goes into the density of components $S_c(F, T)$ and the rates $\mathcal{W}_t(\mathcal{F}|\mathcal{F}')$. These contain all the information about the properties of the unbiased ensemble.

The description of glassy dynamics in terms of a master free-energy equation such as (79) has been wandering around for many years in the literature of the field. Several equations have appeared scattered in the literature during the last decades, but generally written in terms of the energy instead of the free energy, see for instance [38]. These equations describe what are usually known as trap models (see section 6.4). Example master equations are proposed by Dyre [39] and Bouchaud [40]. Other attempts include granular media [41].

4.2.1. Complexity and the effective temperature. Before closing the present discussion let us note that, in equilibrium, both the transition rates $Z_t(\mathcal{F}|\mathcal{F}')$ and $\mathcal{W}_t(\mathcal{F}|\mathcal{F}')$ are time independent and satisfy detailed balance,

$$\frac{Z^{\mathrm{eq}}(\mathcal{F}'|\mathcal{F})}{Z^{\mathrm{eq}}(\mathcal{F}|\mathcal{F}')} = \exp(-\beta(\Phi(\mathcal{F}', T) - \Phi(\mathcal{F}, T))) \tag{84}$$

$$\frac{\mathcal{W}^{\mathrm{eq}}(\mathcal{F}'|\mathcal{F})}{\mathcal{W}^{\mathrm{eq}}(\mathcal{F}|\mathcal{F}')} = \exp(-\beta(\mathcal{F}' - \mathcal{F})) \tag{85}$$

with

$$\Phi(\mathcal{F}, T) = \mathcal{F} - TS_c(\mathcal{F}, T) \tag{86}$$

where $\Phi(\mathcal{F}, T)$ is a new potential where the free energy appears balanced by the complexity. The probability (77) assumes the simple form,

$$\mathbf{P}^{\mathrm{eq}}(\mathcal{F}) = \frac{\exp(-\beta\Phi(\mathcal{F}, T))}{\mathcal{Z}(\beta)} \tag{87}$$

where $\mathcal{Z}(\beta)$ is given by (14). We will describe in section 5.1.2 how this relation provides us with a tool to obtain the configurational entropy as function of both the free energy and the temperature.

The hints on the existence of this new potential were found by Kirkpatrick, Thirumalai and Wolyness [42–44] who identified the marginal transition T_{A} ('A' standing for activated) as the temperature below which different metastable states concur in such a number to compensate the lower equilibrium free energy of the paramagnetic or liquid state. The subindex in T_{A} stands for

[7] The term configurational entropy has often been used with different meanings, leading to confusion. Originally, as used by Adam and Gibbs for their thermodynamic theory, it denotes the part of the total entropy including only the configurational degrees of freedom. More recently, in the context of spin-glass theory, this concept has been coined to denote that part of the configurational entropy that counts the number of metastable states rather than configurations. It is with this last meaning that we understand it here. For a thorough discussion of this concept see section 5.1.

the fact that below that temperature activation is dominant and relaxation occurs in the form of activated jumps from one metastable state to another. T_A is identified with the mode-coupling transition temperature T_c of mode-coupling theories (see section 6.1) and corresponds to a spinodal instability [42–44]. The mathematical argument behind the compensation of the free energy of metastable states by the complexity is as follows. Let us decompose the canonical partition function of the system as a sum over a set of non-overlapping components $\mathcal{R}$ (as explained in section 3.3),

$$\begin{aligned} \mathcal{Z}(T) &= \sum_{\mathcal{C}} \exp(-\beta \mathcal{H}(\mathcal{C})) = \sum_{\mathcal{R}} \exp(-\beta \mathcal{F}(\mathcal{R})) \\ &= \sum_{\mathcal{F}} \Omega(\mathcal{F}, T) \exp(-\beta \mathcal{F}) = \sum_{\mathcal{F}} \exp(-\beta \Phi(\mathcal{F}, T)) \end{aligned} \tag{88}$$

where we have used definition (75) for the free energy of components $\mathcal{F}(\mathcal{R})$ and (83), (86). Due to the extensive character of the variables $\mathcal{F}$, $S_c(\mathcal{F}, T)$ and $\Phi(\mathcal{F}, T)$, the dominant contribution to the sum in (88) is evaluated through the saddle point method. At each temperature T there is a free energy $F^*(T)$ such that its contribution to the exponent (88) is dominant, i.e. $\mathcal{Z}(T) \sim \exp(-\beta \Phi^*(T))$ where we have defined $\Phi^*(T) = \Phi(F^*(T), T)$. The behaviour of this solution depends on the shape of the function $S_c(\mathcal{F}, T)$. In general, this function is a monotonically increasing function of the free energy $\mathcal{F}$. Because the exponential is a positive definite function we have $\Phi(F, T) \geqslant F_{\text{para}}(T)$ where $\mathcal{Z}(T) = \exp(-\beta F_{\text{para}}(T))$ and $F_{\text{para}}(T)$ denotes the paramagnetic free energy.

Above T_A there is no solution $F^*(T)$ which can compensate the equilibrium paramagnetic free energy and $\Phi(F, T) > F_{\text{para}}(T)$. Below T_A a solution appears $F^*(T)$ such that $\Phi^*(T) = F_{\text{para}}(T)$ and gives the dominant contribution to (88) so $F^*(T)$ satisfies the saddle point relation,

$$\frac{1}{T} = \left. \frac{\partial S_c(\mathcal{F}, T)}{\partial \mathcal{F}} \right|_{\mathcal{F}=F^*(T)}. \tag{89}$$

The identity $\Phi^*(T) = F_{\text{para}}(T)$ implies $F_{\text{para}}(T) = F^*(T) - T S_c(F^*(T), T)$. This means that for $T \leqslant T_c$ there is a band of components with free energy $F^*(T) \geqslant F_{\text{para}}(T)$ (therefore with free energy above the equilibrium one) whose difference with $F_{\text{para}}(T)$ is compensated by the complexity $S^*(T) = S_c(F^*(T), T)$. This solution exists as long as $S^*(T) > 0$. Because $S_c(F, T)$ is a monotonically increasing function of F and both $F^*(T)$, $S^*(T)$ decrease with T there is a temperature T_K at which $S^*(T_K) = 0$. Below this temperature, the complexity vanishes and the solution $F^*(T)$ ceases to change with temperature (so equation (89) does not hold anymore) but sticks to its minimum value $F^*(T_K)$. This is the entropy crisis scenario where T_K corresponds to the Kauzmann temperature [45].

In mean-field models it has been shown [46] that the complexity $S_c(F, T)$ defines a free-energy dependent effective temperature through the relation,

$$\frac{1}{T_{\text{eff}}(\mathcal{F})} = \frac{\partial S_c(\mathcal{F}, T)}{\partial \mathcal{F}}. \tag{90}$$

From this relation, it emerges that the configurational entropy plays the role of the thermodynamic potential associated with the effective temperature. Similarly, the entropy is the potential conjugated to bath temperature in the microcanonical ensemble. However, (90) has only been derived in mean-field models close to the asymptotic free-energy threshold where lower free-energy states are inaccessible [46, 47]. In models that do not have a marginal free-energy threshold above the equilibrium value, it is possible to show that free energies are uncorrelated random variables exponentially distributed [48, 35]. The extension of these results beyond mean-field where all free-energy states are accessible through activated

processes is at the roots of the existence of the unbiased component ensemble. Some attempts have been proposed in [49–51]. In particular, it would be very interesting to understand the general form of the transition probabilities Z_t as these lead to very specific predictions amenable to numerical checks. The exponential character of the free-energy distribution of the lower free-energy states below the threshold, and the fact that this distribution is time dependent (as shown by the fact that Z_t is itself time dependent) appear as the two crucial ingredients to understand the emergence of effective temperatures in glassy systems. These features are present in many models of glasses such as mean-field spin-glass models, trap models (see section 6.4) or entropy barrier models (see section 6.5.1).

4.3. The integrated response function (IRF) and fluctuation–dissipation (FD) plots

When a system is in a non-equilibrium state its response to an external perturbation cannot be described, in general, by FDT relations such as (60) since this has been derived assuming that the system is in a stationary state. However, the glassy state is a particular non-equilibrium state characterized by extremely slow relaxation processes. Hence, while the system is not in a real equilibrium state, it may be thought of as being in a sort of quasi-equilibrium regime over timescales much longer than the microscopic timescales but still smaller than the typical relaxation timescales of the slow processes. In this quasi-equilibrium regime, the evolution of the system is quasi-stationary since non-stationary effects are seen only for times of the order of the timescales of the slow processes. In this situation, we may think that relations similar to (60) can still be valid, even if TTI cannot be assumed anymore. Thus a possible generalization of FDT to the glassy regime requires us to introduce the following nondimensional quantity,

$$X_{A,B}(t,s) = \frac{T R_{A,B}(t,s)}{\frac{\partial}{\partial s} C_{A,B}(t,s)} \qquad t > s \tag{91}$$

where $X_{A,B}(t,s)$ is called the fluctuation–dissipation ratio (FDR). In equilibrium $X_{A,B}(t,s) = 1$ whatever times t, s and observables A, B are used (cf (60)). Thus X is a measure of the violation of the true equilibrium in the quasi-equilibrium glassy state. The validity of (91), i.e. the proportionality between the response and the time derivative of the correlation function, can only be checked *a posteriori* since it is based on the quasi-equilibrium hypothesis that up to now it has been proved only in mean-field models. Eliminating one time in favour of the correlation function, the time dependence of $X_{A,B}(t,s)$ can be recast in the form

$$X_{A,B}(t,s) \equiv X_{A,B}[C_{A,B}(t,s), s]. \tag{92}$$

The FDR was first studied in spin glasses where analytical results have shown that glassy systems in general satisfy the weak ergodicity breaking scenario [40], discussed in section 6.2. For the present purpose, it is enough to note that calculations in mean-field spin-glass models [52, 53] have shown that in the limit $s \to \infty$ the FDR is a non-trivial function which depends on the relation between the times t and s only through the correlation function $C_{A,B}(t,s)$. The following specific form of FDT violations has been proposed to be generically valid in the non-equilibrium regime of glassy systems,

$$\lim_{s\to\infty} X_{A,B}(t,s) = X_{A,B}[C_{A,B}(t,s)]. \tag{93}$$

Using (93) and (91) we obtain the differential form of the quasi-FDT (QFDT) relation [32],

$$X_{A,B}(C) = \left[\frac{T R_{A,B}(t,s)}{\frac{\partial}{\partial s} C_{A,B}(t,s)}\right]_{C_{A,B}(t,s)=C} \qquad t > s \tag{94}$$

which describes the response of the system in the (quasi)-equilibrium state to a impulsive perturbation at time $s < t$. Experiments and numerical simulations usually measure integrated

response functions[8] (IRF), i.e., the response at time t to a perturbation switched on or off at time $s < t$. According to definition (43) the variation of the observable $\langle A(t)\rangle_\epsilon$ to linear order in the perturbation intensity ϵ is given by

$$\langle A(t)\rangle_{\epsilon_s} = \langle A(t)\rangle_0 + \epsilon R_{A,B}(t,s) + \mathcal{O}(\epsilon^2) \qquad t > s. \tag{95}$$

Assuming that the perturbation acts for all times $t > s$ and that its intensity is small enough for the accumulated response to be linear in ϵ we get

$$\begin{aligned}\langle A(t)\rangle_{\epsilon_s} &= \langle A(t)\rangle_0 + \sum_{t'=s}^{t} \epsilon_{t'} R_{A,B}(t,t') \\ &= \langle A(t)\rangle_0 + \int_s^t \mathrm{d}t' \epsilon(t') R_{A,B}(t,t')\end{aligned} \tag{96}$$

where $\epsilon_{t'}$ (or $\epsilon(t')$) is the perturbation at time t'. In the particular case of $\epsilon(t') = \epsilon\theta(t'-s)$, i.e., of a constant perturbation, one gets

$$\chi_{A,B}(t,s) = \lim_{\epsilon\to 0} \frac{\langle A(t)\rangle_{\epsilon_s} - \langle A(t)\rangle_0}{\epsilon} = \int_s^t \mathrm{d}t' R_{A,B}(t,t'). \tag{97}$$

which is also called zero field cooled (ZFC) susceptibility. The name zero field cooled follows from the experimental protocol used in spin-glass measurements to distinguish it from the thermoremanent magnetization (TRM). To measure the TRM susceptibility, a constant external perturbation is applied to the system at time $t = 0$ and removed at time $s > 0$ and the subsequent decay of $\langle A(t)\rangle$ is recorded. The TRM susceptibility is given by

$$\chi^{\mathrm{TRM}}_{A,B}(t,s) = \lim_{\epsilon\to 0} \frac{\langle A(t)\rangle_{\epsilon_s} - \langle A(t)\rangle_0}{\epsilon} = \int_0^s \mathrm{d}t' R_{A,B}(t,t'). \tag{98}$$

In the large t, s limit the ZFC (97) and TRM (98) susceptibilities are equivalent since they are related by

$$\chi_{A,B}(t,s) + \chi^{\mathrm{TRM}}_{A,B}(t,s) = \chi_{A,B}(t,0) \tag{99}$$

and $\chi_{A,B}(t\to\infty,0) = \chi^{\mathrm{eq}}_{A,B}$.

Inserting the QFDT relation (94) in (97) we obtain the formula

$$\chi_{A,B}(t,s) = \frac{1}{T}\int_{C_{A,B}(t,s)}^{C_{A,B}(t,t)} \mathrm{d}C' X_{A,B}(C') \tag{100}$$

which relates $\chi_{A,B}(t,s)$ to the FDR $X_{A,B}$ and provides a simple way to calculate $X_{A,B}$ from measurements of $C_{A,B}(t,s)$ and $\chi_{A,B}(t,s)$ in the time sector $t > s$. Suppose indeed we fix the lowest time s and plot $\chi_{A,B}(t,s)$ as function of $C_{A,B}(t,s)$ for different values of t, then the value of the FDR can be obtained from the slope of the resulting curve. In many of the examples considered in this review the equal times correlation function is time independent, for instance $C_{A,B}(t,t) = 1$. In this case, the slope can be simply obtained by derivation of $\chi_{A,B}(t,s)$ with respect to $C_{A,B}(t,s)$ for fixed s which from (100) yields

$$X_{A,B}(C) = -\beta \left.\frac{\partial\chi_{A,B}(t,s)}{\partial C_{A,B}(t,s)}\right|_{C_{A,B}(t,t)=\mathrm{const},s\ \mathrm{fixed}}. \tag{101}$$

Typical FD plots are shown in figure 3 for the three possible scenarios (see section 4.1). In the general case in which $C_{A,B}(t,t)$ is time dependent one needs to be more careful in computing

[8] The integrated response functions are also called time-dependent or non-equilibrium susceptibilities.

the FDR. Sollich and co-workers have proposed [54, 55] to construct FD plots χ versus C with t kept constant and varying the lowest time s. From (91) we have

$$X_{A,B}(C) = -\beta \left.\frac{\partial \chi_{A,B}(t,s)}{\partial C_{A,B}(t,s)}\right|_{t \text{ fixed}}. \tag{102}$$

If $C(t,t)$ changes with time it is convenient to normalize correlations and the IRF by the equal times correlation $C_{A,B}(t,t)$:

$$\widetilde{C}_{A,B}(t,s) = \frac{C_{A,B}(t,s)}{C_{A,B}(t,t)} \qquad \widetilde{\chi}_{A,B}(t,s) = \frac{\chi_{A,B}(t,s)}{C_{A,B}(t,t)}. \tag{103}$$

With these definitions,

$$X_{A,B}(C) = -\beta \left.\frac{\partial \widetilde{\chi}_{A,B}(t,s)}{\partial \widetilde{C}_{A,B}(t,s)}\right|_{t \text{ fixed}}. \tag{104}$$

The importance of normalizing the raw FD plots (102) is well appreciated in trap models discussed in section 6.4 or in kinetically constrained models discussed in section 7.5. In this last case, for example, raw FD plots can lead to awkward representations such as those shown in figure 36.

4.4. The concept of neutral observables

If the FDR (91), (94) has the physical interpretation of a temperature (as has been suggested, see the discussion in section 5.2) then one would expect the FDR to be independent of the observables A, B used to construct correlations and responses. In fact, this is true in equilibrium where $X_{A,B} = 1$ whatever A, B. However, although $X_{A,B} \neq 1$ observable independence is not at all required in the glassy regime. In this section, we present a brief digression on which conditions the observables A, B must satisfy for the FDR to be observable independent. This issue is yet unresolved, so the present discussion is quite speculative.

Albeit restricted, for simplicity we will consider here the case of a glassy system with only two timescales where $A = B$ (so we will denote $X_{A,A}$ simply by X_A) in the time sector where $(t-s)/s \sim \mathcal{O}(1)$ or $X_A \neq 1$. In equilibrium, one could argue that the equality $X_A = 1$ is related to the fact that the entropy $S(E, A)$, as defined in the microcanonical ensemble section 2.1, is maximum (12) for A equal to its equilibrium value. This property is observable independent as well as it is the identity $X_A = 1$. A similar argument, but extended to the glassy regime, would require us to define the configurational entropy $S_c(\mathcal{F}, \mathcal{A})$ (i.e. the equivalent generalization (2) of (83)) where $\mathcal{F}, \mathcal{A}$ denote the component averaged values of the free energy (75) and the corresponding restricted Gibbs average for the observable A. We could then say that A is a neutral observable if its dynamically averaged value at all times $\langle A(t)\rangle$ coincides with the stationary maximum of the function $S_c(\mathcal{F}, \mathcal{A})$ as $\mathcal{A}$ is varied. Of course, if this were not true the value of X_A would then depend on the value of A in the same way that the value of the temperature $1/T = \beta$ in the microcanonical ensemble, and for a given value of the energy E, would depend on the value of the observable A if μ in (83) were not zero.

For instance, the magnetization in mean-field spin-glass models is known to be a neutral observable and nearly all computations of the FDR have used this observable (see section 6.2). In fact, in the framework of the TAP approach it can be shown that the configurational entropy evaluated as a function of the free energy and magnetization of the TAP states is maximum at zero magnetization. Indeed, the fact that the magnetization is not a good order parameter in these models (it vanishes in both the paramagnetic and the spin-glass phase) is related to its neutral character. Not by chance do the majority of numerical studies in glassy systems use the magnetization as the central observable to investigate and measure FDT violations.

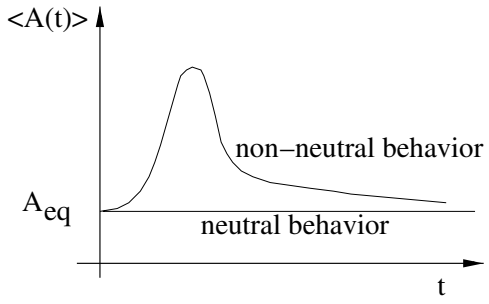

Figure 4. Illustration of the neutrality property of observables. The value of a neutral observable remains fixed at its initial (equilibrium) value despite the fact that the initial state is non-equilibrium.

A non-neutral observable A would correspond to a situation where, starting at time zero from a non-equilibrium initial state where the value of A is taken to coincide with its equilibrium value (this is not a contradiction, since A could coincide with its equilibrium value but not the value of any other observable) the subsequent evolution of A deviates from its initial equilibrium value. In this case A is not neutral because its time evolution is correlated with that of the other observables. In contrast, if A were a neutral observable, then it would stick to the value A forever (as happens for the magnetization in mean-field spin-glass models). Figure 4 illustrates this behaviour. The definition of neutrality can be easily adapted in trap models by assuming that observable values of traps are uncorrelated with their energies [54] (see also section 6.4).

4.5. Numerical approach to component dynamics: Stillinger–Weber decomposition

The increase of computational power and the recent developments in the theory of disordered systems has pushed forward an approach to the glass transition based on the analysis of a reduced dynamics in the component space. The underlying ideas date back more than 30 years ago to a seminal, but talkative, paper of Goldstein [56]. The glass transition is of purely dynamical origin and hence must reflect the properties of the dynamical evolution of the system. Goldstein suggested that the dynamics of a supercooled liquid can be understood in terms of a diffusive process between different *basins* of the potential energy surface. At low temperature the dynamics slows down since the system gets trapped for a long time in a basin. This approach, which focuses on the topological properties of the energy surface, is rather appealing since it naturally leads to a convenient framework for understanding the complex phenomenology of glassy systems.

The implementation of these (qualitative) ideas came some years later by Stillinger and Weber (SW) [57–59] who formalized the concept of basin in configuration space, identifying it with a component in the component space, and proposed a procedure for identifying them: the set of all configurations connected to the same local energy minimum by a steepest descent path on the energy surface uniquely defines the basins of the minimum. Stillinger and Weber (SW) called the local minimum *inherent structure* (IS) to stress its intrinsic nature. Since the identification of ISs is unique, the mapping from configurations to local minima gives a *unique well-defined* decomposition of the phase space into a *disjoint* set of basins. The SW decomposition defines a mapping of the phase space to the component space in which each basin, usually labelled by the energy $E_{\rm IS}$ of the local minimum, is a component.

This decomposition does not cover completely the configuration space since it leaves out the boundaries between different basins. However, under the assumption that those configurations do not contribute to the thermodynamics of the system, e.g., the boundaries between basins are subextensive, it does cover *almost all* the phase space and the partition function can be written as a sum of contributions from different components:

$$\mathcal{Z}(T) \simeq \sum_{E_{\rm IS}} \mathcal{Z}_{\rm IS}(E_{\rm IS}, T). \tag{105}$$

Let $\Omega(E)$ denote the number of IS with energy $E_{\rm IS} = E$, then collecting all components with the same value of $E_{\rm IS}$

$$\begin{aligned}\mathcal{Z}(T) &\simeq \sum_{E} \Omega(E) \sum_{E_{\rm IS}=E} \mathcal{Z}_{\rm IS}(T)/\Omega(E) \\ &= \sum_{E} \exp[S_c(E) - \beta F_b(T, E)].\end{aligned} \tag{106}$$

The term

$$S_c(E) = \log \Omega(E) \tag{107}$$

which accounts from the entropic contribution arising from the number of different basins with the same IS energy, is called the SW *configurational entropy* of *complexity*. This quantity is strongly related to the partitioning, so we add the adjective SW to distinguish it from other definitions of configurational entropy taken from mean-field concepts.

The second term $F_b(T, E)$ is defined as

$$F_b(T, E) = -T \log \left[\frac{1}{\Omega(E)} \sum_{E_{\rm IS}=E} \mathcal{Z}_{\rm IS}(T) \right]. \tag{108}$$

In general, this quantity differs from the average free energy of components with $E_{\rm IS} = E$, however if all these components have similar statistical properties, then $F_b(T, E)$ is the free energy of the system when constrained to any one of the components with $E_{\rm IS} = E$. In the thermodynamic limit, the system populates components with energy $E_{\rm IS} = E_{\rm IS}(T)$ fixed by the condition

$$-\beta F(E) = S_c(E) - \beta F_b(T, E) = \text{maximum over } E \tag{109}$$

and the free energy of the system can be calculated using

$$F(T) = F_b[T, E_{\rm IS}(T)] - T S_c[E_{\rm IS}(T)]. \tag{110}$$

The condition (109) is equivalent to that of $F(T)$ being minimal, i.e.,

$$\frac{\partial F}{\partial E} = \frac{\partial F_b(T, E)}{\partial E} - T \frac{\partial S_c(E)}{\partial E} = 0. \tag{111}$$

Note that the minimum condition follows from the balance between the contribution from the change with the energy of the shape of the basins $(\partial F_b(T, E)/\partial E)$ and its corresponding number $(\partial S_c(E)/\partial E)$. Often the free energy is written as

$$F_b(T, E_{\rm IS}) = E_{\rm IS} + F_v(T, E_{\rm IS}). \tag{112}$$

The first term in (112) takes into account the average energy of IS visited in equilibrium at temperature T, as can be seen from (110): $U(T) = \partial(\beta F_b)/\partial\beta = E_{\rm IS}(T) + \partial(\beta F_v)/\partial\beta$. It can be shown [60, 61] that if the density of states $\Omega(E)$ is Gaussian and the basins have approximately the same shape then $E_{\rm IS} \propto 1/T$. The second term in (112) describes the volume of the corresponding components and is called the 'vibrational' contribution.

To understand the success and limitation of the IS approach we have to analyse the idea behind the SW approach. It is clear that even if the phase space can always be partitioned, not all possible partitions will lead to a physically relevant dynamics in the component space. This is a well-known problem in the theory of dynamical systems, where the component dynamics is called *symbolic dynamics*, see e.g. [22]. To prove that the SW is a physically good partition for a given system is a problem of the same hardness as proving ergodicity. One then adopts a constructive point of view, along the same lines as equilibrium statistical theory: based on some reasonable hypothesis one first assumes that the SW partition is a good partition and then checks if this reproduces the desired features of the dynamics.

The physical motivation behind the SW proposal follows from the observation that the potential energy surface of a supercooled liquid contains a large number of local minima and that the time evolution can be separated into two different processes: thermal relaxation into basins (*intra-basin* motion) and thermally activated potential energy barrier crossing between different basins (*inter-basin* motion). This scenario has been recently confirmed from numerical analysis [60–64]. The timescale separation of the two processes strongly depends on temperature. When the temperature is lowered down to the order of the critical mode-coupling theory (MCT) temperature T_c the typical barrier height is of the order of the thermal energy $k_B T_c$, and the slow inter-basin motion dominates the relaxation dynamics. If the temperature is further reduced the relaxation time eventually becomes of the same order as the physical observation time and the system falls to a non-equilibrium state since there is not enough time to cross barriers and equilibrate. With this picture in mind, it is natural to view the IS partitioning as the natural elements to describe the slow glassy dynamics. This approach is rather appealing since it naturally leads to universality: all glassy systems with similar IS dynamics must have similar glassy behaviour. Recent IS analysis performed on disordered spin systems displaying a transition of fragile glass type does support this conclusion [36, 65–68]. It should be noted [69] that the definition of IS for spin systems is more subtle than for systems with continuous variables. Indeed usually for spin systems IS are defined as one-spin flip stable states, however these may not be stable for two-spin or higher number of spin flips. One possibility of making IS well defined also for spin systems is to define them directly from the $T = 0$ limit of the dynamics, i.e., as states which are stable under the $T = 0$ dynamics [70]. This is the definition used in this review when discussing IS for spin systems.

5. Thermodynamic description of the aging state

We saw in section 4.2 how the self-generated dynamical measure allows a description of the aging dynamics in terms of a probabilistic master equation with transition rates characterized by an extensive quantity that was defined as a configurational entropy or complexity (83). This quantity has received considerable attention in studies of spin glasses since the seminal paper of Thouless, Anderson and Palmer (TAP) [71] on the SK model where a way to compute the configurational entropy was proposed [72]. Later studies in the context of structural glasses [42–44] have shown its importance as the mechanism for an entropy crisis of the supercooled liquid as proposed by Kauzmann many years ago [45].

5.1. Methods to compute the complexity

In this section, we present a schematic overview of some of the analytical and numerical methods that have appeared in the literature to compute the configurational entropy. In the absence of a full solution of the dynamics in many systems, and under the assumption that there is a connection between the effective temperature and the configurational entropy (see the

discussion in section 4.2.1), the calculation of the latter, by using equilibrium methods taken from statistical physics, appears as an alternative way of quantifying FDT violations. In mean-field theories metastable states give a natural partition of the phase space since their lifetime diverges in the thermodynamic limit. For systems with short-range interactions, however, metastable states can be defined unambiguously only referring to some reference timescale. Therefore the identification of metastable states for real systems can be a very hard task. In section 4.5 we have presented a partition scheme, proposed by Stillinger and Weber, which in principle can be applied to any system. The scheme essentially uses a zero-temperature dynamics and thus it is free from the ambiguities due to the finite metastable lifetime. The results described in the next sections must be seen as instructive attempts to evaluate a quantity (the complexity) that governs the slow dynamics of relaxational glassy systems. The extension of these equilibrium concepts to other non-equilibrium systems beyond aging systems (e.g. driven systems) remains an open problem.

5.1.1. Analytical methods. Bray and Moore [72] calculated $S_c(\mathcal{F}, T)$ for the Sherrington–Kirkpatrick model within the TAP approach. The TAP equations give the local magnetization m_i in a system confined to a metastable state, which for mean-field models have infinite lifetime. As a consequence, the number of metastable states (i.e. components) can be readily obtained just by counting the number $\mathcal{N}_s(\mathcal{F}, T)$ of solutions of the TAP equations at temperature T with a free energy $\mathcal{F}$,

$$\mathcal{N}_s(\mathcal{F}, T) = \int_{-1}^{1} \prod_{i=1}^{N} \mathrm{d}m_i |\det H(\{m_i\})| \delta(\mathcal{F} - \mathcal{F}(\{m_i\}, T)) \delta(g_i(\{m_i\})) \quad (113)$$

where $\mathcal{F}(\{m_i\}, T)$ is the TAP free energy at temperature T as a function of the local magnetizations m_i, $g_i(\{m_i\}) = \partial\mathcal{F}(\{m_i\}, T)/\partial m_i = 0$ are the TAP equations and $H_{ij} = \partial g_i(\{m_i\})/\partial m_j$ the Hessian. This type of calculation has been done for other mean-field models, such as p-spin [73] and random orthogonal model (ROM) [74, 75], finding in all cases that $\mathcal{N}_s(\mathcal{F}, T)$ increases exponentially fast with the system size N. This remains true if the number of free-energy minima $\mathcal{N}_m(\mathcal{F}, T)$, instead of the number of stationary points $\mathcal{N}_s(\mathcal{F}, T)$, is considered [76]. Although these types of calculations can be done only in exactly solvable mean-field models the exponential growth with the system size of the number of free-energy local minima or stationary points is generally applicable to any system (mean-field or not) displaying glassy behaviour. Knowledge of the number of minima allows us to define the complexity (78) as

$$S_c(\mathcal{F}, T) = \log \mathcal{N}_m(\mathcal{F}, T) \quad (114)$$

and hence the thermodynamic potential $\Phi(\mathcal{F}, T) = \mathcal{F} - T S_c(\mathcal{F}, T)$ as described in section 4.2.

A general framework to evaluate the complexity has been devised by Monasson [77]. The starting point in his procedure is to consider m interacting copies or replicas of the original system, with an attractive interaction term of the form $\epsilon \sum_{a,b=1}^{m} Q(\mathcal{C}_a, \mathcal{C}_b)$ where $Q(\mathcal{C}_a, \mathcal{C}_b)$ is a suitable overlap function which takes its maximum value only if $\mathcal{C}_a = \mathcal{C}_b$. The free energy of the replicated system is then

$$\mathrm{e}^{-\beta F(T,m)} = \sum_{\mathcal{C}_1,\ldots,\mathcal{C}_m} \exp\left[-\beta \sum_{a=1}^{m} \mathcal{H}(\mathcal{C}_a) + \beta\epsilon \sum_{a,b=1}^{m} Q(\mathcal{C}_a, \mathcal{C}_b) \right]. \quad (115)$$

If the thermodynamic limit is taken before the limit $\epsilon \to 0^+$ then the configurations $\mathcal{C}_a, \mathcal{C}_b$ tend to lie as close as possible since maximization of the coupling term minimizes the global free

energy $F^{(m)}(T)$ and hence, given a phase space partition, the replicas tend to 'condense' into the same component. Thus collecting all components with the same free energy the partition function $\mathcal{Z}(T, m)$ can be decomposed as

$$\begin{aligned}\mathcal{Z}(T, m) &= \sum_{\mathcal{F}} \Omega(\mathcal{F}, T) \exp(-m\beta\mathcal{F}) \\ &= \sum_{\mathcal{F}} \exp[-\beta\Phi(\mathcal{F}, T, m)] \end{aligned} \tag{116}$$

where $\Phi(\mathcal{F}, T, m) = m\mathcal{F} - TS_c(\mathcal{F}, T)$ is basically the potential $\Phi(\mathcal{F}, T)$ discussed in section 4.2 with the term $\mathcal{F}$ multiplied by m (the order of limits, first volume $\to \infty$ and then $\epsilon \to 0^+$, enforces the m replicas to occupy the same component $\mathcal{R}$). In the limit $m \to 1$ we recover the potential $\Phi(\mathcal{F}, T)$: $\Phi(\mathcal{F}, T, m = 1) = \Phi(\mathcal{F}, T)$. Knowledge of $\Phi(\mathcal{F}, T, m)$ allows us to compute the configurational entropy. In the thermodynamic limit the sum in (116) is dominated by the free energy $F^*(T, m)$ that satisfies the relation

$$\frac{m}{T} = \left.\frac{\partial S_c(\mathcal{F}, T)}{\partial \mathcal{F}}\right|_{\mathcal{F}=F^*(T,m)}. \tag{117}$$

Inserting the solution $F^*(T, m)$ into $\Phi(\mathcal{F}, T, m)$ we obtain the free-energy potential $\Phi^*(T, m) = \Phi(F^*(T, m), T, m)$. If m (originally an integer value) is continued to real values then it can be shown that the following relations are satisfied:

$$\frac{\partial}{\partial m}\Phi^*(T, m) = F^*(T, m) \qquad \frac{\partial}{\partial m}\left[\frac{\Phi^*(T, m)}{m}\right] = \frac{T}{m^2}S_c(F^*, T). \tag{118}$$

Varying m allows us to compute the configurational entropy $S_c(\mathcal{F}, T)$ as a function of the two variables $\mathcal{F}$ and T. The potential $\Phi(\mathcal{F}, T, m)$ can be explicitly evaluated with the sole knowledge of the microscopic Hamiltonian of the system and using the replica method. Although this procedure was initially applied only to mean-field disordered systems [77, 78], more recently it has been extended to more realistic interacting potentials such as Lennard-Jones liquids [79, 80] and binary mixtures [81, 82].

This method of computing the configurational entropy can be easily implemented in the framework of the standard replica method for mean-field disordered systems. This has been worked in some detail in [83, 84]. The starting point is free energy at the one-step level of replica symmetry breaking $F(q_0, q_1, m)$, where q_0, q_1 and m are the parameters that describe the Parisi matrix [35] in the one-step replica symmetry breaking scheme. By expanding the free energy around $m = 1$ one gets, $F(q_0, q_1, m) = F_{\rm RS}(q_0) + F^{(1)}(q_0, q_1)(m - 1) + \mathcal{O}((m - 1)^2)$ where q_0 stands for the overlap among replicas belonging to different subboxes and $F_{\rm RS}(q_0)$ is the free energy in the replica symmetric approximation, i.e., in the limit $m \to 1$. Extremization of $F_{\rm RS}(q_0)$ yields $q_0(\beta)$ which inserted into $F(q_0, q_1, m)$ allows us to find $F_{\rm RS}(\beta)$, $F^{(1)}(\beta, q_1)$. Knowledge of these functions fully determines the configurational entropy of the system for temperature $T_{\rm RSB} < T < T_{\rm c}$ (where $T_{\rm c}$ corresponds to the MCT, see section 6.1). Indeed the dynamical transition $T_{\rm c}$ is found solving the equations $(\partial/\partial q_1)F^{(1)}(\beta, q_1) = \left(\partial^2/\partial q_1^2\right)F^{(1)}(\beta, q_1) = 0$ while the static transition $T_{\rm RSB}$, where the configurational entropy vanishes, follows from the solution of $F^{(1)}(\beta, q_1) = (\partial/\partial q_1)F^{(1)}(\beta, q_1) = 0$. Finally, the complexity in the region $T_{\rm RSB} < T < T_{\rm c}$ is given by the value of $F^{(1)}(\beta, q_1)$ evaluated for $q_1(\beta)$ solution of the equation $(\partial/\partial q_1)F^{(1)}(\beta, q_1) = 0$. This approach gives a detailed description of the metastable properties in the range $T_{\rm RSB} < T < T_{\rm c}$. Below $T_{\rm RSB}$ more sophisticated methods are needed to describe the metastable behaviour.

The potential method has been proposed by Franz and Parisi [85] in the framework of the replica approach. The starting point in this procedure is to write down the partition function of a generic system at temperature T whose configurations $\mathcal{C}$ are constrained to have an overlap

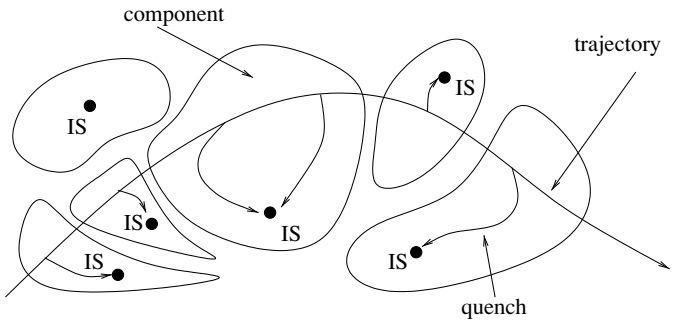

Figure 5. Stillinger and Weber decomposition.

$Q(\mathcal{C}, \mathcal{C}_0)$ with a reference configuration $\mathcal{C}_0$. The free energy of the constrained system is then averaged, using the replica method, over the reference configuration $\mathcal{C}_0$ thermalized at a temperature T' in general different from T. This yields the potential $V(Q, T, T')$. For $T = T'$, and in a given range of temperatures, the potential V, as a function of Q, has two local minima. The difference of the potential at these two values yields the configurational entropy at that temperature. The method has been applied to evaluate the configurational entropy in the hypernetted chain approximation usually employed for liquids [86, 87].

5.1.2. Numerical methods. Among numerical approaches, Speedy [88] has proposed a method that consists in estimating what he defines as the *statistical entropy* (basically identical to the intrastate entropy in the inherent structure approach discussed in section 4.5) and comparing it to the thermal or total entropy obtained from integration of the specific heat. The difference between the thermal entropy and the statistical entropy is the complexity. To compute the statistical entropy, the method considers different reference configurations representative of an amorphous glass state and introduces a coupling term between a reference configuration and the system that forces it to stay within a given distance of that reference configuration. By progressively slowly changing the intensity of the coupling the energy of the system can be evaluated for each value of the coupling. The entropy associated with a particular reference state is then estimated by integrating the energy as a function of the intensity of the coupling. Speedy has applied this approach [88–90] to hard-sphere systems where the centre of the hard spheres is tethered to a spherical region with a variable diameter that regulates the intensity of the coupling.

Probably up to now the most powerful method to compute numerically the configuration entropy is that based on the IS formalism. Moreover, due to its relatively simple implementation, the IS formalism has become an important tool in the numerical analysis of models. For this reason we shall give a more detailed presentation. The calculation of IS, summarized in figure 5, follows directly from the definition. First the system is equilibrated at a given temperature T, then starting from an equilibrium configuration the system is instantaneously quenched down to $T = 0$ by decreasing the energy along the steepest descent path. The procedure is repeated several times starting from uncorrelated equilibrium configurations. In this way the ISs are identified and their probability distribution can be computed. In equilibrium at temperature T the system explores the IS of energy $E_{\mathrm{IS}} = E$ with probability (see (106), (112))

$$\mathcal{P}(E, T) = \exp[S_c(E) - \beta E - \beta F_v(T, E) + \beta F(T)] \tag{119}$$

where $F(T)$ is the equilibrium free energy. Then the SW configurational entropy can be computed just inverting this relation,

$$S_c(E) = \ln \mathcal{P}(E, T) + \beta E + \beta F_v(T, E) - \beta F(T) \tag{120}$$

and using the computed IS probability distribution. If the energy dependence of $F_v(T, E)$ can be neglected, then curves for different temperatures can be superimposed and the resulting curve is, except for an unknown constant, the SW complexity $S_c(E)$. The unknown constant can be fixed by either comparing the numerical results with known theoretical predictions, or using the method described below. This method works rather well for some disordered spin systems such as the random orthogonal model (ROM), where the data collapse is rather good for a quite large energy interval [65]. The vibrational contribution F_v follows from the motion inside the component. Its independence of the energy of IS means that all components are equivalent, i.e., have similar shapes. In general, this is not the case and its contribution must be included. For systems with continuous variables F_v can be calculated at low T in the harmonic approximation by expanding the energy about the IS configuration [91, 92].

An alternative numerical method consists in computing directly the configurational entropy as a function of temperature. This method is free from unknown constants but does not resolve the configurational entropy as a function of IS energy. Considering (110) and (112) we have

$$\begin{aligned} F(T) &= E(T) - TS(T) \\ &= E_{\mathrm{IS}}(T) + E_v(T) - TS_c(T) - TS_v(T) \end{aligned} \tag{121}$$

where $E_{\mathrm{IS}}(T)$ is the average energy of IS seen at equilibrium at temperature T. The total entropy is then the sum of two contributions,

$$S(T) = S_c(T) + S_v(T). \tag{122}$$

The first term accounts for the multiplicity of components of energy $E_{\mathrm{IS}}(T)$ while the second for their 'volume'. The SW configurational entropy can then be computed as a difference between the total and the vibrational entropy.

The total entropy S can be evaluated via thermodynamic integration of the total energy at temperature T from a known reference point:

$$\Delta S = S(T) - S(T^*) = \int_{T^*}^{T} \frac{\mathrm{d}E}{T}. \tag{123}$$

Computing the vibrational contribution is more difficult, however at low temperature the system mainly explores the bottom of the components, near the IS. If the system is described by continuous variables then the vibrational contribution can be computed in the harmonic approximation by expanding about the IS. This leads to

$$S_v(T) \simeq S_{\mathrm{harm}}(T) = \mathcal{N} - \sum_{i=1}^{\mathcal{N}} \log\left[\frac{\hbar\omega_i(T)}{k_B T}\right] \tag{124}$$

where ω_i is the (average) frequency of the ith normal mode and $\mathcal{N}$ the number of normal modes. It is possible to refine this approximation by adding terms which take into account the basin anharmonicities, however usually these are negligible when compared with (124) [92]. For systems with discrete variables, such as for example disordered Ising-spin systems, the vibrational contribution can be estimated from the $T \to 0$ expansion of the TAP entropy, which leads to

$$S_v(T) \simeq \sum_{i=1}^{N} 2\beta|h_i|\exp(-2\beta|h_i|) \tag{125}$$

where N is the number of spins, and h_i is the local field acting on ith spin evaluated at the IS configuration [93].

These methods have been successfully applied to several model systems with both continuous variables such as Lennard-Jones glasses [91, 92, 94] or discrete variables like the ROM [65] or the SK model [65, 95].

Recently in [96] there has been introduced a numerical method to compute directly $S_c(\mathcal{F}, T)$ within the IS decomposition scheme based on the probabilistic definition of the component free energy. The dynamical evolution of the system in equilibrium defines a probability measure $p_{\mathcal{R}}$ over the components. In the case of an ergodic dynamics, and assuming that the observation time τ_{obs} is larger than the equilibration time, the statistical weight of the component $\mathcal{R}$ is

$$p_{\mathcal{R}}(T) = \frac{\tau_{\mathcal{R}}}{\tau_{\text{obs}}} = \exp[-\beta F(\mathcal{R}) + \beta F(T)] \tag{126}$$

where $\tau_{\mathcal{R}}$ denote the time spent by system in the component $\mathcal{R}$ during the total observation time τ_{obs}, $F(T)$ the equilibrium free energy and $F(\mathcal{R})$ the component free energy (see (75)). The probability to find at temperature T a component with free energy equal to $\mathcal{F}$ is

$$\begin{aligned}\mathcal{P}(\mathcal{F}, T) &= \sum_{\mathcal{R}} p_{\mathcal{R}}(T)\delta\left(\mathcal{F} - F(\mathcal{R})\right) \\ &= \exp[S_c(\mathcal{F}, T) - \beta\mathcal{F} + \beta F(T)]\end{aligned} \tag{127}$$

so that

$$S_c(\mathcal{F}, T) = \ln \mathcal{P}(\mathcal{F}, T) + \beta[\mathcal{F} - F(T)]. \tag{128}$$

If the number of different components is not too large $F(\mathcal{R})$ can be estimated directly using (126) and the frequency with which a given component $\mathcal{R}$ appears in a (long) simulation at temperature T:

$$F(\mathcal{R}) = -T \ln\left(\frac{\tau_{\mathcal{R}}}{\tau_{\text{obs}}}\right) + F(T). \tag{129}$$

The equilibrium free energy $F(T)$ can be computed by performing simulations at different temperatures and integrating the energy $E(T)$ of the system from $T = \infty$ down to T,

$$\beta F(T) = \int_0^{\beta} \mathrm{d}\beta'\, E_{\text{eq}}(\beta') - S(\beta = 0) \tag{130}$$

where $S(\beta = 0)$ is the infinite-temperature entropy of the system. From the value of $F(\mathcal{R})$ it is now easy to construct the histogram $\mathcal{P}(\mathcal{F}, T)$ and using (128) compute $S_c(\mathcal{F}, T)$. Because the system is equilibrated, in this approach components with identical free energy are sampled with the same probability. This differs from the previous method where components with the same energy E_{IS} are assumed to be equally probable which is clearly an approximation. The two methods coincide only if components have similar volumes so that the component entropy is the same.

This method has been successfully applied in [96] to the study of the ROM and the SK model, two cases with completely different critical behaviour. In both cases, the computed potential Φ allows for a very precise calculation of critical temperatures using relatively small systems giving confidence on $S_c(\mathcal{F}, T)$. Moreover, the form of Φ clearly discriminates between the two different types of transitions.

5.2. The concept of the effective temperature

There is the long standing idea that the non-equilibrium regime in aging or driven systems can be characterized by the FDR $X_{A,B}(C)$ (94) that has the meaning of a temperature in the thermodynamic sense. This suggestion stems from the observation that (94) can be recast in the following form,

$$\frac{1}{T_{\rm eff}^{(A,B)}(C)} = \frac{X_{A,B}(C)}{T} = \left.\frac{R_{A,B}(t,s)}{\frac{\partial}{\partial s}C_{A,B}(t,s)}\right|_{C_{A,B}(t,s)=C} \qquad t > s \tag{131}$$

defining an effective temperature through the relation

$$T_{\rm eff}^{(A,B)}(C) = \frac{T}{X_{A,B}(C)}. \tag{132}$$

As defined in (131), (132) the effective temperature is nothing other than a suitable parameter which tells that the QFDT becomes the usual FDT by replacing the bath temperature with the effective temperature. In many cases $X_{A,B}(C) < 1$ so the effective temperature $T_{\rm eff}^{(A,B)}$ is larger than the bath temperature.

The idea that some concepts of thermodynamic systems can be applied also to non-equilibrium systems has been wandering around in the literature for a long time (in the context of turbulence see [97] or in the context of structural glasses [2, 98, 99]). The statement that the effective temperature (132) has indeed a thermodynamic meaning faces some conceptual problems and difficulties not found in equilibrium theory. $T_{\rm eff}^{(A,B)}$ should satisfy the following properties:

- *Observable independence*. $T_{\rm eff}^{(A,B)}(C)$ must be independent of the observables A, B used to construct correlations and responses. If this is not always possible, as the present numerical evidence suggests, at least one would still like to know beforehand which set of 'good' observables endows (132) with a physical meaning. These observables have received the name of neutral observables and have been discussed in section 4.4. From many perspectives, this condition appears quite strong. It could be relaxed by only requiring independence of $T_{\rm eff}$ from the measured observable A for a given perturbation B (rather than on both A, B).
- *Zeroth law*. If the slow degrees of freedom of a system described by effective temperature $T_{\rm eff}(C)$ (we have dropped the A, B dependence) are put in contact with a thermal bath at temperature T, the net heat flow between the system and the bath should vanish only if $T_{\rm eff}(C) = T$, where C determines the relevant timescale (as described in section 4.1) at which the thermal bath, acting as a thermometer, responds. The same conclusion must hold between two glassy systems described by two effective temperatures $T_{\rm eff}^{(1)}(C)$, $T_{\rm eff}^{(2)}(C)$. After putting them in contact the net heat current between them, at the relevant timescale defined by the correlation C, vanishes only if $T_{\rm eff}^{(1)}(C) = T_{\rm eff}^{(2)}(C)$. This definition, apparently reasonable, encounters some difficulties that we will describe below. In particular, systems with identical effective temperatures $T_{\rm eff}^{(1)}(C) = T_{\rm eff}^{(2)}(C')$ but at different timescales ($C \neq C'$) cannot be in mutual equilibrium.
- *Existence of a non-equilibrium measure*. The zeroth law carries an associated maximum principle. In standard thermodynamics the zeroth law establishes that after putting in contact two systems at different temperatures the global system reaches a stationary state with a unique temperature. This stationary state is the one that maximizes the global entropy of the compound system compatible with a given total energy. Moreover, fluctuations around this maximum entropy state are ruled by the temperature. By the same token, the aging state of relaxational systems and the stationary state of driven

systems must exhibit some fluctuations or deviations around the aging (or driven) state that are described by the effective temperature $T^{\rm eff}(C)$. The full characterization of these fluctuations is presently unknown.

In section 4.2 we tried to fortify the idea that a thermodynamic description is indeed possible and that the effective temperature shares some properties of thermodynamic temperatures. Cugliandolo *et al* [100] have emphasized these aspects showing that the effective temperature can be defined only regarding the timescale under consideration. They considered a small thermometer that can be mimicked by a single harmonic oscillator of frequency ω that is put in contact with the original system. For definitiveness let us consider that x denotes the oscillator coordinate and $O(y)$ an observable of the system (described by the variable y) to which the oscillator is coupled by an interaction term, $-\epsilon x O(y)$ where ϵ is the intensity of the coupling. If ϵ is small enough, then the interaction between the oscillator and the system can be treated within the linear response theory and the energy of the oscillator evaluated in the stationary state. The equipartition theorem relates this energy to the temperature measured by the oscillator acting as a thermometer. In aging systems, the effective temperature is given by the FDT in the frequency domain (also called Nyquist formula),

$$T_{\rm eff}^{(O)}(\omega, t_w) = \frac{\pi}{2}\frac{\omega S_O(\omega, t_w)}{\chi''_O(\omega, t_w)} \tag{133}$$

where $S_O(\omega, t_w)$ is the power spectrum of correlation $\langle O(t)O(t_w)\rangle$ expressed in Fourier space (see (275)) and $\chi''_O(\omega, t_w)$ the corresponding out-of-phase susceptibility. A similar expression is valid for the stationary non-equilibrium state of driven systems, however because TTI holds the t_w dependence in (133) drops off. The connection between (132) and (133) appears when translating the meaning of ω and t_w into the many-timescales scenario. According to that ω corresponds to $1/(t - t_w)$ and therefore we can define $C^* \equiv C(t, t_w) = C(t_w + 1/\omega, t_w)$. This means that a thermometer put in contact with the system at time t_w and responding at a given frequency ω measures the temperature $T_{\rm eff}(C^*) = T/X(C^*)$. Equivalently, to measure the temperature $T_{\rm eff}(C^*) = T/X(C^*)$ in an aging system a thermometer responding to a timescale $t^* = 1/\omega$ with $C^* \equiv C(t_w + 1/\omega, t_w)$ should be used. In aging systems with two-timescales (such as structural glasses) characterized by the full aging t/t_w, in order to measure the effective temperature associated with the slow process, the frequency of the thermometer must be $\omega \sim 1/t_w$. The thermometer must respond in a timescale of the order of the waiting time!! In this scenario, effective temperatures can be extremely difficult to measure and this raises the question of their true meaning as the system drifts away from that state in the time required for a single measurement. To cope with this problem it has been proposed [101] that an ensemble of small thermometers is needed for the measurement. However, this does not solve the problem of how to measure, using this procedure, the effective temperature of a vitrified piece of glass quenched 1000 years ago. These difficulties are inherent to aging systems but not necessarily in driven systems that reach a stationary TTI state. For these reasons, experimental measurements of FDT violations and effective temperatures could be more suitable in driven rather than aging systems (for concerning experiments see discussion in section 8).

Zeroth law aspects of the effective temperature have been considered in [100, 102] within the spherical p-spin model. It has been shown that in the large $t_w \to \infty$ limit and low frequency limit $\omega \to 0$ there are only two possible ansatz solutions that close the dynamical equations in the aging state: either the two systems remain uncoupled with different effective temperatures or they thermalize and reach a common temperature. These results have been endorsed by a systematic study of these *coupled* solutions in the framework of the oscillator (OSC) model [103]. The OSC model is characterized by a single timescale corresponding

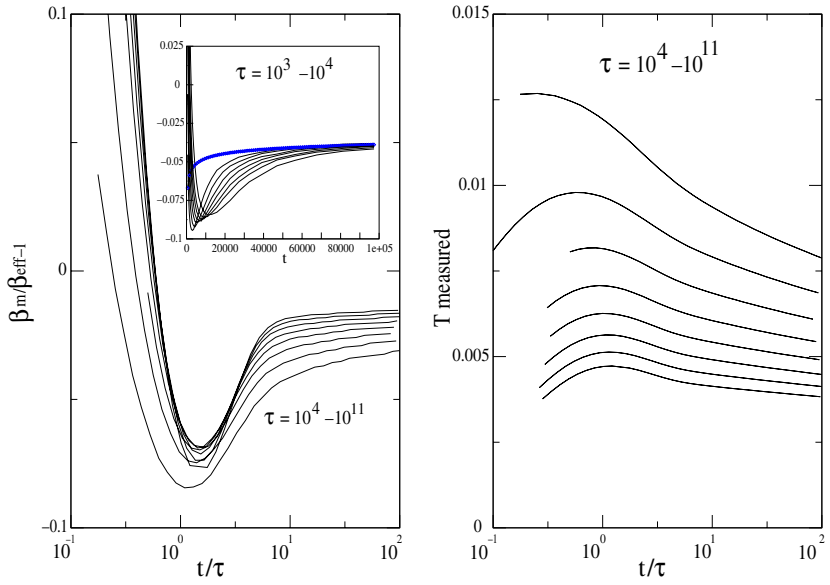

Figure 6. Left panel: relative difference between the measured temperature by a thermometer responding in a timescale $\tau = 1/\omega$ and the glassy OSC model aged at t, plotted against t/τ for different values of $\tau = 10^4, 10^5, 10^6, 10^7, 10^8, 10^9, 10^{10}, 10^{11}$ (from bottom to top). The measured temperature coincides with $T_{\rm eff}$ for $t/\tau \sim \mathcal{O}(1)$. In the inset, the same relative difference but plotted against t for $\tau = 10^3, 10^4$. Right panel: measured temperature plotted as a function of t/τ. From [105].

to the slow process at zero temperature (see section 6.5.1). It has been shown that, in the presence of an interaction term in the Hamiltonian that describes a compound system formed by two ensembles of the OSC model, the dynamics behaves in two different ways: either the effective temperatures equalize or they are different as if the systems were uncoupled. The dynamics remains always uncoupled (independent of the coupling intensity) if the dynamics is sequential on both systems, i.e., the updating is done sequentially over the two ensembles $1 \to 2 \to 1 \to 2$ and so on. In this case the effective temperatures of the two systems differ, each one corresponding to that of the non-interacting OSC ensemble. If dynamics is parallel, i.e., updating is done simultaneously over the two OSC ensembles $1 + 2 \to 1 + 2 \to 1 + 2$ and so on, then the effective temperatures of both models coincide even for a zero value of the coupling ϵ in the Hamiltonian. This result shows that, in general, two glassy systems interacting through a coupling term in the Hamiltonian do not necessarily reach the same effective temperature on timescales of the order of the waiting time.

In all these studies the same question remains always unanswered: why do fast and slow degrees of freedom decouple into different effective temperatures (in two-timescale systems, one is the bath temperature, the other the (higher) effective temperature)? A necessary condition is that the relaxation rate of the energy (or entropy production) decays to zero slowly enough [104]. To better understand this question, in [105] the thermal current between the oscillator model and a thermometer was analysed (see figure 6). There it was shown that the measured temperature $T_{\rm m}$, which makes the net current flow between system and the thermometer vanish, coincides with the effective temperature if $\omega t \sim 1$. However, in the limit $\omega t \ll 1$ the measured temperature is much smaller than the effective temperature, while in the other extreme $\omega t \gg 1$ the thermometer measures tolerably well the effective

temperature. Discrepancies between the measured and the effective temperature have also been reported in the SK model in the presence of asymmetric interactions as an example of a driven system [106]. Another important aspect is that the zeroth law is hardly effective as transport coefficients (such as the thermal conductivity) are exceedingly small, in agreement with the uncoupling of degrees of freedom occurring in glassy systems with many timescales. From another point of view Nieuwenhuizen [49, 107, 108] has formulated a theory to describe the aging regime of glassy systems with two timescales assuming, right from the beginning, that the effective temperature is indeed associated with a thermodynamic potential. In this formulation, the configurational entropy is an extensive thermodynamic potential conjugated to the effective temperature. The first law of thermodynamics, that expresses energy conservation, reads $\mathrm{d}E = \mathrm{d}W + T\,\mathrm{d}S_{\mathrm{eq}} + T_{\mathrm{eff}}\,\mathrm{d}S_c$ where $S = S_{\mathrm{eq}} + S_c$ is the total entropy that receives contributions from the equilibrium (or intrastate) entropy and the configurational entropy. The configurational entropy and the effective temperature manifest in the reported experimental failure of the second Ehrenfest relation (while the first is automatically satisfied by construction) leading to values of the Prigogine–Defay ratio larger than 1 [109].

5.3. The Edwards measure for granular materials

Granular materials are systems made of a large number of individual grains such as sands or powders. At first sight granular systems look quite different from thermodynamical systems since, for example, they interact mainly through frictional forces and hence the energy is not conserved. Moreover, power is supplied to them by tapping, shearing or shaking, all mechanisms quite different from thermal contact with a thermal bath. However, despite these differences, granular materials share with thermal systems the property that their properties are reproducible given the same set of extensive operations, i.e., operations acting upon the system as a whole and not on individual grains. For example, if some sand is poured uniformly and at low density into a container one expects to have a sand of a certain reproducible density. Based on these facts it is then reasonable to hypothesize that granular systems can be described at a macroscopic level by a small number of parameters, analogous, e.g., to temperature or pressure, using some ideas of statistical mechanics [110–114].

The most important variable describing the state of a granular system is its density, or equivalently its volume V. The thermal energy of a granular system at room temperature is indeed negligible. The volume V is the actual volume occupied by the system, for example measured by the position of a piston in the container, and hence it depends on the configurations (position and orientation) of the grains. In principle other variables should be necessary to describe the state of the system, but if we assume that the grains are rigid then all other microscopic details can be neglected. Thus the only valid configurations of grains are stable arrangements where grains can remain at rest under the influence of confining forces, and with no overlap among them. We are then led to a statistical description of all possible stable configurations of grains in the real space, i.e., to a *configurational* statistical mechanical theory for the random packing of grains. Since in a stable configuration grains that cannot move these configurations are also called *blocked states*.

The next step to develop a statistical mechanical description for granular systems consists in the introduction of a *volume function* W [110, 111] which plays the role of energy in statistical mechanics. The function W specifies the volume of the system in terms of the configuration of grains: $V = W(\boldsymbol{q})$, where $\boldsymbol{q}$ denotes all the grain positions and orientations in a blocked state. Under the assumption that for a given volume V all configurations for which $V = W(\boldsymbol{q})$ are equally probable a statistical description can be developed through a

process completely analogous to that of conventional statistical mechanics. It is then possible to introduce a microcanonical ensemble with distribution function

$$\mathrm{e}^{-S}\delta(V - W(\boldsymbol{q})) \tag{134}$$

where $S = S(V)$ is the entropy defined as usual in terms of the total number of blocked states

$$\Omega = \int \mathrm{d}\boldsymbol{q}\,\delta(V - W(\boldsymbol{q})) \qquad S = \ln\Omega. \tag{135}$$

Similar to its thermodynamic counterpart, the entropy S is an extensive quantity as can be seen, for example, in simple toy models [111, 115]. The measure (134), (135) is usually called *Edwards' measure* for granular systems.

To define a canonical ensemble it is necessary to define a parameter analogous to temperature which characterizes the state of the system. This parameter is the *compactivity* X defined as

$$\frac{1}{X} = \frac{\partial S}{\partial V} \tag{136}$$

and thus the partition function is

$$\mathcal{Z} = \mathrm{e}^{-Y(X)/X} = \int \mathrm{d}\boldsymbol{q}\,\mathrm{e}^{-W(\boldsymbol{q})/X} \tag{137}$$

where potential $Y(X)$ is called the *effective volume* and plays the role of a free energy:

$$Y(X) = V(X) - XS. \tag{138}$$

The analogy can be pushed forward and many other relations similar to that of conventional statistical mechanics can be derived. We shall not pursue this here, however, before concluding we shall spend some more words on the compactivity X. The compactivity X measures the packing of grains, indeed from its definition it is clear that it may be interpreted as being characteristic of the number of possible ways of arranging the grains of a system by changing the volume by an amount ΔV, the change in entropy being equal to ΔS. Consequently, the two limits of X are 0 and ∞ corresponding to the most compact and the least compact arrangements, respectively. The compactivity X also describes the balance between the tendency of the system to increase or decrease its volume and the tendency to increase or reduce its entropy.

At first sight blocked states in granular systems resemble IS discussed for glasses. Indeed a connection between the two can be drawn [41, 116–118] introducing a 'tapping' dynamics for glasses, i.e., a dynamics in which each tap consists in raising the temperature and, after a short time, quenching it to zero. Similar to what has been done for other glassy systems, one can try to describe the dynamics of the slow degrees of freedom through an effective temperature defined from the FDR [100, 119]. At the mean-field level this temperature turns out to coincide with the Edwards compactivity, which is related to the derivative of the entropy of *blocked configurations* of a given density. The Edwards ensemble immediately leads to the definition of an entropy $S_{\mathrm{Edw}}(\rho)$ as the logarithm of the number of blocked configurations of given ρ. The soundness of the Edwards approach encounters difficulties reminiscent of those present in the IS approach. At present the correspondence between the Edwards construction and the long-time slow dynamics for non-mean-field models can only be checked *a posteriori* and it is presently unknown how to derive it from first principles.

6. QFDT from exactly solvable models

In the structural glass problem, the spatial randomness is self-generated rather than put in by hand as in random spin-glass models. This suggests that there should be a connection

also with frustrated but regular models. In the last years several spin models, both with and without randomness, displaying structural-glass transition like properties have been found. Interestingly, some of them can be solved in closed form, offering an important tool for understanding the glass transition.

In this section, we shall summarize the main results on violation of FDT obtained from the exact solution of some spin models.

6.1. The mode-coupling theory

A model Hamiltonian or an effective Lagrangian capable of describing relaxation processes in supercooled liquids and structural glasses is difficult to obtain. Early studies based on both dynamical mode-coupling theories or equilibrium density-functional theories suggested that there may be a close connection with mean-field spin-glass models [120]. They thus provide a set of microscopical models where glassy dynamics can be studied analytically. The basic simplification occurring in mean-field models is that after averaging over the disorder and making the number of spins very large ($N \to \infty$) one is left with a closed set of equations for the two-times correlation and response functions. Above a critical temperature T_c those equations admit a TTI solution satisfying the FDT. In this regime they are basically equivalent to the schematic mode-coupling equations introduced by Leutheusser, Götze and others [121–123] as a model for the ideal glass transition. Below T_c the ergodicity is broken and the FDT is violated. This is signalled by the appearance of a finite Edwards–Anderson order parameter q_{EA} at T_c.

The fundamental quantities in the dynamical mode-coupling theory (MCT) are the local particle density correlation functions $\langle \delta\rho(\boldsymbol{x}, t)\delta\rho(\boldsymbol{x})\rangle$ where $\delta\rho(\boldsymbol{x}) = \rho(\boldsymbol{x}) - \rho_0$, with

$$\rho(\boldsymbol{x}) = \sum_{i=1}^{N} \delta(\boldsymbol{x} - \boldsymbol{x}_i) \tag{139}$$

the local particle density, and ρ_0 the uniform fluid density

$$\langle \rho(\boldsymbol{x})\rangle = \rho_0 \qquad \text{(homogeneous state)} \tag{140}$$

where the angle brackets denote an ensemble average. In the glassy phase, the system is trapped into metastable states with nonuniform (average) local density field $\langle \rho(\boldsymbol{x})\rangle \neq \rho_0$ and the density-fluctuation correlation functions do not decay to zero for $t \to \infty$:

$$\lim_{t\to\infty} \langle \delta\rho(\boldsymbol{x}, t)\delta\rho(\boldsymbol{x})\rangle \neq 0. \tag{141}$$

The complete mode-coupling theories lead to the time-evolution equations for the normalized correlation functions

$$\phi_q(t) = \frac{\langle \delta\rho(\boldsymbol{q}, t)^* \delta\rho(\boldsymbol{q}, 0)\rangle}{N S_q} \tag{142}$$

where $S_q = \langle |\delta\rho(\boldsymbol{q})|^2\rangle/N$ is the static structure factor, and $\rho(\boldsymbol{q})$ are the Fourier components of the density field $\rho(\boldsymbol{x})$,

$$\rho(\boldsymbol{q}) = \int \exp(-\mathrm{i}\boldsymbol{q}\cdot\boldsymbol{x})\rho(\boldsymbol{x})\,\mathrm{d}\boldsymbol{x} = \sum_{i=1}^{N} \exp(-\mathrm{i}\boldsymbol{q}\cdot\boldsymbol{x}_i). \tag{143}$$

The basic idea of MCT is to derive the equations of motion for the slow relaxing modes integrating all fast modes. This leads to a set of self-consistent equations involving only slow mode variables in which all information from fast modes are buried into density-fluctuation memory kernels of the form

$$M_q(t) = \mathrm{i}\nu_q + \Omega_q^2 m_q(t) \tag{144}$$

where ν_q is a (white-noise) frictional term arising from fast modes, $\Omega_q > 0$ gives the frequency or timescale of microscopic motion and $m_q(t)$ accounts for slow modes couplings arising from the integration of the fast modes. The general form of the MCT equations is [123]

$$\partial_t^2 \phi_q(t) + \nu_q \partial_t \phi_q(t) + \Omega_q^2 \phi_q(t) + \Omega_q^2 \int_0^t \mathrm{d}s\, m_q(t-s) \partial_s \phi_q(s) = 0 \tag{145}$$

which must be solved with initial conditions:

$$\phi_q(t=0) = 1 \qquad \partial_t \phi_q(t=0) = 0. \tag{146}$$

The fundamental mechanism for the glass transition in the MCT is the feedback between slow density fluctuations expressed through $m_q(t)$. The solution of these equations is a formidable task since the kernel $m_q(t)$ involves higher order correlations between density-fluctuation modes. Therefore when these theories are implemented approximations are generally made. The simplest approximation consists of replacing the average of products with products of averages to obtain a set of closed equations. This is some sort of mean-field approximation. Indeed within this scheme the memory-kernel $m_q(t)$ can be expressed as a functional of the ϕ_q,

$$m_q(t) = \mathcal{F}_q[\mathbf{V}, \{\phi_q\}] \tag{147}$$

with some vertex functions $\mathbf{V}$. Despite this rather strong approximation, similar to a mean-field approach, the theory contains the basic mechanism of the glass transition. We note that due to this approximation, the MCT is not capable of describing activated processes, in the same way they cannot be discussed within mean-field theories. Therefore the appearance of activated-process dominated regimes is signalled in this theory by the divergence of some quantities. Activated processes could, in principle, be included as perturbative terms, however consistent theories which account for them are not yet available.

The main properties of the MCT can best be seen using a simplified version of the theory called *schematic mode-coupling theory* in which only one relaxation function is considered [121–123]:

$$\partial_t^2 \phi(t) + \nu \partial_t \phi(t) + \Omega^2 \phi(t) + \Omega^2 \int_0^t \mathrm{d}s\, m(t-s) \partial_s \phi(s) = 0. \tag{148}$$

The simplest model describing an idealized structural-glass transition is that specified by the two coupling constants (v_1, v_2):

$$m(t) = v_1 \phi(t) + v_2 \phi(t)^2. \tag{149}$$

This theory predicts a transition from an ergodic liquid phase, where $\phi(t \to \infty) \to 0$, to a glass phase, where the ergodicity is broken and $\phi(t \to \infty) \to f > 0$, as the parameter (v_1, v_2) are varied. Depending on the values of (v_1, v_2) the nature of the transition can be either continuous (type A) with f growing continuously from zero or discontinuous (type B) with f jumping from zero to a finite value as the transition line is crossed.

6.2. Disordered spin-glass models

Mean-field spin-glass models can be classified into two broad classes depending on the value of the Edwards–Anderson parameter (q_{EA}) at the transition (for the structural-glass transition this can be identified with the long-time limit of the density correlation functions). The first class, called *discontinuous* models, includes models for which a finite q_{EA} appears discontinuously at T_c. The prototype model in this class, which we discuss here, is the spherical p-spin model. Other models included in this family are: Potts glasses with more than four components

[42, 124], quadrupolar glass models [124, 125] and p-spin interaction spin-glass models [43, 44, 126–128]. The second class includes models such as the Sherrington–Kirkpatrick (SK) model [129, 130], for which $q_{\rm EA}$ starts continuously from 0 at $T_{\rm c}$. Those models are termed *continuous* models.

6.2.1. p-spin spherical model. Among the mean-field spin-glass models with a discontinuous spin-glass transition an important role has been played by the spherical p-spin spin-glass model. Spin-glass models with multispin interactions were first considered in the 1980s for both Ising [126–128] as well as soft spins [43, 44]. However, while the static properties could be computed for arbitrary values of p, dynamical properties were limited to values of p close to 2 [43, 44]. An important step forward came with the introduction of the spherical p-spin spin-glass model [131, 132], since its statics and dynamics can be solved in closed form for any value of p.

The spherical p-spin interaction spin-glass model is defined by the Hamiltonian

$$\mathcal{H} = -\sum_{1\leqslant i_1<\cdots<i_p\leqslant N} J_{i_1\ldots i_p}\sigma_{i_1}\cdots\sigma_{i_p} - h\sum_{i=1}^{N}\sigma_i \tag{150}$$

where h is an external field, which in the following we shall take equal to zero for simplicity. It describes a system of N continuous spins σ_i interacting via randomly quenched infinite range p-spin interactions $J_{i_1\ldots i_p}$ which are taken to be Gaussian with zero mean and variance

$$\overline{\left(J_{i_1,\ldots,i_p}\right)^2} = \frac{J^2 p!}{2N^{p-1}} \qquad 1 \leqslant i_1 < \cdots < i_p \leqslant N. \tag{151}$$

The overbar stands for the average over the couplings. The scaling with N is chosen such that there is a well-defined thermodynamic limit $N \to \infty$. The spins can vary continuously from $-\infty$ to $+\infty$, but are subject to the global spherical constraint

$$\sum_{i=1}^{N}\sigma_i^2 = N \tag{152}$$

which must be satisfied at any time. The relaxational dynamics for $\sigma_i(t)$ is given by the set of Langevin equations [133]

$$\Gamma_0^{-1}\partial_t\sigma_i(t) = -r(t)\sigma_i(t) - \frac{\delta\beta\mathcal{H}}{\delta\sigma_i(t)} + \eta_i(t). \tag{153}$$

The kinetic coefficient Γ_0 sets the timescale of the microscopic dynamics, and will be henceforth set to 1 without loss of generality, while $\beta = 1/T$. The last term in (153) $\eta_i(t)$ is a Gaussian random field with zero mean and variance

$$\langle\eta_i(t)\eta_j(t')\rangle = 2\Gamma_0^{-1}\delta_{ij}\delta(t-t') \tag{154}$$

representing the effects of thermal noise. The average over thermal noise is denoted as usual by angle brackets $\langle\cdots\rangle$. The first term in (153) enforces the spherical constraint at any time, and must be fixed self-consistently. In the mean-field limit $N \to \infty$ the sample-averaged dynamics is entirely described by the evolution of the two-times correlation and linear response functions

$$C(t,s) = \overline{\langle\sigma_i(t)\sigma_i(s)\rangle} \tag{155}$$

$$R(t,s) = \left.\frac{\delta\overline{\langle\sigma_i(t)\rangle}}{\delta h_i(s)}\right|_{h_i=0} \tag{156}$$

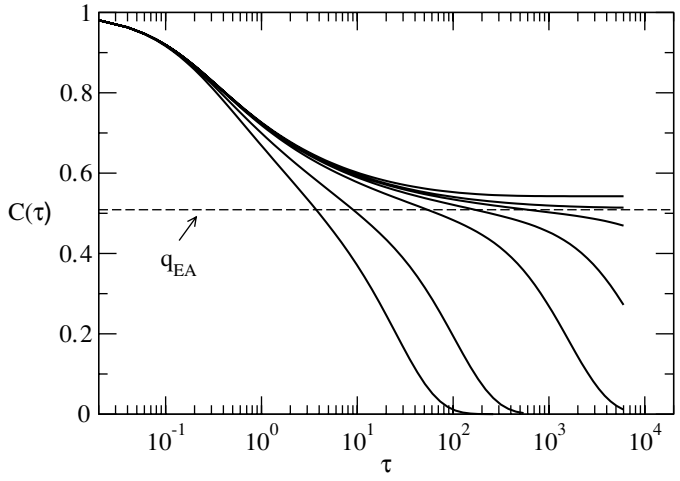

Figure 7. $C(\tau)$ as a function of time for the spherical p-spin model with $p = 3$. Left to right: $T = 0.7, 0.65, 0.62, 0.615, 0.613, 0.612$ and 0.61. The horizontal line is $q_{\rm EA}(T = T_{\rm c}) \sim 0.509\,034$ and $T_{\rm c} = 0.612\,372$.

which vanishes for $t < s$ due to causality. The dynamical equations for C and R are obtained from (153) [132] through standard functional methods [43, 44, 134]. At high temperatures the system is ergodic, thus for initial time $t_{\rm i} \to -\infty$ both TTI and FDT hold. Using the FDT relation the equation for $C(t - s)$ reads [132]

$$\partial_\tau C(\tau) + C(\tau) + \int_0^\tau {\rm d}\tau' m(\tau - \tau')\partial_{\tau'} C(\tau') = 0 \tag{157}$$

where $\tau = t - s$ and

$$m(\tau) = \mu C(\tau)^{p-1} \tag{158}$$

which has the same structure of the schematic MCT equation (148). The correlation always decays to zero for large t. However, slightly above $T_{\rm c}$ there develops a plateau at $C \sim q_{\rm EA}$ before eventually decaying to zero, see figure 7. The length $\tau_p(T)$ of the plateau increases as a power of $T - T_{\rm c}$ and diverges at $T_{\rm c}$. Near the plateau one finds that

$$C(\tau) \sim q_{\rm EA} + c_a \tau^{-a} \qquad C \gtrsim q_{\rm EA} \tag{159}$$

$$C(\tau) \sim q_{\rm EA} - c_b \tau^{b} \qquad C \lesssim q_{\rm EA} \tag{160}$$

where the exponents a and b are related by

$$\frac{\Gamma^2(1-a)}{\Gamma(1-2a)} = \frac{\Gamma^2(1+b)}{\Gamma(1+2b)} = \frac{(p-2)(1-q_{\rm EA})}{2q_{\rm EA}}. \tag{161}$$

The plateau length scale $\tau_p(T)$ sets the equilibration timescale. Therefore, as the temperature is lowered to $T_{\rm c}$ the system undergoes a transition since the length of the plateau diverges and the correlation fails to decay to zero. In the low-temperature spin-glass phase ($T < T_{\rm c}$) the system cannot equilibrate and the ergodicity is broken so the state of the system may depend on its initial state. In this scenario, it is clear that even a mean-field theory can be highly non-trivial. To discuss the dynamics in the low-temperature phase it is convenient to have an understanding of the low-temperature structure of the phase space. A standard method to deal with such a problem is the so-called *replica trick*, see e.g. [35]. The breaking of ergodicity

results in a breaking of the permutation symmetry between replicas [135]. The general form of the breaking is, however, not known. For p-spin models it has been found that the solution is given by the so-called *one-step replica symmetry breaking* (1RSB) form [44, 127, 128, 131]. Physically this means that the phase space is broken into equivalent ergodic components separated by infinite (for $N \to \infty$) barriers and the equilibrium solution is described by only three parameters: the overlap between two different ergodic components, the overlap inside an ergodic component (the Edwards–Anderson order parameter) and the probability that two different replicas will be found in the same ergodic component. For the p-spin spherical model this solution is valid everywhere in the low-temperature phase [131]. Ising-spin p-spin models present an even lower temperature phase with a more complex structure described by an *infinite-step replica symmetry breaking* (∞-RSB) [128]. A similar scenario is also found in Potts glasses with more than four components [124].

Besides the replica approach, which gives essentially information on the lowest lying states which mostly contribute to the equilibrium measure, a good understanding of the landscape topology is given by the TAP approach. Using these methods we have now a rather good knowledge of the landscape [73, 85, 136–140]. Roughly speaking the picture that emerges for the p-spin spherical model is that equilibrium states, whose energy and free energy difference is $O(1)$, are separated by $O(N)$ barriers. As the temperature is changed the solutions neither merge nor bifurcate, and their free energy smoothly changes. The TAP equations for the p-spin spherical model have non-trivial solutions in the free-energy range ($F_{1\mathrm{RSB}}$, F_{thr}), where the threshold free energy F_{thr} is larger that the equilibrium free energy $F_{1\mathrm{RSB}}$ by an $O(N)$ quantity, the difference being the complexity, see section 5.1, which is maximal for $F = F_{\mathrm{thr}}$ and vanishes when $F = F_{1\mathrm{RSB}}$. Below the threshold the equilibrium states are local minima of the TAP free energy separated by $O(N)$ barriers, while above the threshold there are no minima.

To have a meaningful investigation of the non-ergodic phase some regularization scheme of the dynamics on a very long timescale is required. One possibility is to refer to a large finite system. The finiteness of N guarantees ergodicity by allowing the penetration of barriers whose height would diverge for $N \to \infty$ limit, and the system can equilibrate. This approach was first proposed by Sompolinsky for the Sherrington–Kirkpatrick model [141]. In the Sompolinsky scheme TTI holds and FDT is satisfied up to some timescale t_0, which diverges as $N \to \infty$, related to the (free-)energy barrier crossing, but it is violated for timescales larger than t_0 where it is replaced by a modified form called *quasi-fluctuation–dissipation theorem* (QFDT). See section 6.2.2 for a more detailed discussion of the Sompolinsky scheme. In order to consider the motion on the two different time regimes ($t \ll t_0$ and $t \gg t_0$) one writes [32, 132]

$$C(\tau) = C_1(\tau) + C_0(\xi) \qquad R(\tau) = R_1(\tau) + \frac{1}{t_0} R_0(\xi) \tag{162}$$

where $\xi = \tau/t_0$. The functions $C_1(\tau)$ and $R_1(\tau)$ describe the motion in a single ergodic component and vary on timescales $\ll t_0$, while the functions $C_0(\xi)$ and $R_0(\xi)$ describe the motion among different minima and hence vary on timescales $\gg t_0$. Continuity imposes

$$C_1(\tau = 0) = 1 - q_{\mathrm{EA}} \qquad C_1(\tau \to \infty) = 0 \tag{163}$$

$$C_0(\xi = 0) = q_{\mathrm{EA}} \qquad C_0(\xi \to \infty) = 0 \tag{164}$$

thus C_0 describes the slow decay of the correlation function from q_{EA} to zero. The initial conditions for R_0, R_1 are obtained from the FDT, the QFDT and the continuity condition for C.

On timescales $\tau \ll t_0$ FDT holds, so $C_1(\tau)$ obeys a dynamical equation similar to (157). The equations for $C_0(\xi)$ and $R_0(\xi)$ are more complex, however it can be proved [132] that they are related by the QFDT relation

$$R_0(\xi) = -\beta x \theta(\xi) \partial_\xi C_0(\xi) \tag{165}$$

with $0 \leqslant x \leqslant 1$ given by

$$x = \frac{(p-2)(1-q_{\mathrm{EA}})}{q_{\mathrm{EA}}}. \tag{166}$$

Within the replica formalism the parameter x corresponds to the location of the discontinuity in the order parameter $q(x)$. However, different to the static calculation, where x is fixed by the requirement of stationarity of the replica free energy F with respect to x, the dynamical calculation requires that $\partial_x F$ be maximal (marginal condition) [132]. This condition is equivalent to the condition of a maximal configurational entropy [42, 73, 77], so that the dynamics is dominated by the states with the largest degeneracy (threshold states).

The Sompolinsky approach has several similarities with the static approach, and indeed in the static limit it correctly reproduces the static results obtained within the Parisi scheme. However, it suffers from some problems which are difficult to amend since it would require detailed knowledge of the dynamics for a large but finite system. One among the most serious inconsistencies of the Sompolinsky dynamics is that FDT violations, as given in (165), satisfy TTI. This is untenable in the aging regime of purely relaxational systems (although not necessarily in driven systems) where TTI is clearly violated. It must be noted though, that the Sompolinsky approach was never proposed to explain aging, since it is eliminated from the theory at the beginning.

For this reason there have been various attempts to amend the solution. One possibility, proposed by Horner [32, 132, 142, 143], consists of cooling the system, at finite cooling rate from $T > T_{\mathrm{c}}$ to $T < T_{\mathrm{c}}$. This introduces a regularization timescale, the inverse of cooling rate, which is eventually sent to infinity at the end. Another approach [32], consist in making the disorder time-dependent hence restoring ergodicity on timescales larger than the disorder typical timescale.

The above methods assume in one way or another equilibrium, thus cannot describe non-equilibrium properties typical of glasses such as aging, see section 4.1. To tackle them, a different scheme has been proposed by Cugliandolo and Kurchan [52]. The main difference lies in that the thermodynamic limit is taken *before* any large time limit, including the initial limit $t_{\mathrm{i}} \to -\infty$. Differing from the Sompolinsky approach this is a non-equilibrium scheme since the system evolves from a non-equilibrated initial configuration. As the system evolves in time the dynamical free-energy density decreases, and the system explores an ever decreasing portion of phase space. The *weak ergodicity breaking* [40] describes this non-equilibrium regime before equilibrium is reached. In this scenario the important parameter is the *waiting time* t_w, i.e., the time elapsed since the quench into the low-temperature phase. For longer waiting times, the system can explore deeper minima becoming less susceptible to external perturbations and hence ages. The weak ergodicity breaking scenario can be summarized in the following assumptions:

(i) After any time t_w the system continues to drift away and asymptotically reaches the maximum allowable distance. Thus the correlation functions satisfy

$$\partial_\tau C(\tau + t_w, t_w) \leqslant 0 \qquad \partial_s C(t,s) \geqslant 0 \qquad (t > s) \tag{167}$$

and in the absence of external magnetic fields

$$\lim_{\tau \to \infty} C(\tau + t_w, t_w) = 0 \qquad \text{for any fixed } t_w. \tag{168}$$

(ii) The response to a constant small magnetic field applied from $s = 0$ to $s = t_w$,—i.e. the TRM $M^{\mathrm{TRM}}(t, t_w)$—decays to zero after long enough times

$$\lim_{t\to\infty} \int_0^{t_w} \mathrm{d}t' R(t, t') = \lim_{t\to\infty} M^{\mathrm{TRM}}(t, t_w) = 0 \tag{169}$$

for any fixed t_w.

(iii) The evolution of the two-times correlation function presents two distinct regimes. After a long time s, but $\tau = t - s$ small, the correlation decays from 1 at equal time to a plateau value q_{EA} defined as

$$q_{\mathrm{EA}} = \lim_{\tau\to\infty} \lim_{s\to\infty} C(\tau + s, s). \tag{170}$$

This *fast* decay corresponds to a fast relaxation towards a local minimum. In this time sector the system behaves as if it were in a local equilibrium, and both TTI and FDT hold. The value of q_{EA} measures the size of the local minima or, equivalently, the width of the channel through which the system evolves. This fast relaxation is followed by a *slow* decay of C below q_{EA} and the exploration of different minima. Since the depth of minima increases with time, C decays from the plateau in a manner that depends on both s and τ. To show the two processes (i.e. the contribution from fast and slow motion) the response and correlation functions are split into two different terms, in a fashion similar to that used in the Sompolinsky scheme,

$$C(t, s) = C_{\mathrm{st}}(t - s) + C_{\mathrm{ag}}(t, s) \qquad R(t, s) = R_{\mathrm{st}}(t - s) + R_{\mathrm{ag}}(t, s) \tag{171}$$

with

$$C_{\mathrm{st}}(t - s = 0) = 1 - q_{\mathrm{EA}} \qquad C_{\mathrm{st}}(t - s \to \infty) = 0 \tag{172}$$

$$C_{\mathrm{ag}}(t, t) = q_{\mathrm{EA}} \qquad \lim_{t\to\infty} C_{\mathrm{ag}}(t, s) = 0. \tag{173}$$

The assumption of local equilibrium implies that FDT is satisfied by the fast motion:

$$R_{\mathrm{st}}(t - s) = \beta\theta(t - s)\partial_s C_{\mathrm{st}}(t - s). \tag{174}$$

On long timescales, however, FDT is violated and replaced by (cf equation (165))

$$R_{\mathrm{ag}}(t, s) = \beta X[C_{\mathrm{ag}}(t, s)]\theta(t - s)\partial_s C_{\mathrm{ag}}(t, s) \tag{175}$$

with the ansatz that X depends on time only through C_{ag}. The two forms of FDT can conveniently be condensed into one extending the definition of X as $X(z) = 1$ for $q_{\mathrm{EA}} \leqslant z \leqslant 1$. Then we can write

$$R(t, s) = \beta X[C(t, s)]\theta(t - s)\partial_s C(t, s) \tag{176}$$

where C and R are the full correlation and response functions. For the FDT part the MCT-like equations (157) are recovered. To derive the equations for the non-FDT part the time derivatives are neglected since C_{ag} and R_{ag} are slow varying functions:

$$\partial_t C_{\mathrm{ag}}(t, s) \sim \partial_s C_{\mathrm{ag}}(t, s) \sim 0 \qquad \text{for large } t, s. \tag{177}$$

As a consequence the solutions are time-reparametrization invariant, i.e., the solutions are invariant under the transformation

$$C_{\mathrm{ag}}(t, s) \Rightarrow C_{\mathrm{ag}}(h(t), h(s)) \qquad R_{\mathrm{ag}}(t, s) \Rightarrow \left[\frac{\mathrm{d}h(s)}{\mathrm{d}s}\right] R_{\mathrm{ag}}(h(t), h(s)) \tag{178}$$

where $h(t)$ is an arbitrary (well-behaved) function. The full dynamical solution obviously does not have such an invariance. This ambiguity stems from the fact that equations are only

the first order equations of an asymptotic expansion. If higher order terms are included the ambiguity is removed, however we shall not discuss this problem. Motivated by the fact that the relevant timescale in slow relaxation motion is given by the waiting time, one looks for a solution of the form [52]

$$C_{\rm ag}(t,s) \to C_{\rm ag}(h(t)/h(s)). \tag{179}$$

The selection of the correct function $h(t)$ is still an open problem that requires the matching of the short- and long-time regimes. Numerical solution of the dynamical equations [52] suggests a power law $h(t) \sim t^{\lambda}$.

An analysis of the correlation function near the plateau $q_{\rm EA}$ [144], similar to that done in the high-temperature phase [132], reveals the following scenario. As found in the high-temperature phase, the decay of the correlation function to the plateau $q_{\rm EA}$ is a power law with a temperature-dependent exponent. The subsequent departure from the plateau is still a power law with another temperature-dependent exponent, but differing from the high-temperature phase in that it is also t_w dependent,

$$C(\tau + t_w, t_w) \sim q_{\rm EA} + c_a \tau^{-a} \qquad C \gtrsim q_{\rm EA} \tag{180}$$

$$C(\tau + t_w, t_w) \sim q_{\rm EA} - c_b \left(\frac{\tau}{\mathcal{T}_w}\right)^b \qquad C \lesssim q_{\rm EA} \tag{181}$$

with $\mathcal{T}_w = [{\rm d}\ln h(t_w)/{\rm d}t_w]^{-1}$ an effective waiting time. The exponents a and b are related,

$$\frac{\Gamma^2(1-a)}{\Gamma(1-2a)} = X\frac{\Gamma^2(1+b)}{\Gamma(1+2b)} = \frac{(p-2)(1-q_{\rm EA})}{2q_{\rm EA}} \tag{182}$$

where $q_{\rm EA}$ is determined by the marginal condition

$$\mu(p-1)q_{\rm EA}^{p-2} = \frac{1}{(1-q_{\rm EA})^2} \tag{183}$$

$$X(C) = \frac{(p-2)(1-q_{\rm EA})}{q_{\rm EA}} \qquad \text{if} \quad C < q_{\rm EA} \tag{184}$$

and $X(C) = 1$ otherwise.

Here we did not consider the case of non-zero external field, this was studied in [131, 132]. Another extension of the p-spin spherical model is the case of multiple phases treated in [145–148]. It is interesting to note that depending on the degree of non-linearity of the interaction three different scenarios for the transition can be observed [147]. Finally, it is worth noting that the $p = 2$ version of the model has the property of being solvable even for intermediate timescales [149–153] or finite sizes [154].

6.2.2. The Sherrington–Kirkpatrick model. The Sherrington–Kirkpatrick (SK) model [129, 130] belongs to the class of continuous spin-glass models characterized by a low-temperature spin-glass (SG) phase of ∞-RSB type with a continuous order parameter function $q(x)$. The transition to the SG phase is continuous with a $q(x)$ which grows continuously from zero as T is lowered below $T_{\rm c}$. Other models in this class are, e.g., the case of a particle in a long-range correlated random potential [155] or spherical models with mixture of $p = 2$ and $p > 3$ interactions [145, 147]. For $T > T_{\rm c}$ and large times the correlation function decays to zero in the absence of external fields. However, differing from the discontinuous SG models, it does not exhibit a plateau at $q_{\rm EA}$ for T slightly above $T_{\rm c}$. The SK model without external fields is defined by the Hamiltonian

$$\mathcal{H} = -\sum_{i<j} J_{ij}\sigma_i\sigma_j \tag{185}$$

where the interactions J_{ij} are independent quenched Gaussian variables of zero mean and variance

$$\overline{(J_{ij})^2} = \frac{J^2}{N}. \tag{186}$$

As done previously J can be set equal to 1 by rescaling the temperature. The spin variables can be either Ising spins ($\sigma = \pm 1$) or soft spins in which case an extra term may be added to the Hamiltonian to control fluctuations. The first choice is used in static calculations, while the second is preferred in a dynamical approach.

The ∞-RSB structure of the SG phase reflects a completely different topology of the phase space. Again below T_c the phase space is broken into a large number (exponentially in N) states, but now the overlap between states can take any value from 0 to q_{EA}. The equilibrium states are organized in an ultrametric fashion with non-extensive barriers, $O(N^\alpha)$ with $\alpha \sim 1/3$, between them. The TAP analysis shows that the TAP solutions tend to split as the temperature is lowered in a fashion similar to a second order transition. Moreover, the spectrum of the Hessian matrix of the solution extends down to zero, leaving the possibility of finite free-energy barriers. All these facts lead to a dynamical scenario quite different from that discussed in section 6.2.1.

The relaxational dynamics of the soft-spin version is given by Langevin equations similar to (153), (154) and the self-consistent dynamical equations for the two-times correlation and response functions were first derived by Sompolinsky and Zippelius [134, 156]. These are more involved than those of the spherical case because spin variables cannot be integrated away and hence will not be reported here. However, near the critical point the dynamical equations can be written in the MCT form (157), (147) with suitable v_1 and v_2 [157]. The two parameters v_1 and v_2 are not independent and their particular form leaves only the possibility of the type A transition with q_{EA} growing continuously from zero at T_c.

Above the critical temperature T_c no ergodicity breaking occurs, and the solutions are TTI and satisfy FDT. Below T_c the ergodicity is broken and some scheme must be adopted for the long-time dynamics. In the Sompolinsky approach [141], as discussed in the preceding section, one assumes that the initial time is sent to $-\infty$ keeping the system size large but finite so that the system can equilibrate, and only then is N sent to ∞. Two-time quantities such as correlations and responses are then trivially TTI, but FDT may not be necessarily satisfied for the infinite-size system due to the emergence of infinitely high (free-)energy barriers for $N \to \infty$ where freezing of some degrees of freedom confines the system to a portion of the available phase space. In the finite system, in contrast, all barriers can be surmounted in a finite (but large) time, so the degrees of freedom can be frozen only for times smaller than the typical timescale for barrier crossing. The large number and complex structure of states in the phase space led Sompolinsky to postulate a set of very long timescales, eventually diverging for $N \to \infty$, for (free-)energy barrier crossing. The times are organized hierarchically, i.e., denoting them with t_x, where x is an index varying for convenience in [0, 1], then

$$\lim_{N\to\infty} t_x = \infty \qquad \text{but} \quad \frac{t_{x'}}{t_x} \to \infty \quad \text{if} \quad x > x'. \tag{187}$$

to account for the ultrametric organization of states. When the system is observed at time $t_x \ll t \ll t_{x'}$ all degrees of freedom with relaxation times t_x shorter then t will have relaxed completely, while those with longer relaxation times will remain essentially frozen and cannot contribute to the response at time t to an external perturbation at time zero. The FDT must then be modified to account for the missing contribution of the frozen degrees of freedom. This leads to an *anomalous response term* in the response function which measures the degree

of FDT violation. Since barriers with timescale larger than $t = t_x$ cannot be crossed the correlation function cannot decay to zero but relaxes to

$$q(t_x) = \overline{\langle \sigma_i(t_x)\sigma_i(0)\rangle}. \tag{188}$$

In the thermodynamic limit these partially relaxed states will become stable states of typical size $q(x) = q(t_x)$ since barriers with timescale larger than t_x cannot be surmounted anymore, while those with timescale smaller than t_x have already been crossed several times. The overlap $q(x)$ is a non-decreasing function of x and corresponds in the thermodynamic limit to the Parisi order parameter function of the static calculation. The correlation time-persistent part $q(t_x)$ can be written as a sum of contributions from unrelaxed degrees of freedom [141] (cf (162) for one timescale):

$$q(t_x) = \sum_{x'<x} q'_{x'}. \tag{189}$$

Since the system is equilibrated for timescales smaller than t_x FDT must be satisfied on that timescales. The presence of a time-persistent part in the correlation function and the requirement of FDT for timescales smaller than t_x leads to an extra term (cf (162) for one timescale), called the *anomalous response term* and denoted by Δ'_x, in the response function [141, 158].

Like Parisi's, the Sompolinsky derivation of the self-consistent equations for the overlap and the anomalous response term is heuristic but allows for a dynamical theory which presents many similarities with the static solution. Differing from the usual Parisi solution, however, the Sompolinsky solution is expressed in terms of two order parameter functions: the overlap $q(x)$ and the integrated response function $\Delta(x)$, sum of the anomalous response function terms. This extra freedom, called 'gauge invariance', reflects the time-reparametrization invariance of the Sompolinsky solution: any reparametrization $t_x \to h(t_x)$ where $h(t)$ is an arbitrary well-behaved function preserving relations (187) will lead to an acceptable solution. We have already encountered these properties when discussing non-equilibrium solutions of the spherical p-spin model in section 6.2.1. This fact should not be surprising since it only reflects our lack of knowledge on how the barrier-crossing timescales diverge in the thermodynamic limit. Conversely, we may also say that this invariance is intrinsic in any mean-field solution since the details on how barriers diverge are irrelevant, the only important point is that they diverge. We note indeed that the gauge invariance of the Sompolinsky solution has its static counterpart in the invariance of the replica solution under replica permutations. The Parisi solution corresponds to the 'special' gauge [141]

$$\Delta'(x) = -\beta x q'(x) \tag{190}$$

where the prime means derivation, which relates the anomalous response term to the derivative of the overlap (or time-persistent correlation) at timescale t_x (cf (175)). Equation (190), known by the name of *Parisi's gauge*, is actually an FDT relation.

As already noted in section 6.2.1 the Sompolinsky solution, and its variants, are equilibrium solutions and cannot account for aging phenomena found in spin-glass experiments. To deal with them Cugliandolo and Kurchan have proposed a non-equilibrium scheme in which the thermodynamic limit $N \to \infty$ is taken before any large time limit, including the initial time limit $t_i \to -\infty$, to force the system to a non-equilibrium state [52]. This procedure drives the system to a non-equilibrium regime named weak ergodicity breaking in which TTI is lost and the system displays aging, see section 6.2.1 for more details. The TTI is recovered only for small time separations (the so-called FDT regime) where the dynamics is described by Sompolinsky-like equations and the correlation function approaches the plateau $C = q_{EA}$ with the power law form (180) with a temperature-dependent exponent a.

The departure from the plateau, i.e., the aging or non-FDT regime, is more complex since the presence of many different timescales related to different (free-)energy barriers must be taken into account, and representations such as (179) or (181) cannot be adequate. Adapting the Sompolinsky picture of many timescales to the weak ergodicity breaking regime the non-equilibrium relaxation from time s to time t is due to the crossing of (free-)energy barriers with timescales between s and t. Then, using the time-reparametrization invariance of mean-field solutions, (179) is replaced by the asymptotic form valid for large times [53] (cf (189)),

$$C_{\rm ag}(t,s) \sim \sum_i C_{\rm ag}^{(i)}(h_i(t)/h_i(s)) \tag{191}$$

where each contributing term $C_{\rm ag}^{(i)}$ will vary in each separate time sector defined by two successive barrier crossing and, as in the case of one timescale, the functions $h_i(t)$ could be power law with a time sector dependent exponent $h_i(t) \sim t^{\lambda_i}$. Using the fact that correlations decrease as times become more and more separated, it is possible to show that for large times the following relation must hold,

$$C(t_3,t_1) = f[C(t_3,t_2), C(t_2,t_1)] \qquad t_1 \leqslant t_2 \leqslant t_3 \tag{192}$$

where f is an associative function which defines the geometry of the triangles described by the trajectory in the phase space [53]. Next one defines the fixed point q_i of f as $f(q_i,q_i) = q_i$. The intermediate value of the correlation between two successive fixed points defines a time sector. We note that triangles whose sides belong to different timescales, e.g., $C(t_3,t_2) < q_i$ but $C(t_2,t_1) > q_i$, are isosceles with $C(t_3,t_1) = \min[C(t_3,t_2), C(t_2,t_1)]$. This defines an ultrametric geometry analogous to what is found in equilibrium calculations,

$$C(t_3,t_1) = \min[C(t_3,t_2), C(t_2,t_1)] \tag{193}$$

if at least one $C(t_3,t_2), C(t_2,t_1)$ is less then $q_{\rm EA}$.

The set of fixed points q_i can be either discrete or continuous. In the latter case, the correlation (191) is the limit case of a continuous sum of infinitely many scaling functions $C_{\rm ag}^i$. As for the Sompolinsky approach, the term (191) in the correlation function implies an analogous term in the response function (see (171)) which can be related to the correlation function through (175) with an $X(C)$ no longer constant for $C < q_{\rm EA}$ but which coincides with the function $x(q)$ of the static treatment [159].

We note that for the spherical p-spin model $x(q)$ evaluated from statics is different from that evaluated from dynamics [52, 131, 132]. It can be shown that a sufficient condition for the equality between the static $x(q)$ and $X(q)$ is that the system is stochastically stable [160, 161], i.e., the overlap probability distribution $P_\epsilon(q)$ of the system in the presence of a small perturbation must smoothly converge towards the probability distribution of the unperturbed system when $\epsilon \to 0$. Moreover, the limit $\epsilon \to 0$ must also commute with the limit of large times in the dynamics. If this is the case, $x(q)$ and $X(q)$ are then equal. This result holds for mean-field spin glasses with continuous RSB such as the SK model, but not for the spherical p-spin model where the dynamics is dominated by long-lived metastable states.

6.3. Random manifolds and diffusive models

The basic ingredient of a glass behaviour is the appearance of a multitude of long-lived states, that prevent exploration of the whole phase space. This situation is not restricted to glasses but may be present in several, apparently unrelated, far from equilibrium problems. Typical examples have been discussed in the previous sections, here we shall comment a bit on random manifolds and diffusion models.

A typical situation where glassy behaviour shows up is when studying the dynamics of an elastic manifold, with or without internal structure, in a random quenched environment. This problem appears, for example, in flux lattices in high-T_c superconductors [162], interfaces in random fields [163], charge density waves, and surface growth on disordered substrates [164, 165]. The competition between elastic stress and disorder produces a state with many characteristics of a glass: slow dynamics, non-linear macroscopic response, aging and so on [144, 166]. In the mean-field limit a manifold in a random media is described by a field theory with a large number of components. In this case, it is possible to derive a closed set of dynamical equations of the type discussed for spin-glass models. The model of a manifold of dimension d embedded into a random medium of dimension N is described by the Hamiltonian

$$\mathcal{H}[\phi(\boldsymbol{x})] = \int \mathrm{d}^d x \left(\frac{c}{2} |\nabla \phi(\boldsymbol{x})|^2 + V[\phi(\boldsymbol{x}), \boldsymbol{x}] + \frac{\mu}{2} \phi(\boldsymbol{x})^2 \right) \tag{194}$$

where the N component field $\phi = (\phi_1, \phi_2, \ldots, \phi_N)$ gives the displacement of the manifold. The mass term μ constrains the fluctuations of the manifold to a restricted volume of the embedding space. The potential term V is a Gaussian variable of zero mean and correlations

$$\overline{V[\phi, \boldsymbol{x}] V[\phi', \boldsymbol{x}']} = -N \delta(\boldsymbol{x} - \boldsymbol{x}') \mathcal{V} \left[\frac{(\phi - \phi')^2}{N} \right]. \tag{195}$$

A common choice for $\mathcal{V}$ is

$$\mathcal{V}(z) = \frac{(\theta + z)^{1-\gamma}}{2(1-\gamma)} \tag{196}$$

where θ is the free-energy fluctuation exponent. The models are divided into 'long-range' models if $\gamma < 1$ and 'short-range' models for $\gamma > 1$ since in the first case correlations grow with distance, while in the second case they decay.

The study of the static (equilibrium) properties of the $d = 0$ limit [167], i.e. the case of a particle moving in a random potential, reveals that the short-range case is solved by a 1RSB ansatz, while in the opposite case of long range the full RSB scheme is needed.

The manifold dynamics is given by the usual Langevin equations,

$$\frac{\partial}{\partial t} \phi(\boldsymbol{x}, t) = -\frac{\delta \mathcal{H}[\phi(\boldsymbol{x})]}{\delta \phi(\boldsymbol{x}, t)} + \boldsymbol{\eta}(\boldsymbol{x}, t) \tag{197}$$

where $\boldsymbol{\eta}$ is a Gaussian random process of zero mean and variance

$$\langle \eta_\mu(\boldsymbol{x}, t) \eta_\nu(\boldsymbol{x}', t') \rangle = 2T \delta_{\mu\nu} \delta(\boldsymbol{x} - \boldsymbol{x}') \delta(t - t'). \tag{198}$$

To study the long-time dynamics one introduces two-time quantities, which for the simple case of $d = 0$ are the usual correlation and response functions

$$C(t, s) = \frac{1}{N} \overline{\langle \phi(t) \cdot \phi(s) \rangle} \qquad R(t, s) = \frac{1}{N} \frac{\overline{\delta \langle \phi(t) \rangle}}{\delta \boldsymbol{h}(s)} \tag{199}$$

where $\boldsymbol{h}(s)$ is a small perturbation applied at time $s < t$. In addition, one also considers the mean-square displacement correlation function

$$\begin{aligned} B(t, s) &= \frac{1}{N} \overline{\langle [\phi(t) - \phi(s)]^2 \rangle} \\ &= C(t, t) + C(s, s) - 2C(t, s). \end{aligned} \tag{200}$$

The analysis of the long-time dynamics for $N \to \infty$ reveals that in both cases (long- and short-range models), two regimes can be defined in the relaxation from an initial random configuration: (i) FDT regime for large waiting time t_w and not too large time difference; (ii) non-FDT regime for large t_w and time differences. Under the assumption of a weak ergodicity

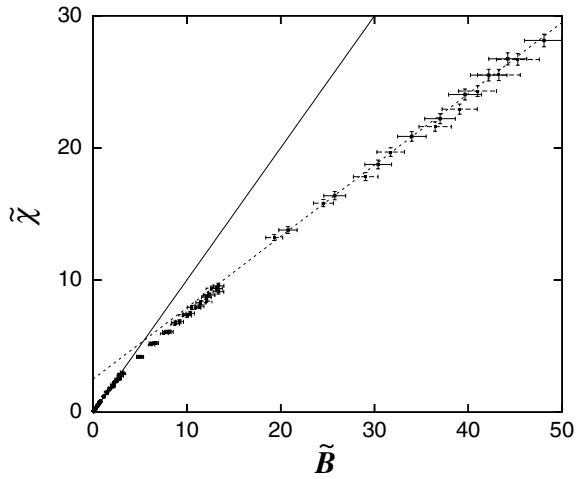

Figure 8. FD plot in the model of directed polymers in random media revealing the 1RSB or two-timescale character of the dynamics. From [168].

breaking scenario, the FDT in the non-FDT regime can be replaced by the generalized form (176) with a function X which is different for short- and long-range models [144]. For short-range models, $X(C)$ is solved with the two-timescale ansatz, i.e., it is 1 in the stationary sector while it is a constant smaller than 1 in the aging sector. For long-range models many timescales are needed, and $X(C)$ is a non-trivial non-constant function, as found for the SK model. This scenario has been extended to the $d > 0$ case in [166].

Related studies have analysed FDT violations in polymer models. Yoshino [168] considered the directed polymer model in random media (i.e. the random manifold (194) with $c = 0$ and $N = d = 1$) and through numerical simulations confirmed the two-timescale character of aging dynamics, see figure 8. Pittard and Shakhnovich [169] have considered a heteropolymer model with uncorrelated monomer–monomer interactions. By analysing the mode-coupling equations they found a two-timescale solution that violates FDT as reported for the random manifold model in the short-range case.

The dynamics of the directed polymer reduces to pure diffusion in the absence of disorder. This is the well-known random walk which in the continuum limit is represented by a stochastic variable $x(t)$ satisfying the (stochastic) differential equation

$$\frac{\mathrm{d}}{\mathrm{d}t}x(t) = \eta(t) \tag{201}$$

where η is a Gaussian random process of zero mean and correlation

$$\langle \eta(t)\eta(s)\rangle = 2T\delta(t-s) \tag{202}$$

and T is the bath temperature. A simple calculation gives for the two-time correlation and response functions

$$C(t,s) = \langle x(t)x(s)\rangle = 2T\min(t,s) \tag{203}$$

$$R(t,s) = \frac{\delta\langle x(t)\rangle}{\delta h(s)} = \theta(t-s) \tag{204}$$

where $h(t)$ is an external field added to the lhs of equation (201). As a consequence, we see that for any t and s

$$X(t,s) \equiv TR(t,s)/[\partial C(t,s)/\partial s] = 1/2 \tag{205}$$

a constant value different from 1 so that the FDT [170]. Despite violation of FDT, the model is simpler than those discussed above, indeed the correlation and the IRF show a rather simple form as a function of the waiting time:

$$C(t,s) = 2Ts \qquad \chi(t,s) = \int_0^s \mathrm{d}t' R(t,t') = s. \tag{206}$$

They both depend on s but not on t (as required by causality). This is a rather extreme example, however other less trivial cases, such as spinodal decomposition, scalar fields at criticality and so on also exhibit non-trivial non-equilibrium behaviour [170]. More complicated non-linear diffusion effective models have been shown [171, 172] to display FDT violations compatible with a one-timescale aging scenario with a single valued FDR $X(t_w) < 1$ that monotonically converges to 1 as in entropic models (section 6.5).

6.4. Trap models

A successful family of models to describe the glass transition are phenomenological trap models. The dynamics in the aging regime can be understood in terms of jumps among different phase space components, each jump corresponding to a new rearrangement of a cooperative spatially localized region. The dynamics of the system can then be viewed as an intermittent motion where some regions remain inactive for a long time (and no net heat current is present between the system and its surroundings) until an activated jump occurs and thermal heat is released from the system to the surroundings, and from there, to the thermal bath. Phenomenological trap models, contrary to mode-coupling theories, are based on the activated nature of glassy dynamics. Although trap models have appeared from time to time in the literature (see [39] and references therein) the most recent and successful study is due to Bouchaud [40] who has considered its relevance to describe aging phenomena in glassy systems.

The trap model corresponds to a set of unstructured energy (or free energy) traps that live in a 'free-energy space' without any explicit reference to real-space configurations. It corresponds, in many aspects, to the coarse-grained description developed in section 4.2 where activated processes are represented as transitions between different phase space components $\mathcal{R}$ that here could be visualized as traps. The number of traps, like the number of components $\mathcal{R}$ in the coarse-grained description of the phase space, is exponentially large with the volume of the system. The model is defined by a set of traps of different depths E (with $E > 0$) with a density $\rho(E)$ and a distribution of escape times given by the Arrhenius expression $\tau(E) = \tau_0 \exp(E/T)$ where τ_0 is a microscopic time and T is the temperature of the bath. Note that, in this last expression, the top level for all barriers is fixed at zero height. The dynamics of the trap model is then described by the ME (79) discussed in section 4.2 in terms of the probability function $P(E,t)$ that specifies the probability that the system stays in a trap of energy E at time t,

$$\frac{\partial P(E,t)}{\partial t} = \sum_{E'} P(E',t) Z(E|E') - \sum_{E'} P(E,t) Z(E'|E). \tag{207}$$

The rates $Z(E|E')$ are assumed to be given by (82)

$$Z(E|E') = \mathcal{W}(E|E')\rho(E) = \frac{\rho(E)}{\tau(E')} \qquad \int_0^\infty \rho(E)\,\mathrm{d}E = 1 \tag{208}$$

where we have identified $\Omega(\mathcal{F}', T) \equiv \rho(E')$ and where the bare rate $\mathcal{W}(E|E') = 1/\tau(E')$ has the dimensions of a frequency. Note that this bare rate only depends on the energy of the departure trap but not on the energy of the arrival trap. Other versions of the trap model

include a dependence on the energy on the arrival trap, see for instance [173]. Inserting (208) into (207) we obtain

$$\frac{\partial P(E,t)}{\partial t} = \omega(t)\rho(E) - \frac{P(E,t)}{\tau(E)} \tag{209}$$

where

$$\omega(t) = \int_0^\infty \mathrm{d}E' \frac{P(E',t)}{\tau(E')}. \tag{210}$$

The rates (208) satisfy detailed balance if $P^{\mathrm{eq}}(E) \propto \rho(E)\tau(E)$, where $\lim_{t\to\infty} P(E,t) = P^{\mathrm{eq}}(E)$. The Bouchaud trap model (BTM) [40] is described by the distribution $\rho(E) = (1/T_{\mathrm{g}})\exp(-E/T_{\mathrm{g}})$. The static formulation of such a model corresponds to the random energy model (REM) of Derrida [174, 175]. Other trap models have considered a Gaussian distribution of energies [39, 176]. However, the main interest of the model proposed by Bouchaud is the existence of a critical temperature T_{g} where the distribution $P^{\mathrm{eq}}(E)$ ceases to be normalizable. In general, for any distribution $\rho(E)$ the temperature T_0 that marks the onset of the non-normalizability of $P^{\mathrm{eq}}(E)$ is given by [177],

$$\frac{1}{T_0} = -\lim_{E\to\infty} \frac{\log(\rho(E))}{E} \tag{211}$$

the BTM corresponding to the case $T_0 = T_{\mathrm{g}}$. Let us note that, in the trap model, energies are not extensive but finite. Comparing the BTM with the REM, where energies are extensive, we observe that the finite T dynamics in the Bouchaud model occurs in a range of finite energies around E_0, the value at which the energy freezes in the REM below T_{g}. The same exponential distribution of states, over a finite free-energy interval, is found in the SK model [35, 48].

Dynamics in the trap model has been exhaustively investigated in many works. In particular, it offers a rather good explanation of magnetic relaxation phenomena observed in spin glasses [40, 178, 179], viscosity anomalies in glasses [176, 177, 180] and, more recently, it has been used as a test model to check whether FDT violations are well described by the ansatz (91) and whether FD plots are meaningful [54, 55]. Correlation and response functions can be defined in the BTM by assigning magnetizations to the different traps as is done to analyse the statics of the REM. The effect of the magnetic field on the traps is to modify the escape time by the relation $\tau_h(E) = \tau_0 \exp((E + mh)/T) = \tau(E)\exp(mh/T)$. The resulting FD plots have been analysed by Sollich and co-workers [54, 55]. As remarked in [54, 55], equal time correlations can be unbounded so proper FD plots are constructed from the raw plots (102) by normalizing correlations and IRF by the equal times correlation at the later time $C_{A,B}(t,t)$ as described in (104). The ME (209), modified to include the effect of the field, is described by a probability distribution $P(E,m,t) = P(E,t)\sigma(m|E)$ where $\sigma(m|E)$ is the probability that a trap of depth E has magnetization m. This probability is assumed to be a Gaussian parametrized by its mean $\overline{m}(E)$ and variance $\Delta^2(E)$. As there is no specific meaning attached to the observable m one can think of the two functions $\overline{m}(E)$, $\Delta^2(E)$ as describing different class of observables. Therefore, observable dependence in the BTM refers to dependence of the FD plots on the choice of these functions. The following cases have been considered [54, 55]: $\overline{m}(E) = \exp(nE/2T)$, $\Delta^2(E) = 0$ or $\overline{m}(E) = 0$, $\Delta^2(E) = \exp(nE/T)$ with $n > T - 1$ in both cases. Figure 9 shows some typical FD plots.

There are three main results of this study: (1) the FD plots strongly depend on the average and the variance of the Gaussian distribution, therefore the FDR and the effective temperature are observable dependent; (2) most importantly, for a given choice of observables the effective temperature (132) smoothly changes with time within a given time sector. In fact, in the trap model the scaling t/t_w is fulfilled in the glassy phase $T < T_{\mathrm{g}}$ but two straight lines (typical

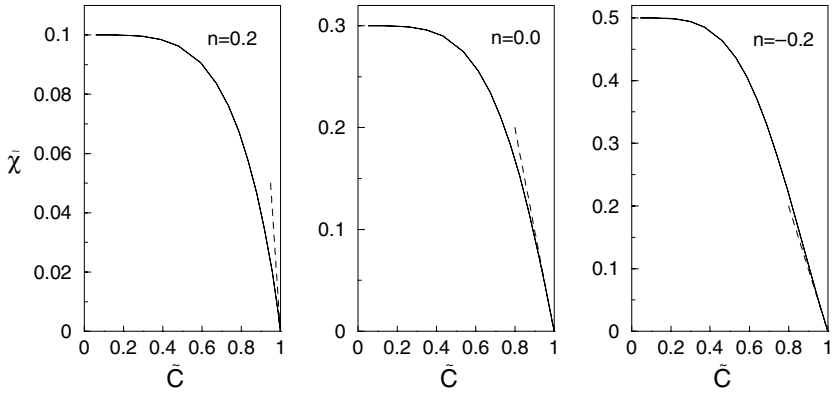

Figure 9. Normalized FD plots (104) for the BTM for a Gaussian distribution of trap magnetizations with zero mean and variance $\Delta(E) = \exp(nE/T)$ for different values of n and $T = 0.3$ ($\tau_0 = T_g = 1$). For each n times shown are $10^6, 10^7$ which are indistinguishable since the limiting FD plot has been reached. Note, however, that a temperature factor has been absorbed in $\tilde{\chi}$ in such a way that the slope is -1 at equilibrium (dashed line). From [54, 55].

of two-timescale glassy systems) are not observed in the FD plots; (3) for all observables $X_\infty = 0$, see (231), supporting the conjecture that this quantity is indeed universal and may have some physical meaning (see section 6.6).

Among these results (2) seems particularly interesting. Why plots FD do not display the characteristic two-step form of relaxational systems with two timescales? Still for observables with zero mean and finite (but E independent) variance where $C(t, t) = \Delta^2$, i.e. for observables that can be considered neutral (see discussion in section 4.4), the one-step shape of the limiting FD plot is absent. The origin of this discrepancy is presently unknown and finding a trap model that shows a two straight-line FD plot remains an interesting open problem[9]. Let us finish these considerations by noting that FD plots, such as that depicted in figure 9, are more characteristic of systems with full RSB where $X(C)$ is a non-trivial function. Quite interestingly, it has been shown [179] that the BTM at the critical temperature $T = T_g$ has correlations that do not fulfil the simple t/t_w scaling but a more complicated dependence with many time sectors and ultrametricity. However, the resulting FD plot at criticality shows only very small deviations from the equilibrium behaviour $X = 1$, being very similar to the FD plot observed in the Ising chain [182] (see section 6.6).

Just before ending this section, let us recall that these results have been endorsed by considering the corresponding driven version of the BTM introduced in [183, 184] in the context of rheology. In this case, as explained in section 7.4.1, the equivalent of the waiting time is the inverse of the shearing rate. In the stationary state TTI is satisfied but FDT violations persist. For the driven model [185], as well as for the purely relaxational model, the same relationship between correlations and responses holds and the two models (the non-driven and the driven one) show similar behaviour.

6.5. Models with entropy barriers

Many of the results described in the previous subsections deal with disordered models with complex thermodynamics. However, many aspects of the violations of the equilibrium FDT

[9] After completion of this work, it has been shown that the influence of the dependence of the perturbed rates in a field (upon the observable value taken at the arrival trap) is crucial to get well-defined limiting FDRs and effective temperatures [181].

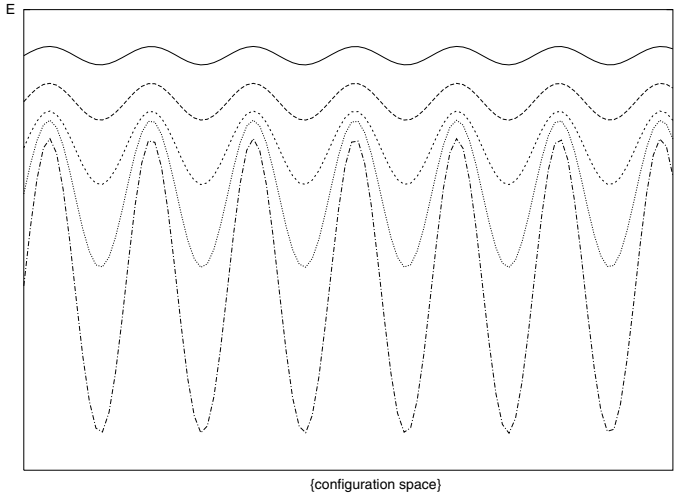

Figure 10. A typical energy landscape in a glassy model determined by the presence of entropy barriers. The *effective* barrier $\log(\tau(E))$ increases as E decreases. From [187].

as well as the existence of an QFDT can be investigated in the framework of simpler models that are exactly solvable but still retain the key ingredients for the emergence of these new properties. In turn, this can help to identify the basic ingredient that any sensible general theory must incorporate.

The scope of this section is mainly illustrative as it intends to present some of the basic ideas of section 4.2 applied to very simple examples. We will focus our discussion on the oscillator (OSC) and the backgammon (BG) models. A comprehensive account of other results about these models can be found in a recent review [15]. Both models have a simple energy landscape and dynamics is determined by the presence of entropy barriers. The intuitive meaning of this term is the following. In general, relaxation in glassy models proceeds by activated jumps over energy barriers that allow the system to escape from a given trap after reaching a barrier of height B, the typical time needed in this process being given by the Arrhenius law $\tau \sim \exp(B/T)$. Activated dynamics is strongly temperature dependent, and for $T = 0$ the dynamics is completely arrested, the system remains trapped forever and correlations no longer decay to zero (ergodicity is broken). When the dynamics is dominated by entropy barriers the relaxational mechanism is different. The system escapes from a trap through a process which involves a timescale τ which does not directly depend on the temperature but, for instance, on the typical energy E of the trap itself, $\tau(E)$, which usually is a decreasing function of the energy E (see figure 10)[10]. At $T = 0$ relaxation is not arrested but proceeds slower as the energy decreases. This type of dynamics is sometimes called marginal dynamics [186] as the system wanders around saddle point configurations, hence is never arrested. Of course, the temperature dependence of the relaxation time in entropic models can appear as effectively activated: at finite (but low) temperatures the maximum value of $\tau(E)$ corresponds to the lowest energy reached, i.e. $\tau(E_{\rm eq}(T))$, $E_{\rm eq}(T)$ denoting the equilibrium energy. The temperature dependence of the relaxation time in equilibrium $\tau(E_{\rm eq}(T))$ is activated in most entropy barrier models. A phenomenological description of these entropy models has been introduced by Barrat and Mezard [173] who have generalized the BTM to the case where the distribution of trapping times is itself a time-dependent function. The oscillator

[10] Now we assume the standard convention for energies being negative rather than positive as in the trap model.

and backgammon models described in this section are microscopic versions of this entropic trap model. According to the scenario presented in section 4.2, the role of entropy appears to be important as relaxation in many glassy systems is accompanied by the emergence of a non-equilibrium microcanonical ensemble which determines fluctuations and responses in the aging state, leading to the existence of QFDT and an effective temperature. This fact suggests that a deep comprehension of the glassy dynamics in exactly solvable entropy barrier models can be a first step towards grasping the leading aspects behind the behaviour of more realistic systems, where both entropy and energy barriers simultaneously intervene.

6.5.1. Oscillator models. We begin our discussion by describing the OSC model in its simplest version. A review of some results can be found in [15, 68, 188]. Originally, oscillator models were introduced indirectly in the analysis of the Monte Carlo dynamics of the spherical Sherrington–Kirkpatrick model, which can be mapped to a set of disordered harmonic oscillators [189, 190]. The OSC model is obtained by simplifying the previous one to an ensemble of identical harmonic oscillators [191]. The OSC model is defined by the following energy function,

$$E = \frac{K}{2} \sum_i x_i^2 \tag{212}$$

where the x_i are real-valued displacement variables for the N oscillators and $K > 0$ is the Hooke constant. The equilibrium properties are trivial due to the absence of interactions, but the Monte Carlo dynamics couples the oscillators in a non-trivial way. Moves are proposed according to the following rule,

$$x_i \to x_i' = x_i + \frac{r_i}{\sqrt{N}} \tag{213}$$

where the r_i are Gaussian random variables with zero mean and variance Δ^2. Moves are accepted according to the usual Metropolis rule. Each move is a parallel update of the whole set of oscillators. Both the energy function (212) and the dynamics (213) are invariant under rotations in the N-dimensional space of the x_i. This symmetry makes the dynamics exactly solvable, and many non-equilibrium quantities, e.g., effective temperatures and FDT violations, can be tackled analytically.

The OSC model is a classical model where the equilibrium entropy is given by $S(T) = \frac{1}{2}\log(T)$, thereby diverging when $T \to 0$ as expected for a continuous model (the ground state is a zero-measure state corresponding to the absolute global minimum of (212), i.e. the configuration $x_i = 0, \forall i$). At $T = 0$ only those moves that decrease the energy are accepted, therefore as the system approaches the global minimum the frequency of accepted moves (213) dramatically decreases. However, that frequency never vanishes so dynamics is never arrested. Dynamics slows down because phase space directions where energy decreases are exceedingly difficult to find. The full solution of the OSC model has been presented in [191].

The main physical quantity containing detailed information about the dynamical evolution is the probability density of energy changes $P(\Delta E)$. This quantity expresses the probability density that a proposed move (213) changes the total energy of the ensemble by the amount ΔE. $P(\Delta E)$ was originally derived in [191] using standard integration tools. Here we present two other alternative derivations which help to understand the mechanisms behind slow relaxation.

The first method relies on the Gaussian form of the distribution while the second one uses a microcanonical argument to count the number of accessible configurations from a reference

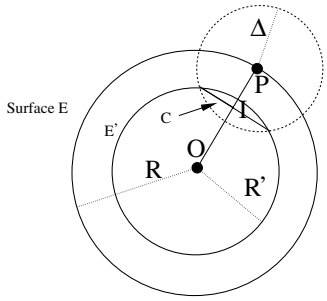

Figure 11. Geometrical construction to compute $P(\Delta E)$. The thick lines denote the departing and final energy hypersurfaces centred at O. The dashed circle indicates the hypersurface accessible from point P. The intersection region between the accessible hypersphere centred at P and the final hypersurface of energy E' defines a hypersurface I of radius C (the radius is represented by a thick line). See the text for explanation.

configuration with a given energy E. The first derivation is rather simple as the distribution for ΔE can be easily obtained. Indeed using (212) and (213)

$$\Delta E = \frac{K}{\sqrt{N}} \sum_i x_i r_i + \frac{K}{2N} \sum_i r_i^2 \tag{214}$$

and the Gaussian property of r_i, it follows that ΔE has a Gaussian distribution. The mean and variance of the distribution are $M_{\Delta E} = \overline{\Delta E} = K\Delta^2/2, \sigma_{\Delta E} = \overline{(\Delta E)^2} - (\overline{\Delta E})^2 = 2EK\Delta^2/N$, yielding [191],

$$P(\Delta E) = \left(4\pi e K \Delta^2\right)^{-\frac{1}{2}} \exp\left[-\frac{\left(\Delta E - \frac{K\Delta^2}{2}\right)^2}{4eK\Delta^2}\right] \tag{215}$$

where $e = E/N$ is the energy per oscillator.

The second method to derive (215) is based on a microcanonical computation. In figure 11 we depict a schematic two-dimensional (2D) representation of the motion of a representative configuration in phase space. The reference configuration $\left\{x_i^0\right\}$ at a given time has an energy E and lies on the spherical hypersurface of radius $R = \sqrt{2E/K}$ (depicted as the point P in the figure) with centre at the origin $\{x_i = 0\}$ (point O in the figure). The smaller dashed circle represents the region of points accessible from $\left\{x_i^0\right\}$ according to the dynamics (213). All accessible points $\{x_i\}$ satisfy $\sum_i \left(x_i - x_i^0\right)^2 = \Delta^2$, i.e. lie at a distance Δ from $\left\{x_i^0\right\}$ which is the radius of the smaller dashed circle. The accessible configurations in a single move lie in a spherical hypersurface of dimension $N-2$ corresponding to the intersection of the hypersurface of energy E' and the smaller spherical hypersurface of radius Δ. We call this region the intersecting region I as shown in figure 11. The final configurations contained in I lie at a distance $R' = \sqrt{2E'/K}$ to the origin O. The change in energy associated with this transition is $\Delta E = E' - E$. The probability of this jump is therefore proportional to the surface of the intersection region, $P(\Delta E) \propto C^{N-2}$, where C is the radius of the intersecting region. The computation of C is quite straightforward as can be deduced from the triangle including the points P, O as vertices and whose three sides are R, R', Δ. In terms of R, R' and Δ, the distance C is given by the relation

$$C^2 = \Delta^2 - \frac{K}{8E}\left(\frac{2\Delta E}{K} + \Delta^2\right)^2. \tag{216}$$

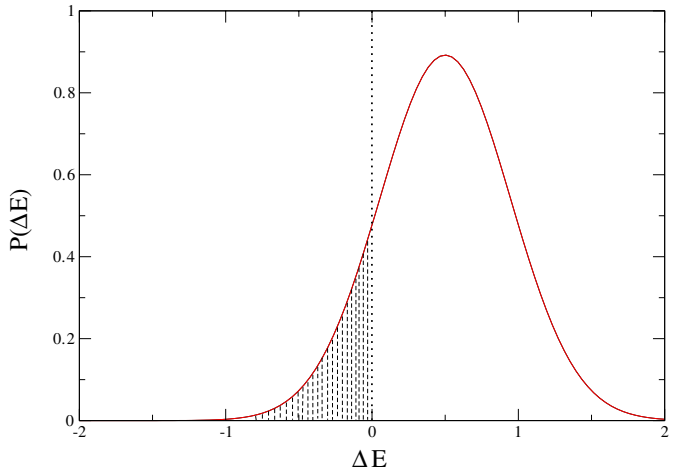

Figure 12. Probability density of the energy of the proposed moves for different values of the energy E as defined in figure 11.

The surface $\Omega(E, \Delta E)$ corresponding to the region I of radius C, relative to the energy E of the reference configuration $\boldsymbol{x}^0$ is

$$\Omega(E, \Delta E) \propto C^{N-2} = \left[\Delta^2 - \frac{K}{8E}\left(\frac{2\Delta E}{K} + \Delta^2\right)^2\right]^{\frac{N-2}{2}}. \tag{217}$$

Using the fact that E is extensive with N this expression can be rewritten as

$$\Omega(E, \Delta E) \propto \exp\left[-\frac{\left(\Delta E - \frac{K\Delta^2}{2}\right)^2}{4(E/N)K\Delta^2}\right] \tag{218}$$

which is proportional to the probability distribution (215).

The distribution $P(\Delta E)$ is depicted in figure 12 for different values of the energy. As E decreases the number of moves with $\Delta E < 0$ shrinks as the total area under the curve with $\Delta E < 0$ decreases. From (215) the dynamical equations immediately follow by defining a Monte Carlo step as a collection of M elementary moves (each elementary move corresponds to a global change of all oscillator coordinates as described in (213)). Because the average change of energy ΔE is finite in an elementary move and the total energy (212) is extensive, the number of moves M in a Monte Carlo step must be proportional to N. For simplicity, we will take $M = N$. In the limit $N \to \infty$, time becomes a continuous variable. This allows us to write a closed equation for the energy E and acceptance rate A, i.e., the average number of accepted moves in a Monte Carlo step,

$$\frac{\partial E}{\partial t} = \int_{-\infty}^{\infty} x\,P(x)W(x)\,\mathrm{d}x \tag{219}$$

$$\frac{\partial A}{\partial t} = \int_{-\infty}^{\infty} P(x)W(x)\,\mathrm{d}x \tag{220}$$

where $P(x)$ is the probability distribution (215) and $W(x)$ is the transition rate which ensures that detailed balance is obeyed. For instance, according to the Metropolis rule

$W(x) = \min[1, \exp(-\beta x)]$ or in heat-bath $W(x) = 1/[1+\exp(\beta x)]$. At zero temperature the transition rate rules $W(x)$ converge to $W(x) = \theta(x)$. In this limit (219), (220) become

$$\frac{\partial E}{\partial t} = \int_{-\infty}^{0} x P(x)\,\mathrm{d}x \tag{221}$$

$$A(t) = \int_{-\infty}^{0} P(x)\,\mathrm{d}x. \tag{222}$$

As shown in figure 12 the acceptance is given by the shaded area enclosed in the negative tail of the distribution. At zero temperature, according to (215), both the mean and the width of the Gaussian decrease as well as the shaded area in figure 12, implying a systematic decrease of the acceptance rate.

We do not want to dwell here on all results one can learn by solving the dynamical equations (221), (222) (see [108, 191]). Interestingly, in the OSC model the FDR (131) for the magnetization $M = \sum_{i=1}^{N} x_i$ can be exactly computed at any temperature [191],

$$T_{\mathrm{eff}}(s) = 2E(s) + \frac{1}{f(s)}\frac{\partial E(s)}{\partial s} \tag{223}$$

and the QFDT is satisfied. At $T = 0$ in the large time limit one gets $T_{\mathrm{eff}}(s) = 2E(s)$ plus subleading corrections. This result shows that FD plots are straight lines starting at $C(s,s) = (2E(s)/K)$, $\chi(s,s) = 0$ and finishing at $C = 0$, $\chi = 1/K$. The relation between the effective temperature and the dynamical energy is exactly the same as the equilibrium relation given by the equipartition theorem. The aging system is in a quasi-stationary state where relations between dynamical quantities are formally the same as in equilibrium. This allows us to define a time-dependent configurational entropy $S_c(E)$ through the relation (90),

$$\frac{1}{T_{\mathrm{eff}}(E)} = \frac{\partial S_c(E)}{\partial E} \qquad S_c(t) = S_c(E(t)) = \frac{1}{2}\ln(E(t)). \tag{224}$$

Until now we have discussed some of the analytical results obtained by solving the dynamical equations of the OSC model. However, an interesting question is the following: can we determine the value of the effective temperature from the sole evolution of the energy E without having to analyse correlations and responses in the framework of the QFDT as described in (223)? Ideally, we would like to apply the ideas presented in section 4.2 to identify the value of T_{eff} solely from the off-equilibrium transition rates $Z(F|F')$. In that description dynamics proceeds by activated jumps over different states, whose dynamics is described by the free-energy ME (79). What are the states in the reduced description of the OSC model? As the energy landscape is a single parabolic well it appears that a reduced description is not possible. The clue to this question is easy to understand if one realizes that at zero temperature the acceptance of the dynamics goes to zero with time, therefore each time a proposed elementary move is accepted we can effectively consider that the system has jumped from one state to another, the typical time for this jump steadily growing with the time elapsed since the system was quenched. In this view, each state corresponds to a configuration and the reduced dynamics simplifies. Moreover, the free energy of the state is simply the energy of the corresponding configuration. In the asymptotic regime $(\mathrm{d}E/\mathrm{d}t)/E \ll 1$, where finite-size effects are not important, i.e. $\Delta \ll \sqrt{2E/K}$, the probability distribution describing the energy change after the first jump is given by

$$P(\Delta E) \sim \exp\Big(\frac{\Delta E}{4e}\Big)\theta(-\Delta E) \tag{225}$$

where we used (215) and expanded it around $\Delta E = 0$ up to linear order. Using relation (224) we can recast (225) in the following form,

$$P(\Delta E) = \frac{1}{2T_{\rm eff}(E)} \exp\left(\frac{\Delta E}{2T_{\rm eff}(E)}\right) \theta(-\Delta E) \tag{226}$$

showing that the statistics of energy jumps is an exponential with a width that directly depends on the effective temperature. This result has two consequences: (1) it shows that the OSC model is a microscopic version of the trap model proposed by Barrat and Mezard [173]; (2) the effective temperature could be computed from the statistics of the first free-energy jumps among components (here corresponding to configurations).

Before finishing, let us note that a number of variants of the oscillator model have been considered, all sharing the feature that oscillators do not interact. For example, Nieuwenhuizen and Leuzzi [108, 192–194] have considered a model with spin variables in addition to oscillators. The new variables are discrete and used to mimic fast relaxational processes not contained in the original formulation; aging, slow relaxation in these models, can still be described in terms of entropy barriers.

6.5.2. The backgammon and urn models. Another instructive model where relaxation is determined by entropic barriers is the backgammon (BG) model [195]. The model belongs to a large class of models under the name of urn models where N particles or balls are distributed among M urns or boxes. The BG model is defined by the energy function,

$$E = -\sum_{r=1}^{M} \delta_{n_r,0} = -N_{\rm empty} \tag{227}$$

where n_r stand for the occupancies for each box and $N_{\rm empty}$ stands for the number of empty boxes. The model has different versions [196] according to whether particles are distinguishable (Maxwell–Boltzmann statistics) or not (Bose–Einstein statistics). The easiest way to compute the thermodynamic properties of the BG model is by expressing the partition function in terms of the occupancies n_r rather than in terms of the set of boxes occupied by the particles. In the Maxwell–Boltzmann case, thermodynamics needs to be corrected by dividing the partition function by the usual $N!$ term to avoid Gibbs' paradox. In the model with Bose–Einstein statistics this is not necessary. The dynamical rules of the BG model directly depend on the type of statistics considered. In the Maxwell–Boltzmann case, a departure box d is selected with a probability proportional to the occupancy n_d of that box and a new arrival box n_a is selected with uniform probability. The proposed move is given by $n_d \to n_d - 1, n_a \to n_a + 1$ and accepted according to the standard Metropolis rule. Instead, in the Bose–Einstein case, the proposed move and the transition rate are the same as for the Maxwell–Boltzmann case but both the departure and the arrival box d and a are selected with a uniform probability $1/M$.

The resulting dynamics of the model is strongly dependent on the type of statistics considered, the interesting one corresponding to the Maxwell–Boltzmann case which displays a strong separation of timescales. In what follows, unless otherwise stated, we will concentrate on the analysis of the model with $M = N$.

The thermodynamics of the model is exactly solvable and the entropy is given by $S(e) = \log(1 + e)$ where $e = E/N$ denotes the entropy per box (or per particle). To analyse the dynamics from the perspective of the scenario described in section 4.2 we follow a similar reasoning as we did for the OSC model. Let us consider a system quenched down to $T = 0$ and the aging regime reached in the asymptotic long-time regime where $(\mathrm{d}E/\mathrm{d}t)/E \ll 1$. In that limit, the system has a number of empty boxes $N_{\rm empty} = -E$ and further decrease of that number by one unit $\Delta E = -1$ requires a time that grows exceedingly as E decreases towards its minimum value $E = -N + 1$ (all particles condensed into a single box) [197, 198]. Therefore, as relaxation slows down, for a long time the system wanders through the constant

energy surface by exchanging particles among occupied boxes. When a new box is emptied the energy decreases by one unit. As we did in the OSC model, also in the $T = 0$ dynamics of the BG model each component $\mathcal{R}$ corresponds to a single configuration with free energy equal to the energy of that configuration.

The transition rate for going from a configuration of energy E to a configuration of energy $E - 1$ is solely a function of the number of available configurations in the initial and final states,

$$\frac{Z_t(E-1|E)}{Z_t(E|E)} = \frac{\Omega(E-1)}{\Omega(E)} \tag{228}$$

where the rate frequency $1/t(E)$ associated with Z_t (for its definition, see section 4.2) has cancelled out from the numerator and denominator on the left-hand side of (228). As E is extensive with N, and using (83), we obtain

$$\frac{Z_t(E-1|E)}{Z_t(E|E)} = \exp\left(-\frac{\partial S(E)}{\partial E}\right) = \exp\left(-\frac{1}{T_{\rm eff}(t)}\right). \tag{229}$$

Equation (229) provides a way to estimate the effective temperature by looking at the number of moves required for a move to decrease the energy by one unit. Inverting (229) yields

$$T_{\rm eff}(t) = \left(\ln\left[\frac{Z_t(E|E)}{Z_t(E-1|E)}\right]\right)^{-1} = \frac{1}{N^*(t)}. \tag{230}$$

Therefore the ratio $Z_t(E|E)/Z_t(E-1|E)$ is simply given by the inverse of the number of *accepted* moves N^* required to decrease the energy by one unit. We stress that N^* is not the number of MC steps but rather the number of accepted elementary moves with $\Delta E = 0$ required until a move with $\Delta E = -1$ is found. This number N^* is independent of the size of the system. Note also that the rate of rejected moves (which gives the acceptance) does not enter into the expression of the effective temperature but rather into the value of the typical timescale $t(E)$ associated with the jump. This is an essential ingredient required in any 'quasi-equilibrium' or microcanonical description of the relaxation. The value of the effective temperature at a given time only depends on the number of accessible states with lower free energy (energy in the present model) and not on the time necessary to escape from that state. This expression is very amenable to numerical calculations.

Note that the energy levels in the BG model are discrete, therefore the relation (226) cannot be applied. However, one can consider a non-degenerate disordered BG model where boxes are assigned different energies [187]. In this case, the distribution $P(\Delta E)$ has been derived and shown to have an exponential time-dependent behaviour characteristic of trap models. However, the computation of the effective temperature in that model and the verification of (226) have not yet been done.

The backgammon model as well as some of its variants have been solved by the technique of the generating function [196,199–205]. A discussion of some of the main results and analytical techniques has been presented in [15]. The origin of the effective temperature as derived from the QFDT remains as yet not completely understood. No neutral observable has yet been identified in the BG model. Although all studied observables show that the QFDT (94) is verified in a one-timescale scenario, there seem to be different effective temperatures depending upon the observable considered [202, 204, 206]. On the other hand, none of the different effective temperatures associated with these observables appear to be linked to the *effective* temperature obtained within the adiabatic approximation [199]. An interesting variant of the urn model is the zeta-urn model introduced in the context of quantum gravity that shows a finite-temperature Bose–Einstein condensation transition [207, 208], see section 6.6.

6.6. Ferromagnetic models at criticality

A new emerging line of research related to the mainstream of research on FDT violations in glassy systems, is the study of FDT violations at critical points. At critical points the relaxation time diverges and one can investigate, for instance through field-theoretical methods, the time dependence of correlations, responses and the resulting FDR (91) in the asymptotic regime $s \to \infty$. These types of investigations are no different from those undertaken in the study of coarsening behaviour in ordered phases. The main difference between the slow dynamics at a critical point and coarsening is that, in the former case, critical slowing down is at the origin of the slow dynamics. Interfaces have no stiffness tension and their motion is subdiffusive (or diffusive) and only a consequence of the curvature of the interface. Growing domains are not islands of up or down spins but regions of spatially and temporally correlated spins of zero net magnetization. At T_c the dynamics is described by the renormalization-group dynamical equations of the corresponding finite-temperature fixed point. However, in coarsening systems below T_c activated processes are important and interfaces have non-zero tension as they separate domains of up and down spins. Competition between the curvature of the surface and its tension leads to different growth laws, described by the zero-temperature fixed point. Because the origin of slow dynamics at T_c is different from that in standard glassy systems, the main ansatz (91) may not hold. Indeed, many studies of the FDR at criticality reveal that $X(t, s)$ is not a single function of the correlation $C(t, s)$.

One among the first studies of ferromagnetic models at criticality is the Ising chain solved by Glauber in 1963 [209]. Strictly speaking, the dynamics of this model is that of a coarsening model as the system orders at the critical point $T = 0$ where the magnetization discontinuously jumps from 0 (for $T > 0$) to 1 (at $T = 0$), i.e. the critical exponent β vanishes. We will see below that the ferromagnetic Ising chain has some peculiar properties. Starting from a random initial configuration the coarsening dynamics at $T = 0$ has long been studied in [210] and revisited in [211]. In the asymptotic long-time limit, the aging part of the two-times correlation functions scales like $C_{ag}(t, s) \sim F(L(t)/L(s))$ (252) with $L(t) \sim t^{1/2}$ corresponding to a diffusive process of the interfaces (see section 7.3). More recently, and nearly at the same time, the FDR has been analytically computed [212, 182] for a random staggered perturbation finding $X(C) = 1/[2 - \sin^2(\pi C/2)]$ in agreement with the ansatz (91); or, in terms of times, $X(t, s) = \frac{1}{2}(1 + s/t)$ showing that $X \to 1/2$ if $t \to \infty$ or $C \to 0$. This last result coincides with that found in the random walk or in the Gaussian model [170], all models characterized by diffusive dynamics. This has led to the proposal [205, 213] that, in systems at criticality, the limiting value $X(t, s)$ for $t \to \infty$ is a universal quantity,

$$X_\infty = \lim_{s\to\infty} \lim_{t\to\infty} X(t, s). \tag{231}$$

This conclusion has been substantiated by the exact solution of the ferromagnetic spherical model in general d dimensions [205, 213]. The authors have noted how X_∞ is only a function of amplitude ratios describing the leading scaling behaviour of correlations and responses. This conclusion is endorsed by the following result: $X_\infty = 1/2$ for $d > d_{ucd} = 4$ and $X_\infty = 1 - 2/d$ for $2 < d < d_{ucd} = 4$ where d_{ucd} stands for the upper critical dimension (below $d = 2$ there is no finite T transition in the model). Interestingly, for $d = 2$ the FDTR $X(C)$ has a non-trivial form [214], similar to what is found for the ferromagnetic Ising chain. Numerical results in the Ising model show that $X_\infty \simeq 0.26$ in two dimensions[11] and preliminary results in three dimensions give $X_\infty \simeq 0.4$. In figure 13 we show the IRF corresponding to the TRM susceptibility (98) as a function of C in the 2D Ising model at the

[11] After completion of this review we learned of recent results finding a slightly different value $X_\infty \simeq 0.34$ in two dimensions [215]. More work is necessary to accurately estimate that number.

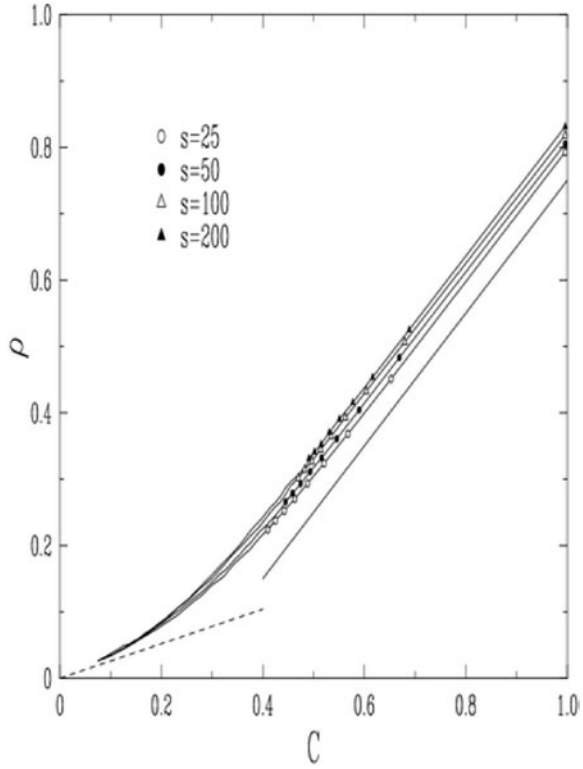

Figure 13. IRF (98) corresponding to the thermoremanent magnetization in the 2D Ising model at criticality. The full and broken lines correspond to the quasi-stationary regimes $X = 1$ and $X_\infty = 0.26$ respectively. From [205].

critical point. The general scenario about ferromagnetic models at criticality is as follows [213]. Let us consider a system that is quenched from a random configuration to a temperature below T_c. If $\tau = t - s \ll s$ the system is in equilibrium, TTI holds and FDT is not violated ($X(t, s) = 1$). However, if $t/s \sim \mathcal{O}(1)$ the system ages, and both TTI and FDT are violated. A solution for the correlation $C_{ag}(t, s)$ and response $R_{ag}(t, s)$ that matches the intermediate regime between the stationary $X = 1$ and the aging regimes is given by

$$C_{ag}(t, s) = m_{eq}^2 \hat{C}\left(\frac{t}{s}\right) \qquad R_{ag}(t, s) = s^{-a-1}\hat{R}\left(\frac{t}{s}\right) \tag{232}$$

where $a > 0$ is a coarsening exponent. From (232) $X(t, s) \sim s^{-a}/m_{eq}^2$, therefore $X \to 0$ for coarsening systems where m_{eq} is finite. The same expression is valid for the critical point but replacing m_{eq} by its time dependence at T_c. Using $m_{eq} \sim (T_c - T)^\beta$, $\xi \sim (T_c - T)^{-\nu}$, $t \sim \xi^z$ where β, ν, z_c are the correlation length and dynamical exponents respectively. Substituting these relations into (232) and using $a_c = 2\beta/z_c\nu$ gives at T_c

$$C_{ag}(t, s) = s^{-a_c}\hat{C}\left(\frac{t}{s}\right) \qquad R_{ag}(t, s) = s^{-a_c-1}\hat{R}\left(\frac{t}{s}\right) \tag{233}$$

leading to $X(t, s) = \hat{X}(t/s)$. This result has two consequences: (1) for $t \to \infty$, $X(t, s) \to X_\infty$ and (2) only for $a_c = 0$, according to the left expression in (233), can $X(t, s)$ be expressed as solely a function of C_{ag}. This is the case of the aforementioned Ising chain where the ansatz (91) is valid because $\beta = 0$. It has been suggested [216] that $R_{ag}(t, s)$ covariantly scales under

conformal transformations of time leading to specific predictions for the scaling function $\hat{R}$. An important implication of the result $a_c = 0$ is that the aging part of the IRF (97) does not vanish in the asymptotic long-time limit. As noted in [217] the non-vanishing of the aging part of IRF in the large s limit is related to the failure of the scheme that links static and dynamical properties [160, 161] in the Ising chain. In fact, as discussed in section 6.2.2 the stochastic stability property links the equilibrium $P(q)$ with the behaviour of IRF,

$$P(q) = -T \left.\frac{\mathrm{d}^2\chi(C)}{\mathrm{d}C^2}\right|_{C=q} = \left.\frac{\mathrm{d}X(C)}{\mathrm{d}C}\right|_{C=q} \tag{234}$$

where we have used (100). In the Ising chain $P(q) = \delta(q-1)$. Equation (234) is not fulfilled in the Ising chain as can be easily checked by inserting the result $X(C) = 1/(2-\sin^2(\pi C/2))$ (discussed in the paragraph preceding (231). As soon as T_c is finite ($d > 1$), $X(C) = \theta\left(C - m_{\mathrm{eq}}^2\right)$ for $T < T_c$ and (234) is again satisfied. Despite its simplicity, the Ising chain appears to be an interesting solvable example that allows us to check many results. For instance, observable independence has also been recently addressed [55] showing that $X_\infty = 0$ for a large class of observables. Recent progress in the study of the FDR at criticality has been achieved by Calabrese and Gambassi [218, 219] who have considered the FDR in momentum space $X_{\vec{q}}(t, s)$. The study of $O(N)$ models using field-theoretical techniques yields estimates for the value of X_∞ (231) in an $\epsilon = 4 - d$ expansion. Two-loop computations [219] give, for the Ising case $N = 1$, the following values: $X_\infty\,(3\mathrm{D}) = 0.429(6)$, $X_\infty\,(2\mathrm{D}) = 0.30(5)$ compatible with the results obtained from numerical simulations [205, 215].

Other studies of models at criticality include the XY model with a Kosterlitz–Thouless transition [220]. This model has a low-temperature phase where correlation functions decay algebraically, therefore correlations are critical below T_c. A failure of the stochastic stability property, similar to that reported in the Ising chain, appears in the 2D XY model at low temperatures where the density of vortices increases.

Finally, let us comment on results for zeta-urn models that have confirmed the validity of the relation (231) [15, 207, 208]. Zeta-urn models show a quite rich phase diagram described in terms of the density ρ of balls (i.e. the number of balls divided by the number of boxes) and the temperature. There is a critical line $\rho_c(\beta)$ that separates a fluid regime ($\rho < \rho_c(\beta)$) from a condensed regime ($\rho > \rho_c(\beta)$) with glassy dynamics. Along the so-called regular part of the critical line ($\beta > 3$) $X_\infty = \frac{\beta+1}{\beta+2}$ is temperature dependent. This number lies in the interval $[4/5, 1]$ quite far from the values $X_\infty < 1/2$ found in ferromagnets. In the condensed phase $X_\infty \to T^{1/2}$ at low temperatures. It vanishes at $T = 0$ as in coarsening systems, however the condensation dynamics in urn models is totally inhomogeneous in contrast to the homogeneous character of coarsening in ferromagnets.

7. QFDT: the numerical evidence

Computer simulations have the great advantage, over the real experiment, of direct access to the microscopic level, even if only relatively small timescales and system sizes can be studied. Although this can be a serious limitations, the true fact is that numerical study of aging phenomena and FDT violations has been successfully done during the last years for several systems.

7.1. Structural glasses

Using ideas developed in the field of spin glasses, many conjectures have been formulated concerning the structure of the phase space of glassy systems. However, obtaining direct

information, either from experiments or from numerical simulations, is a difficult challenge. Relaxation times in a glass are so long as to preclude equilibration within experimental times. Numerical or experimental exploration of the phase space in these systems is therefore necessarily incomplete. The increase in computational power and the recent developments in the theory of disordered systems has pushed forward an approach which should not suffer from these limitations. The idea, which was actively developed in the study of spin glasses, is that relevant information on the phase space structure should be hard-encoded into the non-equilibrium dynamics of glassy systems.

According to the conjecture of the similarity between structural glasses and some spin-glass models, $X(C)$ for structural glasses is a two-valued function with $X(C) = 1$ at short times, and $X(C) = m < 1$ in the long-time aging regime. This scenario has been largely studied using numerical simulations.

In a numerical investigation of aging effects not only the waiting time must be changed over several orders of magnitude, but for a given waiting time the subsequent dynamics must also be studied over a long time. For these reasons, aging phenomena have been studied for models that are simple enough to be simulated over long times, but at the same time still catch the essential features of real glasses. Moreover, to maintain the systems in a non-equilibrium state for very long times, crystallization must be strongly inhibited. This is obtained either with a particular choice of interaction potential parameters or by adding a (small) extra term in the potential. In the following we discuss results obtained for several models.

7.1.1. Mixtures of soft particles of different sizes. See [221–226]. This system consists of N particles half of which are of type A and half of type B interacting via the Hamiltonian

$$\mathcal{H} = \sum_{i<j} \left(\frac{r_i + r_j}{|\boldsymbol{x}_i - \boldsymbol{x}_j|} \right)^{12} \tag{235}$$

where the radius r_i depends on the type of particle. It is known that the choice of two different types of radius such that $r_B/r_A = 1.2$ prevents crystallization and the system can be brought into a glassy state.

Due to the simple scaling of the potential, the thermodynamic quantities depend only on $\Gamma = \rho\beta^4$, where ρ is the density which can be taken equal to 1. This model presents a glass transition at about $\Gamma_c = 1.45$ [222]. In figure 14 we report the response of the particle to a force of strength ϵ

$$\chi(t_w + \tau, t_w) \simeq \frac{1}{N\epsilon} \sum_{i=1}^{N} \langle \boldsymbol{f}_i \cdot \boldsymbol{x}_i(t_w + \tau) \rangle \tag{236}$$

where $\boldsymbol{f}_i$ is a random Gaussian vector of squared length equal to the space dimension d, versus the self-diffusion function

$$\Delta(t_w + \tau, t_w) = \frac{1}{N} \sum_{i=1}^{N} \langle |\boldsymbol{x}_i(t_w + \tau) - \boldsymbol{x}_i(t_w)|^2 \rangle. \tag{237}$$

The average is over different initial states at t_w and realization of $\boldsymbol{f}$. Two linear regions with different slopes, one with $X(C) = 1$ and one with $X(C) = m < 1$, are clearly seen, in agreement with the two-timescale scenario. The dependence of m with T is well fitted by the spin-glass model prediction $m(T) = T/T_c$, see figure 15. Similar results have been obtained in monoatomic Lennard-Jones glasses [227, 228], see section 7.1.3.

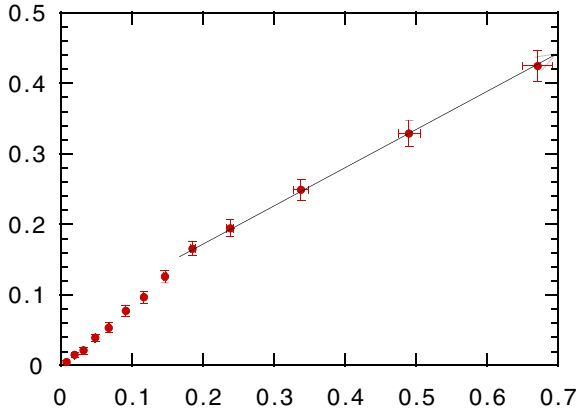

Figure 14. χ versus $\beta\Delta$ at $\Gamma = 1.6$ for $t_w = t_w = 8192$ and $t_w = 2048$. From [225].

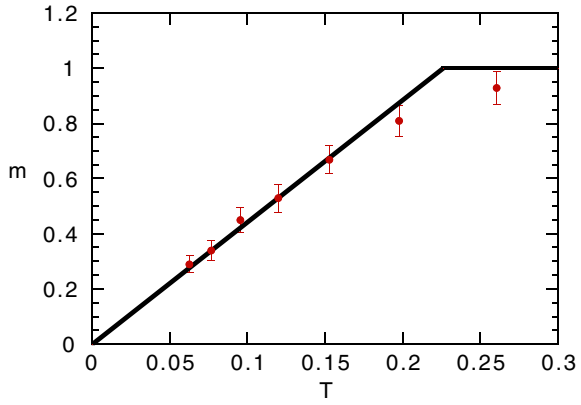

Figure 15. The quantity $m \equiv \frac{\partial\chi}{\partial\beta\Delta}$ as $t_w = 2048$ as a function of the temperature. The straight line is the prediction of the approximation $m(T) = T/T_c$. From [225].

7.1.2. Lennard-Jones binary mixtures. See [229–232]. The system consists of a mixture of particles of types A and B of equal mass m interacting via a 12–6 Lennard-Jones potential of the form

$$V_{\alpha\beta}(r) = 4\epsilon_{\alpha\beta}\left[\left(\frac{\sigma_{\alpha\beta}}{r}\right)^{12} - \left(\frac{\sigma_{\alpha\beta}}{r}\right)^{6}\right] \tag{238}$$

where $\epsilon_{\alpha\beta}$ and $\sigma_{\alpha\beta}$ depend on the particle pair type and are chosen to prevent crystallization. For a 80 : 20 mixture, and using ϵ_{AA} and σ_{AA} as units of energy and length and $\left(m\sigma_{AA}^2/48\epsilon_{AA}\right)^{1/2}$ as the unit of time, these are $\epsilon_{AA} = 1$, $\sigma_{AA} = 1$, $\epsilon_{AB} = 1.5$, $\sigma_{AB} = 0.8$, $\epsilon_{BB} = 0.5$ and $\sigma_{BB} = 0.88$. The atomic dynamics of this model is well described by the mode-coupling theory with a critical temperature of $T_c = 0.435$ in reduced units.

Typical FD plots numerically obtained by Barrat and Kob [233–235] are shown in figure 16. The correlation is given by the incoherent scattering function for a wave vector $\boldsymbol{k}$

$$C_k(t_w + \tau, t_w) = \frac{1}{N}\sum_j \mathrm{e}^{\mathrm{i}\boldsymbol{k}\cdot[\boldsymbol{r}_j(t_w+\tau)-\boldsymbol{r}_j(t_w)]} \tag{239}$$

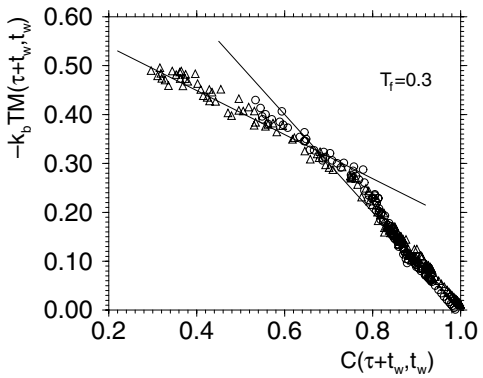

Figure 16. Parametric plot of the integrated response function $M(t_w + \tau, t_w)$ and the correlation function $C(t_w + \tau, t_w)$ for $k = 7.25$. Final quench temperature $T_f = 0.3$, $t_w = 1000$. Circles: $t_w = 10\,000$. The straight lines have slopes -1.0 and -0.45. From [234].

while the response is measured by adding to the potential a term of the form

$$\delta V = V_0 \sum_j \epsilon_j \cos(\boldsymbol{k} \cdot \boldsymbol{r}_j) \tag{240}$$

where $\epsilon_j = \pm 1$ with equal probability and $V_0 < T$. Again a two-timescale scenario is clearly seen. Moreover, the effective temperature in the slow regime where $m < 1$ is in reasonable agreement with the glass transition temperature T_g of the system[12].

Thus the FDT is broken as the system fails to equilibrate, as expected from spin-glass models.

7.1.3. Monoatomic Lennard-Jones systems. See [227, 228, 236, 237]. The system consists of equal particles interacting via the potential $V = V_{LJ} + \delta V$, where V_{LJ} is the usual 12−6 Lennard-Jones potential (expressed in reduced units), and δV is a many-body term that inhibits crystallization:

$$\delta V = \frac{\alpha}{2} \sum_{\boldsymbol{q}} \theta(S(\boldsymbol{q}) - S_0)(S(\boldsymbol{q}) - S_0)^2 \tag{241}$$

where $S(\boldsymbol{q})$ is the static structure function, $\alpha = 0.8$ and $S_0 = 1$. The sum is made over all $\boldsymbol{q}$ with $q_{max} - \Delta < |\boldsymbol{q}| < q_{max} + \Delta$, where $q_{max} = 7.12\rho^{1/3}$ and $\Delta = 0.34$, ρ being the particle density.

In figure 17 we report the parametric plot of the mean-square displacement Δ and IRF in a crunch experiment. It is important to note that the temperature below which $m < 1$ coincides with the glass transition temperature of the system at the density reached after the crunch. This shows that the breaking of FDT does not depend on the initial state nor on the path followed in the (T, ρ) plane, but only on the final (non-equilibrium) state to which the system is brought.

The FD plots for glass forming liquids discussed here reveal the typical two-timescale (or 1RSB) scenario found in some spin-glass models. This supports the original Goldstein's idea [56] that the phase space of supercooled liquids is divided by high barriers into different

[12] The glass transition T_g is defined as the temperature below which the system fails to equilibrate on the experimental timescale. For structural glasses T_g is defined as the temperature at which the viscosity is equal to 10^{13} Poise or, equivalently, a relaxation time of several minutes.

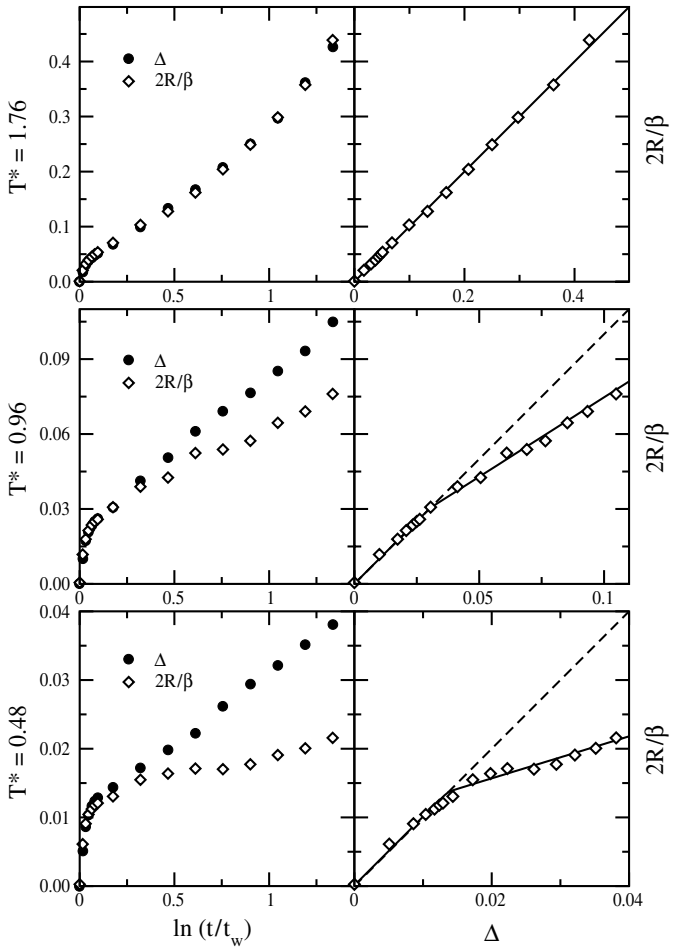

Figure 17. Mean-square displacement Δ and integrated response function $2R/\beta$ in reduced units at $\rho_2^* = 1.24$ for three temperatures $T^* = 0.48, 0.96, 1.76$. The left side shows the log time dependence of the two quantities. On the right side is response function versus Δ. Dashed lines indicate equilibrium FDT, while full lines fit the off-equilibrium aging region. From [227].

valleys each with its own statistical properties. This picture has been recently confirmed by a direct analysis of the motion of a glass forming liquid in terms of IS [62].

In the right panel of figure 18 [238] we show the temporal behaviour of the average energy of minima for a binary mixture Lennard-Jones system visited in the non-equilibrium motion following a quench to a low temperature. As a consequence, when the system is quenched from a high-temperature state to temperature T, the fast intra-component degrees of freedom will quickly equilibrate with the thermal bath temperature T. Applying the condition of minimum free energy to the system, constrained to stay in components of depth $E_{\rm IS}$, allows us to define an effective temperature

$$T_{\rm eff}(E_{\rm IS}, T) = \frac{(\partial/\partial E_{\rm IS})F_v(T, E_{\rm IS})}{(\partial/\partial E_{\rm IS})S_c(E_{\rm IS})} \tag{242}$$

which reflects the non-equilibrium net heat flow from the system to the thermal bath [100]. This expression coincides with that proposed in [46] in the context of p-spin models, once the

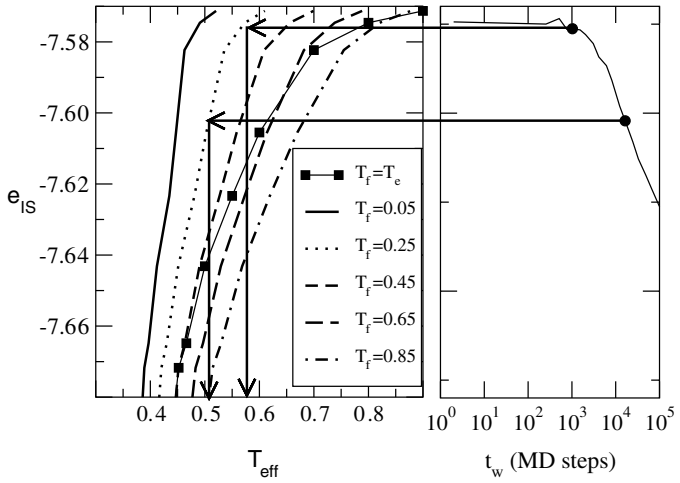

Figure 18. Left: solutions of (242) for several values of the final quench temperature $T_{\rm f}$ for the BMLJ system. Right: $e_{\rm IS}$ as a function of time, following the temperature quench. The arrows show graphically the procedure which connects the $e_{\rm IS}(t)$ value to the $T_{\rm eff}$ value, once $T_{\rm f}$ is known. (Data courtesy of Sciortino and Tartaglia, see also [238]). From [36].

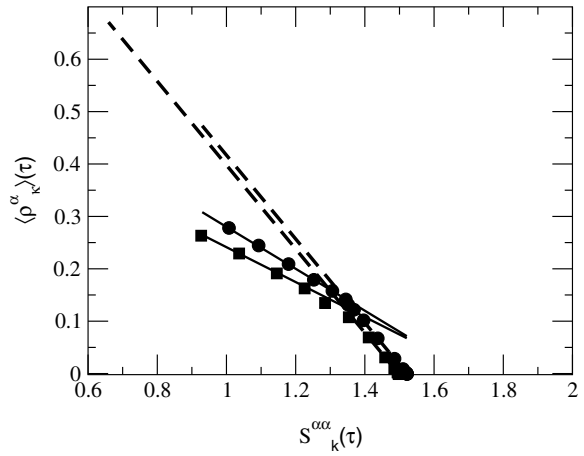

Figure 19. Response $\langle \rho^{\alpha}_{\mathbf{k}}(\tau)\rangle$ versus the dynamical structure factor $S^{\alpha\alpha}_{\mathbf{k}}(t) \equiv \langle \rho^{\alpha}_{\mathbf{k}}(t)\rho^{\alpha *}_{\mathbf{k}}(0)\rangle$, where $\rho^{\alpha}_{\mathbf{k}}$ is the Fourier transform component of the density of $\alpha = A, B$ particles at wave vector $\mathbf{k}$, for the binary mixture Lennard-Jones particle system for a quench from initial temperature $T_{\rm i} = 0.8$ to final temperature $T_{\rm f} = 0.25$ and two waiting times $t_w = 1024$ (square) and $t_w = 16\,384$ (circle). Dashed lines have slope $T_{\rm f}^{-1}$ while thick lines have slope $T_{\rm eff}^{-1}$. (Data courtesy of Sciortino and Tartaglia, see also [238]). From [36].

components are identified with the Thouless–Andreson–Palmer states [71, 73], see also the discussion after (90). Inserting into (242) the value of $E_{\rm IS}$ as a function of time one finally gets the function $T_{\rm eff}(t)$. The definition of $T_{\rm eff}$ is shown graphically in figure 18 [238].

The two-timescale scenario is rather well confirmed by numerical results, as shown in the FD plots of figure 19 [238], where the FD plot for the binary mixture Lennard-Jones system is reported. The full lines are the prediction from (242), the agreement is rather good.

7.1.4. Finite-size mean-field glasses. See [36, 65–67]. We have seen in the previous sections that the essential features of MCT for glass forming systems are also common to some fully connected spin-glass models, called mean-field p-spin glasses with $p > 2$. In the thermodynamic limit, the high-temperature paramagnetic phase is described by the schematic mode MCT for supercooled liquids. At the critical temperature T_c an ergodic to non-ergodic transition takes place. In mean-field models the relaxation time diverges at T_c as barriers separating different ergodic components become proportional to the system size, thereby diverging in the thermodynamic limit. In real systems, or the glass models just described, the barriers are of finite height and the transition to a glassy state appears at the glass transition temperature $T_g < T_c$, where the typical activation time over barriers is of the same order as the observation time.

Despite these differences mean-field models, having the clear advantage of being analytically tractable, are a very useful tool to study the phase space structure of glassy systems, especially between the dynamical temperature T_c and the static temperature T_{RSB} (Kauzmann temperature T_K in glass language). The main drawback is that, since activated processes are not captured by mean-field models, the picture that emerges is not complete. To go beyond the mean field it is necessary to include activated processes, a very difficult task since it implies knowledge of the excitations involved in the dynamics. A simple approach is to include *finite-size effects* in the dynamics of an infinite mean-field system just extending the analysis to *finite-size* mean-field. This approach has been suggested by Nieuwenhuizen [49] and is somehow reminiscent of the dynamical approach of Sompolinsky [141], see also section 6.2.2. We stress that the assumption that finite-size mean-field models capture the physics of glasses beyond MCT is not trivial. In fact, the activated process in finite-size mean-field models could be different from those of supercooled liquids, making the behaviour different. This, for example, seems to be the case for the Potts glass model, where recent studies on a finite-size version indicate some differences with the fragile-glass scenario [239, 240].

A spin-glass model in the p-spin universality class, that displays fragile-glass behaviour, is the random orthogonal model (ROM) [74, 241]. The model is defined by the Hamiltonian[13]

$$\mathcal{H} = -2 \sum_{ij} J_{ij} \sigma_i \sigma_j \tag{243}$$

where σ_i are N Ising spin variables ($\sigma = \pm 1$) and J_{ij} is a random $N \times N$ symmetric orthogonal matrix with zero diagonal elements. We note that, differing from previously discussed spin models, the condition of orthogonality leads to a strong correlation among the matrix elements. In the limit $N \to \infty$ this model has the same thermodynamic properties as the p-spin model. The dynamical transition is at $T_c = 0.536$ with threshold energy per spin $e_{th} = -1.87$. A static transition occurs at $T_{RSB} = 0.256$ and the critical energy per spin is $e_{1RSB} = -1.936$ where the complexity vanishes [74, 241]. The analysis in the mean-field limit gives a rather clear 'geometrical' interpretation of the two transitions. The phase space is composed of an exponentially large (in N) number of components, separated by infinitely large (for $N \to \infty$) barriers. Each component is labelled by the energy density e of its minimum and the largest allowable value of e is e_{th} [76, 242]. Components with e equal to e_{th} have the largest (exponentially with N) statistical weight and become dominant, in a thermodynamic sense, at the dynamical transition $T = T_c$. Since components with e smaller than e_{1RSB} have negligible

[13] The factor 2 in (243) is set only for convenience to match the values of all relevant temperatures with those reported in the original paper [241]. The Hamiltonian studied in [74] differs by a factor 4 from the present definition. To compare the results discussed here with those in [74] temperatures and energies must be properly scaled by a factor 4.

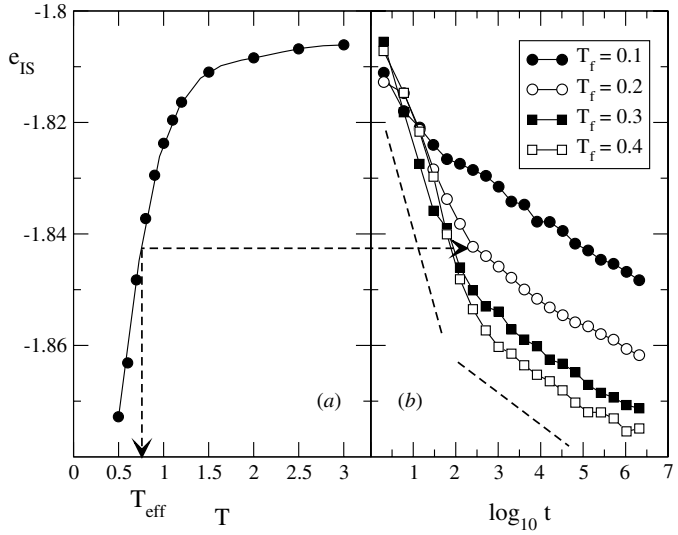

Figure 20. (*a*) Equilibrium average $e_{\rm IS}$ as a function of temperature. The arrows indicate the construction of the effective temperature $T_{\rm eff}\,(e_{\rm IS})$. (*b*) Average inherent structure energy for the ROM as a function of time for initial equilibrium temperatures $T_{\rm i} = 3.0$ and final quench temperatures $T_{\rm f} = 0.1, 0.2, 0.3$ and 0.4. The average is over 300 initial configurations. The system size is $N = 300$. The lines denote the two regimes; see also [66]. From [36].

statistical weight [73, 74], the static transition is ruled by components with $e = e_{\rm 1RSB}$, i.e., the lowest accessible ones [42, 73].

For finite N the scenario is different since not only basins with $e < e_{\rm th}$ acquire statistical weight, but basins with $e > e_{\rm th}$ with few negative directions [76] may become stable, simply because for finite N there are not enough degrees of freedom to hit them. The ROM for finite N has been largely studied during the last few years [36, 65–67, 243] and its behaviour has been compared with that of supercooled liquids finding a remarkable agreement.

In the left panel of figure 20 is shown the average energy minima of basins (IS) as a function of temperature for the ROM with $N = 300$ obtained from a Monte Carlo simulation. It can be shown [60, 61] that if the density of states $\Omega(E)$ is Gaussian and if the basins have approximately the same shape or are, to a good degree, harmonic, then the IS energy density $e_{\rm IS} \propto 1/T$. The data in the figure can be well fitted by

$$e_{\rm IS} = e_\infty + e_1 T^{-1} + O(T^{-2}) \tag{244}$$

indicating that for a relatively large energy range the basins are roughly of the same shape. This means that the contribution $f_v(T, e_{\rm IS})$ to the free-energy density of the system is of the form $f_v(T, e_{\rm IS}) = e_{\rm IS} + \delta f_v(T)$, with the second term independent of $e_{\rm IS}$, i.e., of the component [65]. This in turn implies that the effective temperature for the ROM is completely determined once the complexity (density) $s_c(e)$ is known [66]. Indeed from (90), (242) we have

$$\frac{1}{T_{\rm eff}(e_{\rm IS})} = \frac{\partial s_c(e_{\rm IS})}{\partial e_{\rm IS}}. \tag{245}$$

Furthermore, in an aging experiment $T_{\rm eff}$ depends on time only through $e_{\rm IS}(t)$. For each time t the effective temperature $T_{\rm eff}$ can be obtained graphically as shown in figure 20. The left panel in that figure shows the average $e_{\rm IS}$ energy as a function of time in a typical aging

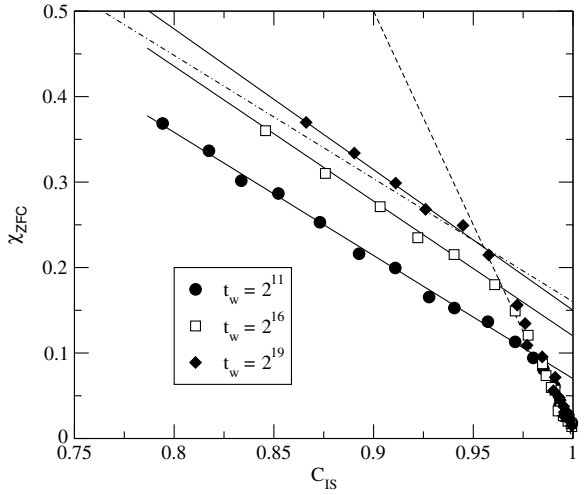

Figure 21. Integrated response function as a function of IS correlation function, i.e, the correlation between different IS configurations, for the ROM. The dashed line has slope $T_f^{-1} = 5.0$, where T_f is the final quench temperature, while the full lines are the prediction (245): $T_{eff}(2^{11}) \simeq 0.694$, $T_{eff}(2^{16}) \simeq 0.634$ and $T_{eff}(2^{19}) \simeq 0.608$. The dot-dashed line is T_{eff} for $t_w = 2^{11}$ drawn for comparison; see also [66]. From [36].

experiment. We note the two-regime decay also observed in supercooled liquids [244]. The two regimes are associated with different relaxation processes. In the first part the system has enough energy and relaxation is mainly due to *path search* out of basins through saddles of energy lower than T, where T is the temperature after the quench. This part depends only on the temperature of the equilibrium state from which the system has been quenched. This process stops when all barrier heights become of $O(T)$ and relaxation slows down since it must proceed via activated inter component processes. In figure 21 is shown the response versus correlation plot for the ROM. Correlations and responses were computed by projecting over the IS, the corresponding FDT also holds in equilibrium as discussed in section 3.3. The figure clearly shows the two-timescale scenario with $X = 1$ at short times and $X = T/T_{eff} < 1$ at later times, with T_{eff} in very good agreement with the value predicted by (242). Also notorious is the fact that the effective temperature shifts with time as expected.

7.2. Spin glasses and other random systems

As we have explained in section 6, spin glasses represent the most important motif of many results regarding FDT violations. Particularly, numerical simulations have been the most widespread tools to investigate many aspects of the equilibrium behaviour of spin glasses that cannot be tackled by analytic means (for a review see [245]). It is usually said that the advantage that numerical simulations offer in the study of non-equilibrium properties, as compared to equilibrium ones, relies on the fact that systems do not need to be equilibrated. However, this observation is naive and deceitful as many dynamical aspects cannot be observed in the range of accessible timescales. Indeed, it is widely believed that many dynamical results in spin glasses are suspect because the asymptotic dynamical regime, defined as that regime where the dynamic correlation length ξ is many lattice spacings, is usually not reached. Establishing whether the range of simulated timescales reaches the asymptotic long-time regime is at the heart of a present controversy in the field. Indeed, not by chance, this controversy

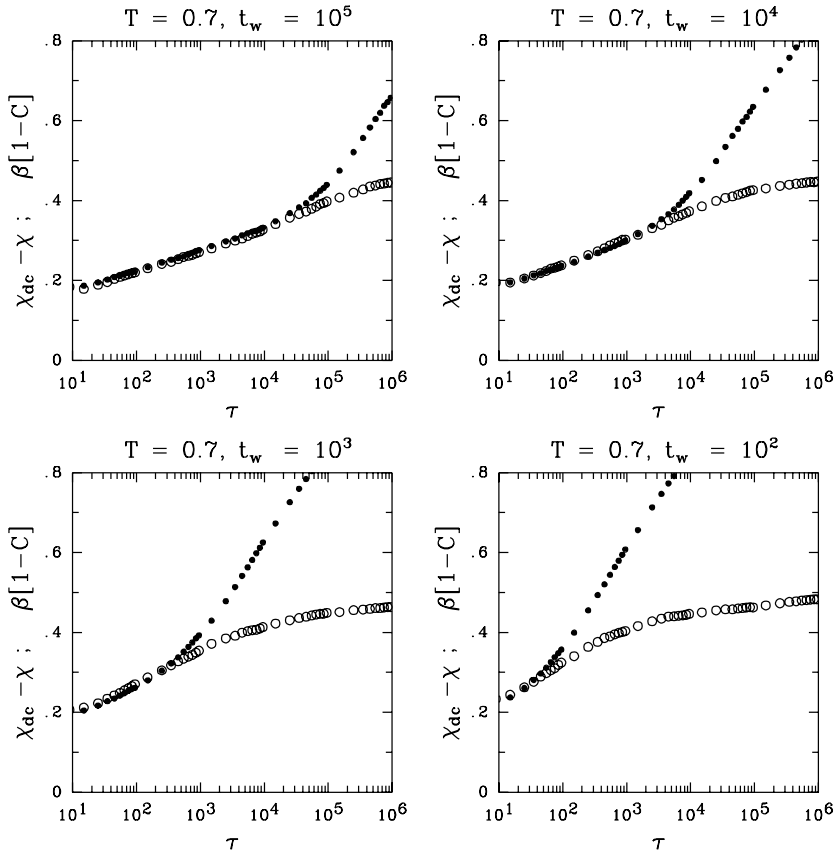

Figure 22. Zero-field cooled IRF $\chi_{\rm ZFC}(t, t_w) = M_{\rm ZFC}(t, t_w)/h = \chi_{dc} - \chi_{\rm FC}(t, t_w)$ (empty circles) in the 3D EA model plotted as a function of the time $t \equiv \tau$ for different values of t_w at $T = 0.7$. For times $t \equiv \tau > t_w$ deviations from the FD relation $\chi_{\rm ZFC}(t, t_w) = \beta(1 - C(t, t_w))$ (full circles) are noticeable. From [247].

is quite reminiscent of another parallel ongoing discussion concerning the magnitude of finite-size effects in the equilibrium properties. Stochastic stability arguments linking non-equilibrium with static properties [160, 161] confirm that any strong finite-size corrections to the equilibrium properties should manifest as strong finite timescale corrections in dynamical experiments. Unfortunately, a precise theory that quantifies (even in an approximate way) these corrections is presently unknown. We will not deal here with the difficult issue of ascertaining in which cases simulations do reach the asymptotic time regime, but present the evidence on FDT violations for the accessible simulated timescales.

7.2.1. Spin glasses. We begin our tour by reporting the first numerical evidence of FDT violations in three-dimensional (3D) Edward–Anderson (EA) spin glasses [246] and their representation in the form of FD plots [247]. In [246] it was shown that deviations from the equilibrium FDT appear at timescales comparable or larger than the age of the system. In figure 22 we show TRM measurements by Franz and Rieger [247] on the 3D EA model. In those measurements the system starts from a random initial configuration and a magnetic field h is applied for time t_w. The field is cut off at t_w and the subsequent decay of the $M_{\rm TRM}(t, t_w)$

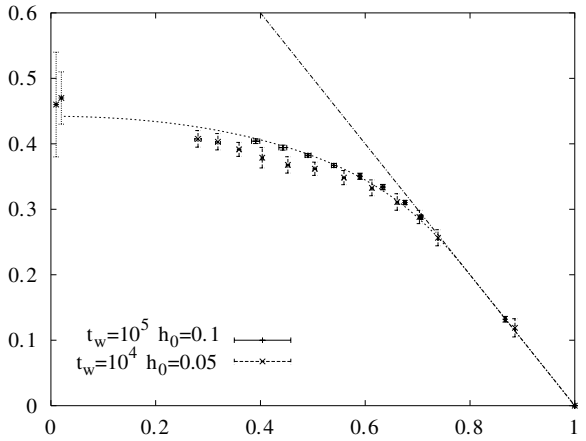

Figure 23. $S(C)$ versus C in the 3D EA model at $T = 0.7 < T_c \simeq 1$ for $L = 64$. The continuous line is the prediction obtained from equilibrium data for $L = 16$ (averaged over 900 samples) as explained in the text. The straight line is the FDT prediction. From [249].

recorded. In the linear response regime this experiment is equivalent [248] to a ZFC set-up where the field is initially zero and switched on at t_w, the resulting $M_{\rm ZFC}(t, t_w)$ being given by $M_{\rm TRM}(t, t_w) + M_{\rm ZFC}(t, t_w) = M_{\rm FC}$ for t large enough (see (99)) where $M_{\rm FC}$ is the equilibrium magnetization. Most of the numerical simulations use the ZFC procedure. The most extensive simulations and the most clarifying FD plots, as described in section 4.3, have been done in $d = 3$ and $d = 4$ [249–253]. In those papers, the authors consider the IRF associated with the global and the spin–spin autocorrelation functions as described in section 4.3. The system is quenched at low temperatures for a time t_w and a small magnetic field is subsequently applied and the $M(t)$ measured. Typical FD plots in the 3D EA model using this construction are shown in figure 23. There we show $S(C)$ at two different magnetic field intensities as well as two different waiting times. FD plots reveal that a constant slope $X(C)$ for $C < q_{\rm EA}$ is a good approximation to the data (although more accurate data in four dimensions hint at the existence of a curvature in $S(C)$ [251, 250]). This constancy of the slope $X(C)$ (i.e. the linearity of $S(C)$ in the region where FDT is violated) can also be interpreted as complementary evidence of the accuracy of the t/t_w scaling in the correlation function [254]. Stochastic stability arguments [160, 161] state that the dynamical $X(C)$ is related to the static function $x(q)$ by the relation $P(q) = x'(q)$ or

$$x(q) = \int_0^q {\rm d}q' P(q') \tag{246}$$

where $P(q)$ is the probability distribution of overlaps between replicas of the same system. This identity offers a way to obtain $S(C)$ from equilibrium data. The derivative of relation (101) with respect to C yields $P(C) = -{\rm d}^2 S(C)/{\rm d}C^2$. Inverting this identity and inserting an estimate of $P(C)$ as obtained from equilibrium simulations allows an alternative way to compute $S(C)$. The applicability of this method is shown in figure 23. Quantitative evidence of the mean-field character of the FDT violations has also been reported by checking the accuracy of the Parisi–Toulouse approximation in spin glasses (this approximation states that the order parameter function $q(x)$ is a function of the argument x/T, see [255, 256] for an exposition). Within this approximation (which works pretty well in MF spin glasses) it can be shown [249, 253] that $\chi(t, t_w) \equiv \chi(C) = \beta S(C)$ is independent of temperature in the

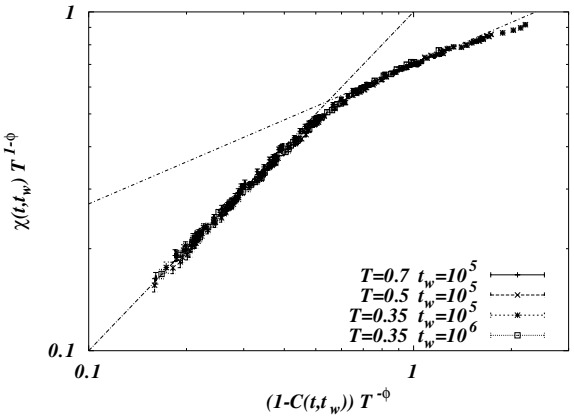

Figure 24. Scaling plot as described in the text for a cubic lattice, $d = 3$ with $L = 64$ showing the existence of two dynamical regimes described by two different scalings for the scaling function $\hat{\chi}(x)$ where $x = (1 - C)T^{-\phi}$. In the FDT regime $\hat{\chi}(x) \sim x$ while for $x > 1$, $\hat{\chi}(x) \sim x^B$ with $B \simeq 0.41$. From [253].

region $C < q_{\rm EA}$ where FDT is violated. In the SK model it can be proved that this function $\chi(C) \simeq \sqrt{(1 - C)}$. In general, for any short-range system one can assume the following behaviour: (a) $\chi(C) = \beta(1 - C)$ for $C > q_{\rm EA}$ when FDT holds and (b) $\chi(C) = A(1 - C)^B$ for $C < q_{\rm EA}$. Multiplying $\chi(C)$ by $T^{1-\phi}$ with $\phi = 1/(1 - B)$ one finds that the resulting quantity is solely a function of the argument $(1 - C)T^{-\phi}$: $T^{1-\phi}\chi(C) = \hat{\chi}((1 - C)T^{-\phi})$ thereby showing that data for different waiting times and temperatures should collapse on a single master curve. In both $d = 3, 4$ a best collapse is obtained taking $B = 0.41$ [249, 253] which is quite close to the mean-field result $B = 1/2$, see figure 24.

Apart from the EA model many other results have been obtained studying short-range versions of the disordered p-spin model. Two different models have been considered. On the one hand, there is the so-called *disordered plaquette model* [257] where spins occupy the vertexes of a finite-dimensional lattice and the interaction occurs between p spins belonging to a given plaquette. The Hamiltonian of this model reads

$$\mathcal{H} = -\sum_{\square} J_{\square} \prod_{i \in \square} \sigma_i \tag{247}$$

where '$\square$' denotes a plaquette (not necessarily a square plaquette) that connects different spins. As usual, $J_{\square}$ are quenched variables of zero mean and finite variance and $\sigma_i = \pm 1$ denote Ising variables. The simplest case, the one considered in [257], is a disordered version of the $p = 4$ model and consists of a regular lattice of side L and dimension D where spins occupy the vertices and plaquettes correspond to the different faces of the lattice. Each face contains four spins and each spin belongs to $4\binom{D}{2}$ plaquettes. A schematic picture of the lattice in $d = 2$ is shown in figure 25. The study of the static and dynamic properties of this model revealed that, although there was no compelling evidence in favour of a finite T spin-glass transition, the relaxation time shows superactivation effects and stretching of correlation functions characteristic of fragile glasses. The relaxation time can be fitted both to a VTF law with $T_0 = 0.65$ or to an exponential inverse temperature squared law with $T_0 = 0$. The study of the equilibrium properties confirmed both possible scenarios ($T_{\rm c} \sim T_0 = 0.65$ or $T_{\rm c} \simeq 0$) but show that, whatever scenario holds, the relaxation time τ and the equilibrium correlation length ξ are linked by the relation $\tau = A \exp(B\xi/T)$, supporting a scenario of cooperative

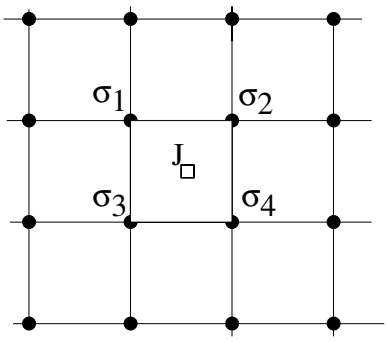

Figure 25. Schematic figure of the disordered plaquette model in $d = 2$.

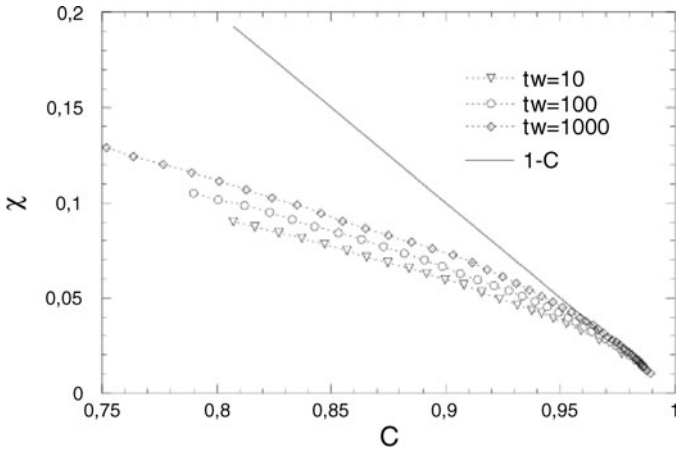

Figure 26. FD plot for the disordered plaquette model (with $p = 4$) in a cubic lattice of lattice size $L = 20$ at $T = 0.7$ and three different waiting time values. From [257].

dynamics. Also, the trap-like character of the dynamics was confirmed by studying the overlap among identical replicas at t_w but evolving with different noises, $Q(t_w, t_w + t)$. This quantity should coincide with $C(t_w, t_w + 2t)$ if jumps among configurations are uncorrelated or entropically driven. Numerical results are compatible with this prediction. Accordingly, the FD plot (figure 26) measured at $T = 0.7$ (just above the suspected finite T_c) showed strong deviations from the equilibrium line $\chi = \beta(1 - C)$ with a FDR $x \sim 0.4$, and in agreement with the one-step pattern characteristic of structural glasses (see section 7.1).

On the other hand, there is another short-range version of the p-spin model [152, 258–261] where M spins $\left(s_i^1, \ldots, s_i^M\right)$ occupy the different sites i of a cubic lattice. For each two adjacent sites i and j one considers all possible groupings of different p spins that can be formed by taking k spins from site i and $p - k$ spins from site j. In an obvious abuse of notation, we can write

$$\mathcal{H} = -\sum_{(i,j)} \sum_{g \in (i,j)} J_g \prod_{k \in g} \sigma_k \tag{248}$$

where the sum runs over all possible nearest neighbours (i, j) and all different groups of p spins as described above. Again, the J are quenched variables with zero mean and finite variance. Two cases have been considered: $M = 2$, $p = 3$ [258, 261] and $M = 3, 4$, $p = 4$

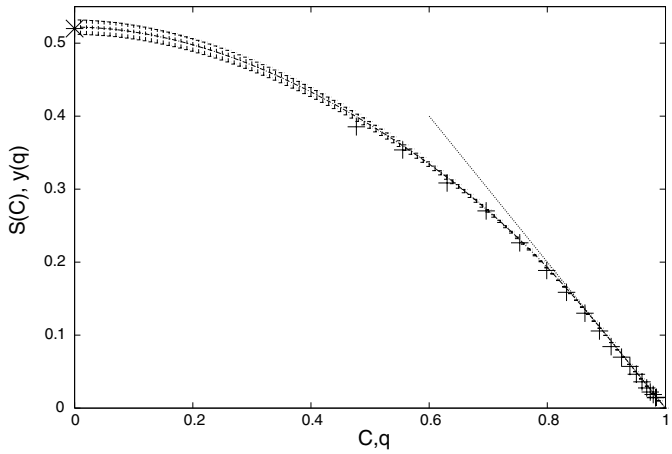

Figure 27. FD plot for the short-range version of the p-spin model (with $p = 4$, $M = 3$) in a cubic lattice of lattice size $L = 16$ at $T = 2.0 = 0.77T_c$ and $t_w = 2^{17}$. The continuous line with error bars is the shape of $X(C)$ derived by numerical integration of the relation $P(q) = x'(q)$ and measuring the equilibrium $P(q)$ for $L = 5$, the dotted line is the equilibrium line $S(C) = 1 - C$ and the isolated cross at $C = 0$ corresponds to the FC magnetization. From [260].

[259, 260] (for $M = 2$, $p = 4$ the model reduces to the standard EA model [259]). In the first case, the model is not time-reversal invariant while in the second case it is. FD violations have been measured in this last case [260]. Finite-size scaling studies of the model show some evidence of a second order phase transition at $T_c = 2.6$ characterized by a divergent spin-glass susceptibility. This result is confirmed by a study of the FDT violations in this model that show the existence of a non-trivial $X(C)$ characteristic of a full RSB scenario. As for the EA model, the $X(C)$ appears to be linked to the static $P(q)$ via the relation $P(q) = X'(q)$, see figure 27. The main message conveyed by most of these results is that FDT violations are qualitatively and quantitatively well described in the framework of MF theories of spin glasses. However, the implications of these similarities must not be taken too far. In particular, the already old but recurrent issue about the validity of the many state picture in finite-dimensional spin glasses cannot be answered from such a point of view. As discussed previously, the precise link between statics and dynamics proposed by stochastic stability arguments confirms that the dynamic $X(C)$ is related to the static $x(q)$ after introducing a coherence length $l(t_w)$ (related to the spin-glass correlation length $\xi(t_w)$ obtained from the two-point replica correlation function) which depends on the waiting time t_w according to the relation $x(q, l(t_w)) = X(C(t, t_w))$. A numerical study of FDT violations in $d = 2$ [262] shows that such an assumption is indeed true and $l(t_w) \propto \xi(t_w)$. More important, the resulting FD plots are extremely similar to those found in $d = 3, 4$ and the scaling ansatz for $S(C)$, as derived from the assumption that the low T phase has many states, also works pretty well. However, as in $d = 2$ there is no finite T transition these results show that statements in favour of the validity (or not) of the mean-field picture in the accessible range of timescales (in off-equilibrium experiments) or sizes (in equilibrium measurements) are inconclusive. The stochastic stability property is well satisfied also in the XY model at not too low temperatures [220] where critical fluctuations dominate, the overall resulting behaviour being quite similar to that of the 3D EA model. From a completely different perspective, the overall presence of mean-field aspects in the analysis of off-equilibrium data suggests that the many-state picture is effectively valid and that only for experimentally inaccessible sizes or timescales (therefore

irrelevant from a practical point of view) is the true scenario (whether mean-field or droplet) recovered.

We finish this subsection by commenting on some recent results [263] aiming to identify and quantify the low-energy fluctuations that locally result in deviations from the average QFDT as measured in the bulk. Local deviations from the bulk QFDT curve $\chi(C)$ are the equivalent of fluctuations from the average magnetization in a Heisenberg magnet, where transverse fluctuations correspond to low-energy spin-wave excitations and the longitudinal fluctuations that modify the length of the magnetization vector are the massive ones. Numerical results in the 3D EA model show that local correlations $C_l(t, t_w)$ and IRFs $\chi_l(t, t_w)$ measured over local boxes spread over the whole lattice generate a two-dimensional surface $\rho(C_l, \chi_l)$ with a prominent maximum centred around the bulk curve. The contour lines of this density map gently deform along the QFDT bulk curve $\chi(C)$ and deviations far away from that curve appear to be penalized. This study offers the possibility of understanding the connections between the mean-field character of the FDT violations and the existence of deviations due to short-scale cooperative processes in an eventual (but yet unclear) heterogeneous scenario.

7.2.2. Other random systems. Apart from spin glasses other lattice models with quenched randomness have been considered in the literature aiming to elucidate whether off-equilibrium studies can tell something about the character of the low-temperature phase. Many of the conclusions of these numerical studies need to be taken cautiously as no conclusive evidence in support of a given scenario or in refusal of other ones is ever reached.

Let us start the discussion with the ferromagnetic diluted and random field Ising models (RFIMs). The 3D version of both models has been investigated in [250]. Simulations in the low T phase and in the Griffiths phase (i.e. the region of temperatures between the critical temperature of the pure system and that of the random system) show that FD plots in ferromagnetic diluted and RFIMs are very similar to each other but quite different to those measured in spin-glass systems (see the preceding section 7.2.1). The former are characteristic of a ferromagnetic phase with $X = 0$ while the latter are described by a non-trivial function $X(C)$. These studies exclude the possibility of a spin-glass and Griffiths phase in both models described by mean-field like RSB solutions.

Another finite-dimensional model with interesting behaviour is the frustrated Ising lattice gas (FILG) [264] defined by the Hamiltonian,

$$\beta\mathcal{H} = -J\sum_{\langle i,j\rangle}(\epsilon_{ij}\sigma_i\sigma_j - 1)n_i n_j - \mu\sum_{i=1}^{V} n_i \tag{249}$$

where the $\sigma_i = \pm 1$ are Ising spins and $n_i = 0, 1$ are occupancies which may take the value 1 or 0 depending whether site i is occupied by a spin or not. The sum is over near neighbours on a d-dimensional lattice. The ϵ_i are quenched random variables that may take the values ± 1 and μ stands for a chemical potential. The average particle density $\rho = \frac{1}{V}\sum_i n_i$ is a monotonically increasing function of μ. In the limit $J \to \infty$ the model converges to the site frustrated percolation problem [264] (a variant of the standard percolation problem where clusters are made out of sites connected by non-frustrated links). This model has been simulated in 3D [265, 266] where different regimes have been singled out. The percolation transition occurs at a given value of the chemical potential μ_p and manifests in the onset of two different relaxational regimes (a fast exponential relaxation followed by a slow stretched decay). A second transition is observed at a higher value of μ, $\mu_d > \mu_p$ where the relaxation time grows extremely fast and dynamics arrests. However, it is unclear whether the relaxation time diverges at μ_d. Less clear is, in the case of the existence of a dynamical singularity

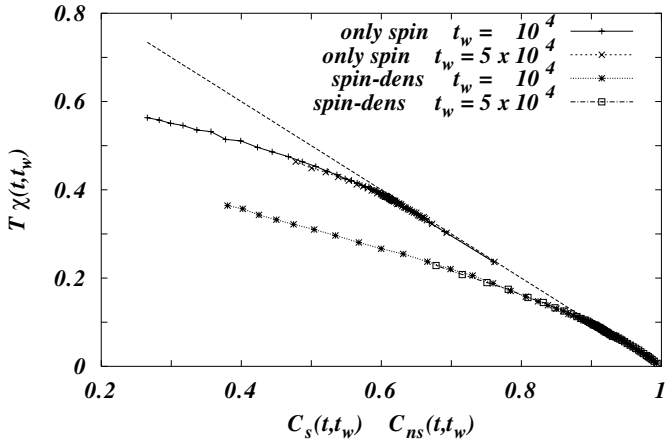

Figure 28. FD plot for the 3D FILG (249) with lattice size $L = 30$ at $T = 1$, $J = 10$, $\mu \simeq 5.5$. Spin density and spin autocorrelations (see the text) yield FD plots compatible with the same effective temperature. From [266].

at μ_d, whether this is associated with a thermodynamic singularity. For the FILG (249) different correlation functions can be constructed depending on whether spin variables σ or occupancies n are considered. A study of FDT violations in this model leads to the following conclusions [266]: (1) in the glassy regime $\mu > \mu_d$ dynamics is one-step like, i.e. a two-timescale scenario with two temperatures describes the relaxational behaviour pretty well; (2) the effective temperature $T_{\rm eff}$, as derived from the slope of the FD plots, is pretty independent of the observable, whether this corresponds to spin variables ($C(t, t_w) = \langle\sigma(t)\sigma(t_w)\rangle$) or mixed spin-occupancy variables ($C(t, t_w) = \langle\sigma(t)n(t)\sigma(t_w)n(t_w)\rangle$) and (3) $T_{\rm eff}$ is apparently independent of the waiting time. However, this last result has to be taken with caution as the range of waiting times considered in [266] may not be large enough[14] to display such a small effect (compare for instance with the results described in section 7.1, figure 21). The observable independence of $T_{\rm eff}$ is shown in figure 28. It should be noted that the above scenario is reminiscent of 1RSB behaviour and occurs in finite D rather than in the mean-field limit $D \to \infty$. Actually the mean-field version of the model does not have a 1RSB low-temperature phase [267].

7.3. Coarsening systems

Although coarsening has been briefly sketched in section 6.6 here we present a more detailed account of results. Coarsening systems are the paradigm of systems which do not reach equilibrium. In such systems TTI does not hold, and all time-dependent correlation functions for large times are of the form $C(t, s) = C(L(t)/L(s))$ where $L(t) \propto t^{1/z}$ is the typical size of the coarsening regions [268]. The dynamic exponent z is characteristic of the universality class of the system and its value depends on whether dynamics conserves or not the value of the order parameter. This functional form is similar to that found for the long-time correlation functions of glasses in the aging regime, and indeed a certain type of coarsening has been advocated as responsible for slow relaxation in glasses [51, 269–271]. The difference between the two systems only becomes manifest when one also considers the response functions associated with the correlation functions. Glasses, such as spin glasses or molecular glasses,

[14] In fact, the range of waiting times explored does not even cover one order of magnitude.

are characterized by long-term memory which results in a non-zero FDR X. On the other hand, for stochastically stable systems [160, 161] the FDR $X(C)$ coincides with the static Parisi function (246). For a ferromagnetic system $P(q)$ is trivial

$$P(q) = \delta(q - m^2) \tag{250}$$

where $m = m(T)$ is the magnetization at temperature T, and hence X is 1 if $1 > C > m^2$ and 0 if $C < m^2$. The argument can be easily extended to the case of a few separate phases. Therefore we expect that in systems in which two (or few) phases separate, X should vanish for long times, signalling the presence of weak long-term memory.

The simplest model displaying domain growth is a ferromagnetic Ising model on a square or cubic lattice of linear size L with single-spin-flip Glauber dynamics. When the system is quenched at time $t = 0$ from a random configuration ($T = \infty$) to a finite temperature T below the critical temperature T_c, domains of 'up' and 'down' spins start to form and grow. This is well reflected by the behaviour of the two-times spin–spin correlation function

$$C(t, s) = \frac{1}{N} \sum_{i=1}^{N} \langle \sigma_i(t)\sigma_i(s) \rangle \tag{251}$$

which for times $t - s \ll s$ (assuming $s < t$) is TTI and rapidly decays from 1 to m^2, m being the average magnetization at temperature T. Later, for more separate times $t - s \gg s$ the TTI is lost, and the aging part of the correlation scales as

$$C_{\mathrm{ag}}(t, s) = F\left[\frac{L(t)}{L(s)}\right] \tag{252}$$

where $L(t)$ is the typical size of the domains at time t. The calculation of the linear response proceeds as usual, i.e., at a certain waiting time t_w a small magnetic field h_i is applied and the induced magnetization is computed. For disordered systems, such as spin glasses, the applied field can be either uniform or random. The advantage of an uniform field is that averaging over different realizations of the field is avoided. However, for systems without disorder, such as ferromagnetic systems, a uniform field would favour one of the phases making it grow faster. In this case, a random field must be used and the correct quantity to measure is the staggered magnetization [272],

$$M(t, s) = \frac{1}{N} \sum_{i=1}^{N} \overline{\langle \sigma_i(t) h_i \rangle} \tag{253}$$

where h_i is the local (quenched) random field, and the overbar denotes average over the field realizations.

In figure 29 we show the curves $\chi(t, t_w) = M(t, t_w)/h$ versus $C(t, t_w)$ obtained with a bimodal field distribution $h_i = \pm h$ [272]. The FDT region and the flattening of the curve are well evident. Two aspects of these curves are worth noting. First of all the value of the plateau reached by the magnetization decreases as t_w increases. Moreover, for fixed t_w the magnetization first grows in the non-aging part as $h(1 - C)/T$, then saturates and eventually goes down again. Indeed, the comparison [273] with the equilibrium response function shows that the equilibrium value of the response lies rather below the plateau. The study of a soft spin version with Langevin dynamics [272, 273] leads to similar results.

There are two contributions to the staggered magnetization: one from the domain walls, the other from the domain bulk. The difference between the plateau and the equilibrium values of $M(t, t_w)$ can be attributed to the domain wall response. After a time t_w the domains have reached a certain typical size, and the domain walls have a certain total length. The effect of the random field is to try to flip some spins. Clearly, the flipping is easier at the domain walls

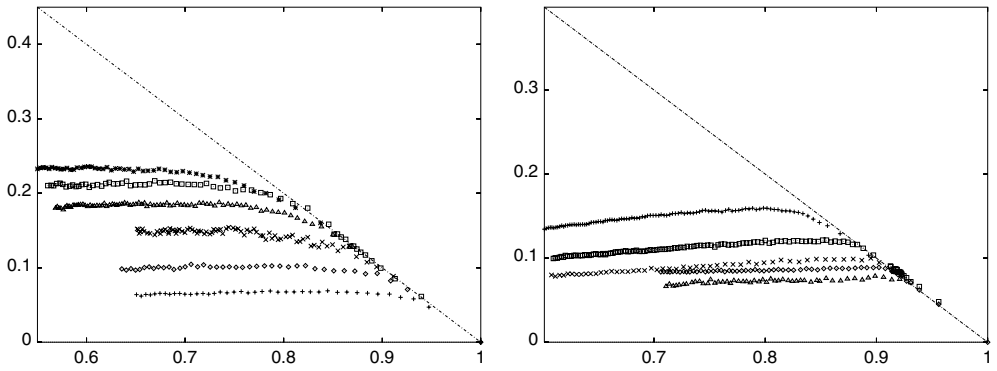

Figure 29. $TM(t, t_w)/h$ versus $C(t, t_w)$ domain growth. Left panel: 2D case with $T_c = 2.27$, at temperatures (from top to bottom) $T = 1.7$ and $t_w = 200, 400, 800, 2000$, $T = 1.3$ and $t_w = 800$, $T = 1$ and $t_w = 800$. Right panel: 3D case with $T = 2.5$ ($T_c \approx 3.5$), $t_w = 100, 300, 600, 1000, 1500$. The straight line is $M = 1 - C$: we see that FDT holds at short times t, and the violation of FDT with $X = 0$ at longer time separation. From [272].

where the spins are less constrained by their neighbours. As time proceeds the domains grow, increasing the bulk at the expense of the total domain wall length. Therefore the contribution from the interfaces decreases with time. On the other hand, the contribution of the bulk is almost independent of t_w since the effect of a random field on 'up' and 'down' domains is the same on average. Therefore, after the initial quasi-equilibrium growth, the total staggered magnetization decreases as t_w increases and, for a fixed value of t_w it decreases as t increases. Analytical results [273] show that the aging part of the IRF is of the form

$$M_{ag}(t, s) \sim A(s) F\left[\frac{L(t)}{L(s)}\right] \qquad C_{ag}(t, s) \sim F\left[\frac{L(t)}{L(s)}\right] \tag{254}$$

where

$$\begin{aligned} A(t) &\sim \frac{1}{L(t)} && d > 2 \\ &\sim \frac{\ln(L(t))}{L(t)} && d = 2. \end{aligned} \tag{255}$$

Because $X(s) \sim \left|\frac{\partial A(L(s))}{\partial L(s)}\right|$ the results (255) explain the slower decrease of the IRF for the two-dimensional case observed in figure 29. The numerical test of the scaling law (255) in two dimensions is shown in figure 30.

This scenario leads to the conclusion that coarsening systems do not display a non-trivial $X(C)$. Recent results [217], however, indicate the possibility of non-trivial $X(C)$ also in these systems. The motion of the domain wall in the presence of an external random field follows from two competing processes: the tendency to reduce the interface curvature due to surface tension and the pinning of the domain wall in favourable positions introduced by the external field. This introduces a dependence on the space dimension since the curvature process, which dominates at large enough dimensions, weakens as the dimension decreases. When the dimension reaches the lower critical dimension the curvature process disappears and the response of the system becomes non-trivial [214, 217] as is indeed seen for the ferromagnetic Ising chain ($d = 1$) [182, 212][15].

[15] See also the discussion in section 6.6. Similar effects are also observed in kinetically constrained models described in section 7.5.

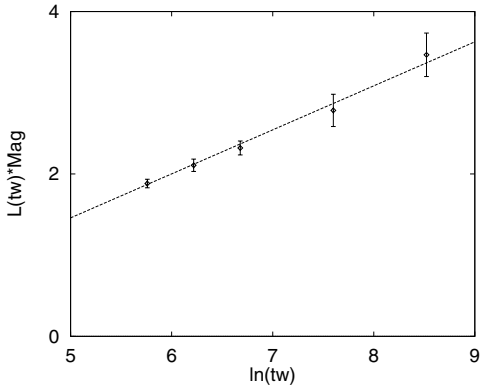

Figure 30. Test of the scaling (254), (255) which predicts a linear dependence of $L(s)M_{ag}(t,s)$ w.r.t. $\ln(s)$ with $s = t_w$. The dashed line fits this dependence very well. From [273].

The domain walls may give a large contribution to the response also at the early FDT part, but almost exclusively from their deformation on relatively short lengths. These fluctuations can be considered thermalized and hence do not spoil the $1/T$ behaviour but, on the contrary, contribute to making the $1/T$ slope of the initial part in the FD plot longer. A generalization of the Ising model to include some frustration via long-range antiferromagnetic interactions has been studied in [274]. Models of this type have been proposed to study, among others, the avoided phase transition in supercooled liquids [275] and charge density waves in doped antiferromagnets [276][16]. They are described by the Hamiltonian

$$\mathcal{H} = -\delta \sum_{\langle i,j \rangle} \sigma_i \sigma_j + \sum_{(i,j)} \frac{\sigma_i \sigma_j}{r_{ij}^3} \tag{256}$$

where σ_i are Ising spins, the first sum runs over all pairs of nearest neighbour sites of the lattice, the second over all distinct pairs, and r_{ij} is the distance between sites i and j. The parameter δ represents the local/non-local exchange ratio. It is known [278] that for a two-dimensional square lattice the ground state of the model is antiferromagnetic for $\delta < 0.85$. For $\delta > 0.85$ the antiferromagnetic state becomes unstable with respect to the formation of striped domains. The study of the non-equilibrium dynamics reveals a crossover from a logarithmic decay for $\delta < \delta_c \sim 2.7$ to an algebraic decay for $\delta > \delta_c$ [274]. However, despite this richer scenario, the FD plot leads in both cases to a vanishing X, and hence to a coarsening scenario. Similar results are found in other coarsening-like systems such as the Migdal–Kadanoff spin glass [279] although in that model the definition of the dynamics appears rather tricky as most of the spins occupy the deepest hierarchical layer in the model.

We conclude this section on coarsening by discussing a hard-sphere lattice gas model in the spherical approximation originally introduced by Lebowitz and Percus (LP) [280]. The interest in this model is twofold. On the one hand, its dynamical behaviour can be solved analytically, hence allowing a detailed investigation of the non-equilibrium behaviour. On the other hand, it is known that hard-sphere models have a fragile-glass behaviour [90].

Lattice-gas models are defined on a lattice of finite dimensions. On each site there can be a density $\rho(\boldsymbol{x})$ of particles, which in the limit of hard spheres can take only the values 0

[16] These models are of interest for information storage in ultra-thin ferromagnetic films [277].

(*empty*) or 1 (*occupied*). In the LP model this restriction is relaxed and ρ takes any continuous value allowed by a spherical constraint:

$$\sigma_1 \equiv \sum_{\boldsymbol{x}} \rho(\boldsymbol{x})^2 - \sum_{\boldsymbol{x}} \rho(\boldsymbol{x}) = 0. \tag{257}$$

There is the additional restriction that the density–density correlation function between nearest neighbours vanishes. This is added to mimic some kind of extended hard-core,

$$\sigma_2 \equiv \sum_{\boldsymbol{x}} \sum_{\boldsymbol{q}} \rho(\boldsymbol{x})\rho(\boldsymbol{x}+\boldsymbol{q}) = 0 \tag{258}$$

where $\boldsymbol{q}$ are the vectors that join a lattice site $\boldsymbol{x}$ to its nearest neighbours. In [31] the following Langevin dynamics for an open system has been studied,

$$\frac{\partial}{\partial t}\rho(\boldsymbol{x}', t) = \mu - \frac{\partial}{\partial \rho(\boldsymbol{x}')}\mathcal{H}[\rho(\boldsymbol{x}'), t] + \eta(\boldsymbol{x}', t) \tag{259}$$

where μ is the chemical potential, η the thermal noise, and $\mathcal{H}$ the Hamiltonian

$$\mathcal{H} = \lambda_0(t) \sum_{\boldsymbol{x}} [\rho(\boldsymbol{x})^2 - \rho(\boldsymbol{x})] + \lambda_1(t) \sum_{\boldsymbol{x}} \sum_{\boldsymbol{q}} \rho(\boldsymbol{x})\rho(\boldsymbol{x}+\boldsymbol{q}). \tag{260}$$

Strictly speaking in this model there is no energy, but only entropy. The role of $\lambda_0(t)$ and $\lambda_1(t)$ in the Hamiltonian is to make the dynamics fulfil the constraints (257) and (258) at all times. The non-equilibrium dynamics of this model shares a large number of features with that of the spherical SK model [149, 150, 281] where the dynamics is driven by the macroscopic condensation of the system onto the disordered ground state. A positive chemical potential would increase the local density, thus starting from an empty state the local density relaxes towards the equilibrium value. The relaxation can be divided into two regimes, the first one where the system is filled in a spatially uncorrelated way. The typical time for this process is order $t^* \sim O(1)$. It is only later that slow relaxation starts when the system is spatially correlated and needs to reorganize large regions in order to increase its density. The model has no built-in disorder, and the slowing down is a purely entropic, direct consequence of the decrease in the number of available configurations imposed by the short-range constraints. When the temperature is below the critical temperature T_c the two motions have well-separated timescales and the two-times correlation function shows the usual two-step form with the first part TTI and the second part scaling as t/t_w, see figure 2 (the plot corresponds to the 3D model at $T = 0.1$; different waiting times from top to bottom are $t_w = 10\,000$, 1000, 300, 100, 30, 10, 3, 1). Study of the FDR reveals that there is no anomaly in the response function [31] and X vanishes for values of C below the plateau value of the correlation. The glassy scenario of this model corresponds to that of phase-ordering kinetics with non-conserved order parameter. Similar results have been reported in spherical models with long-range ferromagnetic interactions [282].

7.4. Non-relaxational driven systems

We have been underlining throughout this review that aging systems are characterized by non-equilibrium behaviour with lack of TTI and by the presence of FDT violations. The relevant parameter which *controls* the aging non-equilibrium state is the waiting time or time elapsed since the system was quenched. However, there is another way to generate a non-equilibrium state that can be characterized by a given timescale in the same fashion as the waiting time characterizes the aging state. For instance, adding a time-dependent perturbation

of frequency ω to a time-independent Hamiltonian. In the regime where $\omega t_w \ll 1$ the perturbation oscillates slow enough to probe only slow processes occurring at timescales $\tau \gg t_w$. While in the opposite regime $\omega t_w \gg 1$ the oscillatory perturbation probes fast relaxation processes occurring at timescales $\tau \ll t_w$. The line $\omega t_w \sim 1$ marks the onset of glassy behaviour, the shape of this line depending also on the intensity of the perturbation.

Driven systems have advantages when compared to aging systems. One of the most important differences is that driven systems, in the stationary state, are TTI but FDT is still violated. Again the concept of an effective temperature can be introduced as a measure of these violations. However, as the non-equilibrium stationary state of driven systems can be described by the intensity of the driving force, they are more experimentally accessible than aging systems, where the waiting time appears as an external parameter difficult to control. For this reason, it has been advocated that experimental measurements of FDT violations and the effective temperature should be made in driven systems rather than aging systems.

There are many ways to put a system into a driven stationary state and these have been investigated in the literature for different types of models. Driven systems can be classified into the following two main groups:

- *Sheared systems.* In this case one considers systems where, in addition to conservative forces, other non-conservative forces (i.e. that cannot be derived from a potential function) act upon the system. In these systems the non-conservative forces may be time dependent or not. In both cases, the non-conservative forces do not work along a given closed dynamical path. This implies that energy power is continually supplied to the system by the driving force. The parameter which describes the stationary state is the intensity of the shearing or driving force which we will identify by the symbol ϵ or $\dot{\gamma}$. These systems include models that violate the action–reaction principle (such as models with asymmetric couplings) and sheared fluids. These systems are described in section 7.4.1.
- *Tapped systems.* In this class, systems are driven to a non-equilibrium state by a time-dependent force which, however, derives from a time-dependent potential. This means that the driving force, if constant in time, does not exert work upon the system whatever its intensity ϵ. This class of systems includes spin-glass models in a oscillating magnetic field and tapped granular systems where the relevant parameter is the frequency of the driving force. These systems are described in section 7.4.2.

7.4.1. Sheared systems. Studies of models described by non-conservative forces go back to the study of neural network models described by synaptic interactions that are non-symmetric [283]. This has inspired future investigations of disordered models where couplings among spins include an important degree of asymmetry. In [284, 285] was considered the relaxational dynamics of the $p = 2$ spherical spin glass with pairwise interactions J_{ij} given by $J_{ij} = J_{ij}^S + \epsilon J_{ij}^A$ where $J_{ij}^S = J_{ji}^S$ denotes the symmetric (therefore conservative) part and $J_{ij}^A = -J_{ij}^A$ stands for the antisymmetric (therefore non-conservative) part. It was shown that any finite amount of asymmetry is enough to destroy the spin-glass phase. The relaxational time of the system was found to diverge as ϵ^{-6} for $\epsilon \to 0$. Importantly, this result suggests the following general scenario: whatever the intensity of the non-conservative force, the stationary state has a finite relaxation time, therefore the stationary state, although of non-equilibrium nature, must be TTI (and, therefore, correlations and response functions do not display aging). Subsequent investigations have confirmed this result showing that this is a generic feature of driven systems.

Among this family of asymmetric spin-glass models, one which has been intensively investigated in past years is the p-spin spherical spin-glass Hamiltonian (150), (151) with

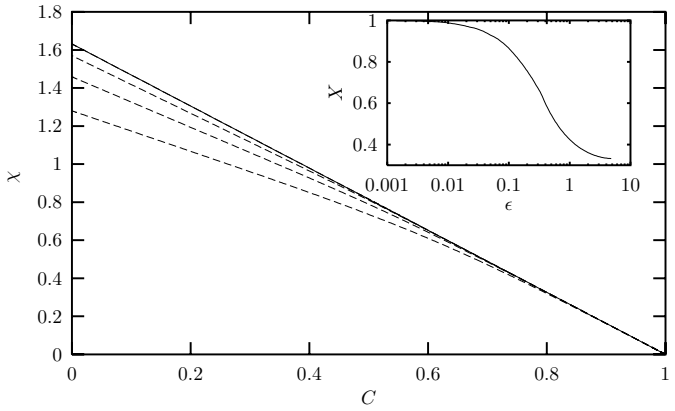

Figure 31. FD plot for the model (261)–(263) with $k = p = 3$ and $T = 0.613 > T_c = 0.612$. The full line is the $\epsilon = 0$ equilibrium curve. Dashed lines correspond to (from bottom to top) $\epsilon = 0.333, 0.143, 0.05, 0$. The inset is the FDR as a function of the intensity of the perturbation. From [287].

asymmetry in the interactions. The model is defined according to the following Langevin dynamics [286, 287]:

$$\frac{\partial \sigma_i(t)}{\partial t} = -r(t)\sigma_i(t) + F_i(\{\sigma\}) + \eta_i. \tag{261}$$

This dynamics is the same as (153) but now the force $F_i(\{\sigma\})$ is replaced by

$$\begin{aligned} F_i(\{\sigma\}) &= -\frac{\delta \mathcal{H}}{\delta \sigma_i} + F_i^{\text{drive}}(\{\sigma\}) \\ &= -\frac{\delta \mathcal{H}}{\delta \sigma_i} + \epsilon \sum_{j_1 < \cdots < j_{k-1}} K_i^{j_1, j_2, \ldots, j_{k-1}} \sigma_{j_1, \ldots, \sigma_{j_{k-1}}} \end{aligned} \tag{262}$$

where $\mathcal{H}$ is the Hamiltonian given in (150) and the driving force $F_i^{\text{drive}}(\{\sigma\})$ describes a k-spin interaction term where the couplings $K_i^{j_1, j_2, \ldots, j_{k-1}}$ are uncorrelated among all permutations of the k different indices $(i, j_1, j_2, \ldots, j_{k-1})$,

$$\overline{K_i^{j_1, j_2, \ldots, j_{k-1}} K_{j_r}^{j_1, j_2, \ldots, j_{r-1}, i, j_{r+1}, \ldots, j_{k-1}}} = 0. \tag{263}$$

These models show the following behaviour. In the regime above the mode-coupling temperature T_c, the relaxation time is finite for the unsheared model $\epsilon = 0$. Therefore both TTI and FDT hold in the stationary state. A small driving force $\epsilon > 0$ puts the system in a new stationary state where TTI holds but FDT is violated. Numerical analysis of the mean-field equations [287] reveals that both FD plots and the value of the FDR are very similar to those found in aging systems. Figure 31 shows these quantities above T_c for the model with parameters $k = p = 3$. Below T_c a new phenomenon, called 'shear thinning', occurs. At $\epsilon = 0$ the relaxation time diverges (as is common in mean-field (MF) models where activated processes are neglected, see discussion in section 6.1). However, as $\epsilon > 0$ the relaxation time becomes finite and decreases with ϵ (shear thinning). Again, numerical analysis of the mean-field equations reveals that for finite ϵ the resulting FD plots are the same as for an aging system with a waiting time t_w given by $t_w \sim \epsilon^{-\alpha(T)}$ where $\alpha(T)$ is a temperature-dependent exponent that takes the value 2 at T_c and slowly increases as T decreases. This scenario, as derived from the study of MF spin-glass models, has been confirmed in numerical studies of

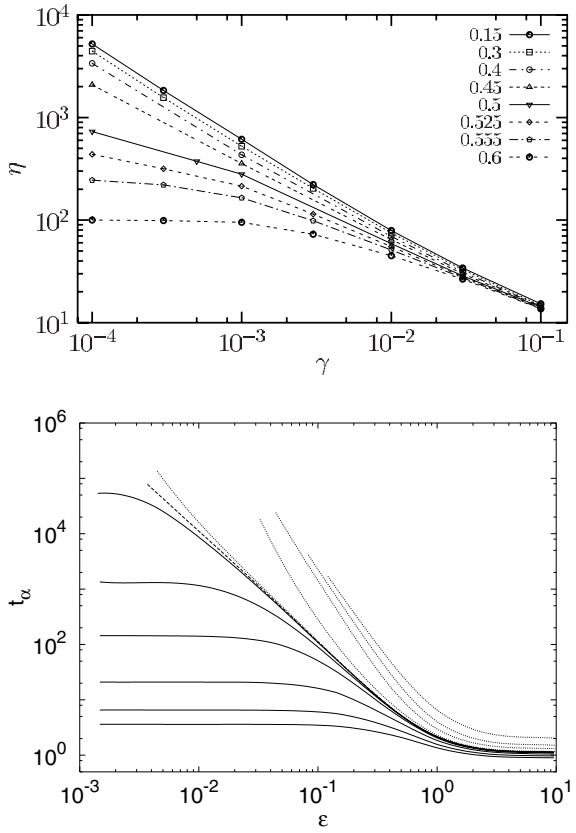

Figure 32. Viscosity as a function of the shear rate for the LJ (top panel) and MF spin-glass models (bottom panel). The viscosity η and shear rate $\dot{\gamma}$ in the LJ fluid correspond to the terminal time τ_α and ϵ/τ_α, respectively, in the MF model. $T_c \simeq 0.435$ in the LJ model and $T_c \simeq 0.612$ in the MF model. Temperatures (from bottom to top): (bottom panel) 0.9, 0.8.0.7, 0.64, 0.62, 0.613, T_c, 0.6115, 0.58, 0.45, 0.3, 0.01 and (upper panel) as indicated in the box. From [287] (top panel) and [289].

binary mixtures of Lennard-Jones (LJ) sheared fluids (see section 7.1.2). In a series of papers, Barrat and Berthier [288–290] have shown that driven short-range systems display the same features as their equivalent MF disordered models. These similarities have been confirmed by other studies that measure the temperature dependence of the shearing rate at which the average potential energy deviates from its equilibrium value [291]. The similarity between LJ models and MF spin glasses is striking concerning rheological properties. In a sheared fluid the velocity field $\boldsymbol{v} = \dot{\gamma} y \boldsymbol{e}_x$ induces a stress σ_{xy} that is well described by the phenomenological law: $\sigma_{xy} = \sigma_0 + a\dot{\gamma}^n$. This law is commonly found in rheological systems [292]. The viscosity is defined by $\eta = \sigma/\dot{\gamma}$: for Newtonian fluids $n = 1$ and $\sigma_0 = 0$, the viscosity is therefore independent of the stress. However, this is known to be inaccurate as many complex fluids show transport coefficients (such as the viscosity) that depend on the shear rate (for a discussion on these effects in the framework of non-equilibrium thermodynamic theories see [293, 294]). In figure 32 we show the flow curves for the viscosity as a function of the shear rate for both the LJ fluid and the MF spin glass, the viscosity η and the shear $\dot{\gamma}$ in the LJ model corresponding to the terminal relaxation time τ_α and ϵ/τ_α in the MF spin glass respectively. The similarity

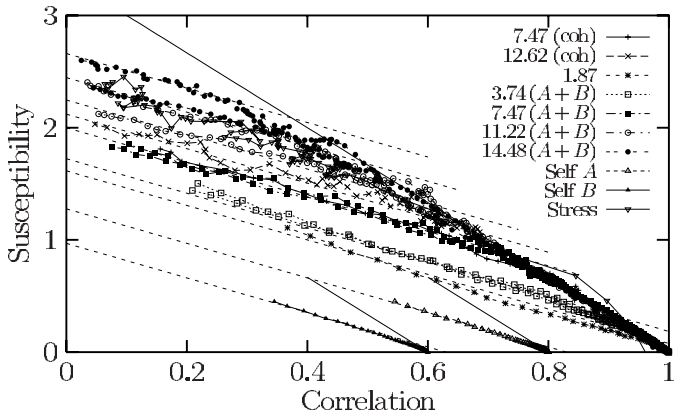

Figure 33. Fourteen FD parametric plots in the LJ model showing the independence of the effective temperature from the observable. The numbers in the key of the figure indicate different values of the wave vectors; 1.87 refers to class 1 in the text. 'coh' stands for coherent or global scattering functions (class 2). A and B refer to the two different chemical species, $(A + B)$ standing for incoherent scattering observables independently measured for A and B species (class 3). 'self' indicates the use of the mean-square displacement (class 4). 'stress' refers to class 5. The value of the effective temperature is compatible with $T_{\rm eff} = 0.65 > T = 0.3$ for all cases. From [289].

is noteworthy. There are two regimes depending on whether $T > T_{\rm c}$ or $T < T_{\rm c}$. In the first regime the fluid is Newtonian at low shearing rates so the viscosity is shear independent. In this regime, standard non-equilibrium thermodynamics [295] is applicable. However, for $T < T_{\rm c}$ the fluid is non-Newtonian and the viscosity diverges at zero shear, $\eta \sim \dot{\gamma}^{-\alpha(T)}$ with $\alpha(T)$ between $2/3$ (at $T_{\rm c}$) and 1 (for $T \to 0$) in agreement with the aforementioned results found in the MF spin glass. The central question addressed in [288–290] was the dependence of the resulting FD plots on the type of observable used as a perturbation. They considered five different classes of observables: (1) the incoherent part of scattering functions (corresponding to single particle density fluctuations), (2) the coherent part or the correlations, (3) the 'chemical' observables associated with correlations of a single species of particles in the binary mixture, (4) the mean-square displacement of particles associated with a constant small force transverse to the flow and (5) the stress in the transverse direction after compression of the box; (1), (2) and (3) were measured at different wave vectors. In all cases, the effective temperature was found to be the same within numerical accuracy. A compendium of their results is shown in figure 33. There have been other studies on driven systems that have investigated the shear thinning effect, i.e. whether a driving force of rate $\dot{\gamma}$ stops aging up to a timescale proportional to $1/\dot{\gamma}$ by restoring TTI. Corberi *et al* [296] have investigated coarsening models in the presence of a driving force. In particular, they have considered a N-component ferromagnetic model with non-conserved order parameter in the large N limit. The authors find that, above the ferro–paramagnetic transition temperature $T_{\rm c}$, the inverse of the driving rate $1/\dot{\gamma}$ sets the timescale after which aging stops and the system becomes TTI. However, below $T_{\rm c}$, contrary to what is observed in MF spin glasses, aging never stops even in the presence of shearing. The origin of this difference is unclear. It could be related to the fact that in coarsening systems the mechanism responsible for aging is different from that in MF spin glasses or LJ glasses. This difference can be traced back to the absence of complexity in the coarsening model as compared to the other cases. Moreover, this behaviour has to be contrasted with what is found in tapped systems such as MF spin glasses in an AC field

[297] where aging survives below T_c in a certain range of magnetic field values (see further discussion on this model in section 7.4.2). Other, studies have considered models such as vortex glasses with random pinning centres in two dimensions [298] where the external driving force is uniform over all vortices. Also in this case FDT violations appear to be described by an effective temperature related to the slow motion of vortices. Trapping dynamics due to pinning defects has also been considered in the study of a driven classical particle subjected to a force [299, 300]

A common feature of all the studies reported here, that has not been emphasized enough in the existing literature, is that measured correlations must be transverse to the direction of the shear flow to yield a meaningful effective temperature. FDT violations for longitudinal observables are apparently not described by an effective temperature. This suggests that neutral observables describing an effective temperature are restricted to the transverse direction, a fact that as yet lacks a clear explanation.

7.4.2. Tapped systems. As already mentioned, another class of driven systems corresponds to those where the external force derives from a time-dependent potential that pumps energy into the system. This also includes driven granular media that have recently received considerable attention.

In [297], the authors have studied the MF p-spin glass model in an oscillating AC field. This problem is interesting as it shows a behaviour different from that observed in sheared MF spin glasses or LJ glasses (see section 7.4.1). The model considered was again (150) but in the presence of an uniform AC field of frequency ω and intensity h. The phase diagram of the model is described by three parameters T, h, ω. Below T_c, at fixed ω, the glassy phase survives below a critical field $h^*_\omega(T)$ meaning that, contrary to sheared systems, a small driving force does not destroy the glassy phase and aging never stops, hence TTI is not restored. This justifies the use of AC fields in experiments to explore the aging regime within the linear response region. A striking result in these studies is the presence of reentrant behaviour at constant field h, as ω is varied, indicating that $\lim_{\omega\to 0} h^*_\omega(T,\omega) < h^*_\omega(T,\omega=0)$, a result that still needs to be clarified. All over the glassy phase of the driven model FDT is violated with the characteristic FD plots of the corresponding relaxational model.

Granular systems may present very slow processes, analogous to what is seen in glasses. Similar to what has been done for other glassy systems one can try to describe the dynamics of the slow degrees of freedom through an effective temperature defined from the FDR [100]. The first example we consider is the kinetically constrained Kob–Andersen model [301] that, even if very schematic, reproduces rather well several aspects of glasses [302] and of granular compaction [303]. Although section 7.5 is devoted to kinetically constrained models we prefer to describe the Kob–Andersen model here since it is a good model for granular media. This model consists of N particles in a cubic lattice, with periodic boundary conditions. There can be at most one particle per site. Apart from the hard-core repulsion there are no other static interactions among particles. At each time step a particle can move to a neighbouring empty site of a three-dimensional lattice only if it has less than four neighbours in the initial and final positions. In its simpler version there is no gravity, but the system is subject to a constant pressure on its surface, obtained by adding or destroying particles on the topmost layer with a chemical potential μ. The dynamic rule guarantees that at equilibrium all configurations of a given density are equally probable. Indeed when the density is of the order of the jamming density $\rho_g \simeq 0.88$ the particle diffusion becomes extremely slow, due to the kinetic constraints, slowing down the whole compaction process. As done for glasses, one can try to describe the slow non-equilibrium motion through an effective dynamical temperature $T_{\rm eff}$ which can be defined via a generalization of the Einstein–Stokes relation between the diffusion coefficient

and the viscosity to a non-equilibrium (aging) situation,

$$\frac{\partial}{\partial \boldsymbol{f}}\langle \boldsymbol{r}(t) - \boldsymbol{r}(t_w)\rangle = -\frac{X(B)}{2T}\frac{\partial}{\partial t_w}\langle(\boldsymbol{r}(t) - \boldsymbol{r}(t_w))^2\rangle \tag{264}$$

where $\boldsymbol{r}$ is the particle position, $\boldsymbol{f}$ a (small) perturbing field, $t > t_w$ two widely separated times, and $B(t, t_w)$ the mean-square displacement:

$$\begin{aligned} B(t, t_w) &= \langle(\boldsymbol{r}(t) - \boldsymbol{r}(t_w))^2\rangle \\ &= \frac{1}{3N}\sum_{a=1}^{3}\sum_{i=1}^{N}\left\langle\left[r_i^a(t) - r_i^a(t_w)\right]^2\right\rangle. \end{aligned} \tag{265}$$

The linear response function can be computed numerically by applying a small random perturbation at time t_w of the form [304]

$$\delta\mathcal{H}_\epsilon = \epsilon\sum_{a=1}^{3}\sum_{i=1}^{N} f_i^a r_i^a \tag{266}$$

where f_i^a are independent quenched random variables which take the value ± 1 with equal probability. With this choice the IRF is defined as

$$\chi(t, t_w) = \frac{1}{3N}\sum_{a=1}^{3}\sum_{i=1}^{N}\left\langle f_i^a \Delta r_i^a(t)\right\rangle \tag{267}$$

where $\Delta\boldsymbol{r}(t + t_w)$ is the difference between the displacement of the same particle in two identical copies of the system, one evolving in presence of the external perturbation and one without. From (264) χ is related to B through

$$\begin{aligned} \chi(t, t_w) &= \frac{\epsilon}{2T}\int_0^{B(t,t_w)} X(B)\,\mathrm{d}B \\ &= \frac{\epsilon}{2T_{\mathrm{eff}}}B(t, t_w) \qquad \text{if} \quad X(B) = m = \text{const} \end{aligned} \tag{268}$$

with $T_{\mathrm{eff}} = T/m$. The numerical simulations show a two-regime scenario [304] similar to what is seen in glasses, i.e., for $t - t_w$ smaller than t_w $m = 1$ and FDT holds, while for $t - t_w \gg t_w$ FDT is violated with $m < 1$, see figure 34. As discussed in section 5.3 the value of the observables attained dynamically in a granular system could be computed from the usual equilibrium microcanonical distribution at the corresponding density ρ restricted to the subset of *blocked* configurations (Edwards ensemble), i.e., only to those configurations in which every grain is unable to move. Very similar to the IS analysis in glassy systems (section 4.5), the Edwards ensemble leads to the definition of a temperature, called the Edwards temperature, as

$$\frac{1}{T_{\mathrm{Edw}}(\rho)} = -\frac{1}{\mu}\frac{\partial s_{\mathrm{Edw}}(\rho)}{\partial\rho} \tag{269}$$

where $s_{\mathrm{Edw}}(\rho)$ is the Edwards entropy density obtained from the logarithm of the number of blocked configurations of given ρ, see (135). The chemical potential fixes the dimension [305, 306].

The Edwards entropy for this model has been computed in [305, 306] through the use of an auxiliary model in which each particle has energy equal to 1 if the dynamic rules allow it to move, and zero otherwise. The auxiliary energy E_{aux} is hence equal to the number of mobile particles. The configurations of the auxiliary model are sampled with a Monte Carlo procedure with non-local moves at the auxiliary temperature $1/\beta_{\mathrm{aux}}$. These non-local moves have nothing to do with the true dynamics of the original model, and the auxiliary model is not

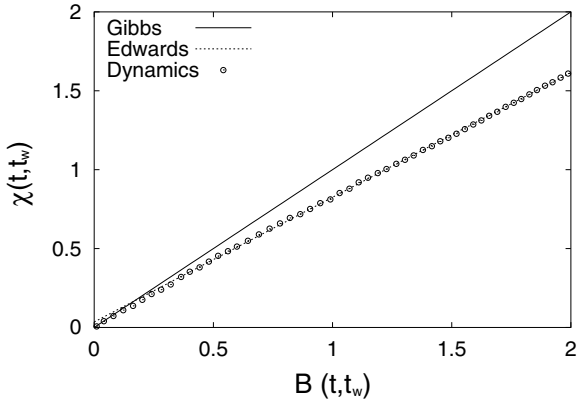

Figure 34. Einstein relation in the Kob–Andersen model: plot of the mobility $\chi(t, t_w)$ versus the mean-square displacement $B(t, t_w)$ (data shown as circles). The slope of the full straight line corresponds to the equilibrium temperature ($T = 1$), and the slope of the dashed one to Edwards' prescription obtained from figure 35 at $\rho(t_w) = 0.848$. From [305].

glassy. This allows us to obtain equilibrium properties such as the auxiliary energy density $e_{\rm aux}$ from which the entropy density can be obtained via thermodynamic integration,

$$s_{\rm aux}(\beta_{\rm aux}, \rho) = s_{\rm equil}(\rho) + \beta_{\rm aux} e_{\rm aux}(\beta_{\rm aux}, \rho) - \int_0^{\beta_{\rm aux}} e_{\rm aux}(\beta'_{\rm aux}, \rho)\, {\rm d}\beta'_{\rm aux} \tag{270}$$

since $s_{\rm aux}(0, \rho) = s_{\rm equil}(\rho)$. The blocked configurations at a given density can be computed performing a simulated annealing down to $\beta_{\rm aux} \to \infty$ of the auxiliary model at fixed particle density. The Edwards entropy density is then obtained as

$$\begin{aligned} s_{\rm Edw}(\rho) &= \lim_{\beta_{\rm aux}\to\infty} s_{\rm aux}(\beta_{\rm aux}, \rho) \\ &= s_{\rm equil}(\rho) - \int_0^{\infty} e_{\rm aux}(\beta_{\rm aux}, \rho)\, {\rm d}\beta_{\rm aux}. \end{aligned} \tag{271}$$

since $e(\beta_{\rm aux}, \rho)$ vanishes for $\beta_{\rm aux} \to \infty$. The Edwards entropy is shown in figure 35 as a function of density. We are now in a position to compare the long-time non-equilibrium results with those obtained from the Edwards measure. In figure 34 is shown the mobility $\chi(t, t_w)$ versus the mean-square displacement $B(t, t_w)$. The agreement between $T_{\rm eff}$ and $T_{\rm Edw}$ is clearly satisfactory.

Similar results have also been found [305–307] for models with geometrical, rather than kinetical, constraints, the so-called 'Tetris' models [308, 309]. These models are defined on a two-dimensional lattice with particles of randomly chosen shapes and sizes. The only constraint is that particles cannot overlap: for two nearest neighbour particles the sum of the arms oriented along the bond connecting them has to be smaller than the bond length.

Tapped granular matter [310, 311] has been considered in several models such as the one-dimensional (1D) model ferromagnet [312] showing that the Edwards measure provides a very good description of the stationary state. A similar agreement is found in simulations of sheared granular matter [313]. Real compaction occurs in the presence of gravity [314]. The gravity introduces an extra term in the Hamiltonian

$$\mathcal{H}_g = mg \sum_{i=1}^{N} h_i \tag{272}$$

where g is the gravity constant, m the particle mass and h_i the height of the ith particle.

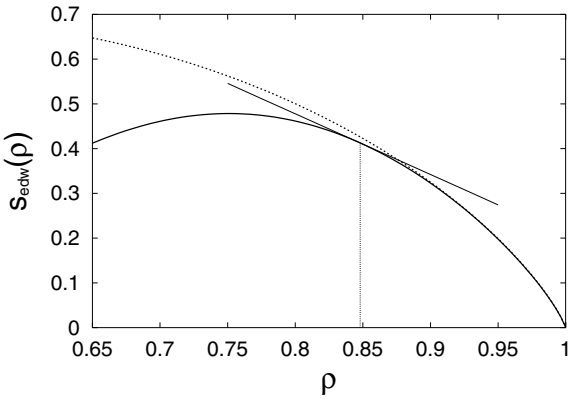

Figure 35. The Edwards entropy per particle of the Kob–Andersen model versus density (full curve). For comparison we also show the equilibrium entropy (dashed curve). At high enough density the curves are indistinguishable, and join exactly only at $\rho = 1$. The slope of the tangent to $s_{\rm Edw}(\rho)$ for a generic ρ allows us to extract $T_{\rm Edw}(\rho)$ from the relation $T_{\rm Edw}(\rho)\frac{ds_{\rm Edw}}{d\rho} = \mu$. From [305].

The simplest way of including gravity in the above models is assuming that particles can move up and down (if they respect the geometrical or kinetical constraints) with different probabilities, $p = \min[1, \exp(-mg\Delta h/T)]$ where $\Delta h = -1, 0, 1$ is the elementary vertical displacement. A closed boundary is situated at the bottom of the system. The control parameter $x = \exp(-mg/T)$ represents the 'vibration'. The presence of gravity introduces a preferred direction in the diffusive motion (downwards) which in turn may produce inhomogeneities in the vertical density profile making the situation more complicated, moreover horizontal (transversal) and vertical (longitudinal) quantities must be treated separately.

Inhomogeneities are only along the vertical direction, so transversal observables when measured well inside the bulk are not too sensitive to the detailed form of the density profile. Indeed if homogeneity of the bulk is imposed, the dynamical temperature obtained from the FDT ratio for the horizontal displacement mobility coincides with the Edwards temperature [307].

The analysis of the FDT ratio for the longitudinal motion [315, 316] also shows a two-slope scenario, however the comparison with the Edwards measure is more complex due to the presence of inhomogeneities. In [316], based on the observation that the density profile far from the top and bottom layers is rather flat, the effective dynamical temperature for longitudinal observables and the Edwards temperature have been compared assuming a homogeneous density. The comparison, however, reveals strong deviations when inhomogeneities are stronger indicating that inhomogeneities of the density profile must be included. This could be done by using the recently introduced restricted Edwards measure [116, 317], a route not yet explored.

We stress that the Edwards measure is constructed from a white sampling of blocked configurations, hence it reproduces the physical quantities at large times only if this condition is satisfied by the long-time dynamics. In other words, the Edwards measure can be inappropriate even though the system presents a slow dynamics. This is for example the case of the three-dimensional Ising model in a weak random magnetic field [305, 306]. Here the long-time configurations at low temperatures are made of domains of 'up' and 'down' spins of similar volumes, so that the global magnetization is zero. This is quite different from either the equilibrium or blocked configurations since both of them are magnetized. Other studies have

extended this method to the study of kinetically constrained models (KCMs) (see section 7.5) such as the Kob–Andersen model [318].

7.5. Kinetically constrained models

A category of statistical models that has received considerably attention during the last few years is kinetically constrained models (KCMs). In a nutshell, KCMs are models with trivial thermodynamics but complicated dynamics arising from a, put by hand, set of forbidden transitions in configurational space. Allowed transitions are selected according to a given transition rule that constrains the dynamics of the system. There are different ways to justify KCMs as valuable models for glassy dynamics. One can think of KCMs as effective models in which the slowest degrees of freedom are idealized as quenched variables that manifest as dynamical constraints. Therefore, the statistical variables of KCMs can be seen as the fast dynamical variables that are slaved, through the dynamical constraints, to the motion of the slowest ones. These constraints are of local nature as also is the interaction between the original degrees of freedom.

KCMs display most (if not all) of the features characteristic of glassy systems including slow relaxation, activated behaviour, cooperativity and non-equilibrium phenomena such as aging and FDT violations. Recently, a review on KCMs has been written that covers all these aspects. For this reason, here in this review we will not dwell much on discussing FDT violations on these models but content ourselves with underlining some of the most important results. We refer the reader to [15] for a comprehensive and exhaustive survey.

The most representative families of KCMs are spin-facilitated models [319, 320], lattice gases [301, 302, 304, 321, 322], topological cellular models [323, 324] and plaquette models [325–327]. We already discussed in section 7.4.2 the Kob–Andersen model as an example of kinetically constrained lattice gas for granular matter. There are two aspects of KCMs that make them especially attractive from a theoretical point of view. On the one hand, the thermodynamics of KCMs is straightforward, there is no underlying thermodynamic singularity, and even more astonishing, often the model is purely non-interacting from the point of view of its equilibrium properties. On the other hand, the non-interacting character of the energy function entails that the slow dynamics is described by representing the original variables in terms of a new set of effective variables. Relaxation can be visualized as a dynamical process where defects diffuse (in either a free or cooperative way) and annihilate each other, leading to a more tractable problem from the analytical point of view.

We begin our tour by presenting the simplest among these types of models. Our intention is to illustrate with an example what type of models KCMs are. Maybe the simplest KCM is the spin-facilitated model (SFM) introduced by Fredrickson and Andersen (FA) [319, 320] consisting of free 'spins' in a field. The model is defined by

$$E = h \sum_{i=1}^{N} n_i \tag{273}$$

where $n_i = 0, 1$ corresponding to two possible orientations of the spins ($n = 1$ up, $n = 0$ down)[17] that occupy a D-dimensional lattice. This model would be trivial if it were not for the dynamical rules that describe how spins can flip. In the standard SFM model transitions $n_i \to 1 - n_i$ are allowed if at least f among the possible nearest neighbours are up or $n = 1$. This model defines the f, d-SFM that shows different behaviour according to whether

[17] The variables n cannot be considered as occupancies and (273) does not define a lattice gas model. In lattice gas models the total number of particles (i.e. the energy E in (273)) is conserved while in the SFM it is not. See [15] for a thorough discussion. However, we will continue denoting the spins by n.

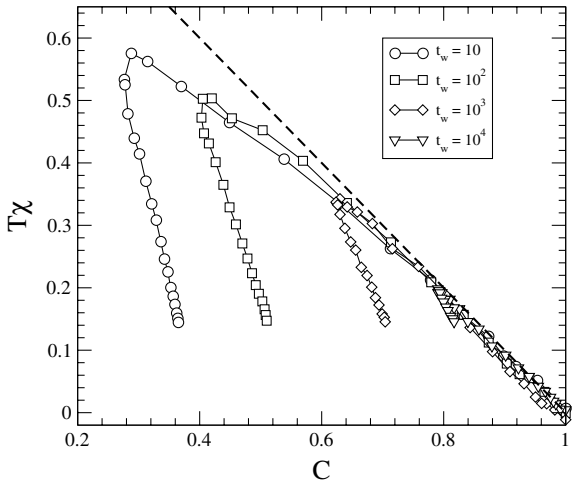

Figure 36. FD plots for the 1, 1-SFM (273) with $N = 10^5$, quench temperature $T = 0.3$ and different waiting times (see the box). The straight line is the FDT relation. From [70].

$f = 1$ (diffusive) or $f > 2$ (cooperative). Variations of the SFM include KCMs with directed constraints such as the 1D East model [328] or the 2D North-East model [329], defined again by (273), but where a spin n_i can flip only if the spin on its left is up (East model) and if both spins that are nearest neighbours in two fixed orthogonal directions (North-East model), point up. In one dimension, it is also possible to define a model that interpolates between the 1, 1-SFM and the East model [330].

In what follows we concentrate our attention on FDT violations in diffusive KCMs where some understanding has been recently gained. A generic aspect of KCMs is that dynamics is determined by the motion and annihilation of isolated defects. Slow dynamics strictly occurs at temperatures close to $T = 0$ (and timescales larger than an initial fast transient). The relevant relaxing variable is the number of isolated defects $c(t)$ (e.g. in the 1, 1-SFM this corresponds to the number of up spins). This has interesting consequences [217, 327, 331] in the behaviour of the IRF. The IRF in the presence of an external random staggered field $\chi(t, t_w)$ is then proportional to the product of the number of isolated defects $c(t)$ and the individual local response typical of one defect $\chi_{\rm eff}$. This local response is TTI as the defect is isolated leading to

$$\chi(t, t_w) \simeq \chi_{\rm ag}(t, t_w) = c(t)\chi_{\rm eff}\Big(\frac{t - t_w}{\tau(T)}\Big) \tag{274}$$

where $\tau(T)$ is the relaxation time of the defect. This relation has two important consequences: (1) the function $\chi(t, t_w)/c(t)$ is TTI, a result which is characteristic of coarsening systems (see below) but not of other (cooperative) glassy models where the IRF is a genuine aging function depending, for instance, on the ratio $h(t)/h(t_w)$ and (2) $\chi(t, t_w)$ has a maximum as a function of $t - t_w$ when the defect concentration (that decreases with time) compensates the growth of the monotonically increasing effective response $\chi_{\rm eff}$.

Non-equilibrium measurements for the 1, 1-SFM [70, 332] and related models such as the 2D triangle model [333, 334] or topological cellular models [323, 324] show an IRF (274) displaying a maximum as a function of $t - t_w$ and leading to awkward FD plots. One example is shown in figure 36. Buhot and Garrahan [327] have explained how to recover well-defined FD plots by using (274) and plotting $\chi(t, t_w)$ as a function of the difference $C_c(t, t) - C_c(t, t_w)$

where C_c is the standard connected correlation function $C_c(t,s) = \langle (n(t)-c(t))(n(s)-c(s))\rangle$ with $c(t) = \langle n(t)\rangle$ for the 1, 1-SFM. In this case, the resulting FD curve corresponds to a straight line (corresponding to the equilibrium result) casting doubts on the usefulness of FD plots for non-cooperative models.

The origin of the maximum in the IRF has also been considered in the 1D RFIM with infinite-ferromagnetic coupling $J = \infty$ [331]. Actually, in this limit the model turns out to be a KCM as transitions are only allowed on the spins sitting on the interfaces of the ferromagnetic domains, i.e. a spin can flip only if its left and right neighbours point in different directions (meaning that the ferromagnetic contribution to the local field acting on that spin vanishes). If quenched at low enough temperature this model displays a coarsening behaviour with two well-separated regimes. If the average distance between interfaces (or average domain length) $L(t)$ is smaller than a length scale $L_g \sim (T/h_0)^2$ (where h_0 is the mean-square deviation of the intensity of the random field) then dynamics is diffusive. However, if $L(t) > L_g$ dynamics becomes activated of the Sinai type. In the Sinai regime the IRF is well described by the relation (274), $\chi(t,t_w) = \chi_{\rm ag}(t,t_w) = c(t)\chi_{\rm eff}(t,t_w)$, leading to a maximum of the IRF at intermediate times where $L(t) \sim L_g$. This relation sets a crossover timescale where pure diffusion takes over from Sinai diffusion. Comparing this result with (70) we note that there is no stationary contribution to the IRF because for $J = \infty$ thermal fluctuations within domains are suppressed. Again this leads to FD plots similar to figure 36. For the 1D RFIM in the asymptotic long-time limit $L(t) \gg L_g$ the $\chi(t,t_w)$ decays to zero, a property required to establish a link between static and dynamic properties. As remarked in section 6.6, however, this property does not hold for the 1D Ising model.

A description of the IRF for the 2D plaquette model along the same lines as (274), but modified to account for the diffusion and annihilation of oscillating pairs of defects, has been presented in [327]. The resulting FD plots have been shown to display the characteristic two slope curves of two-timescale systems. However, it is unclear what is the physical meaning of the piece of the curve with slope $X < 1$ and whether indeed $T_{\rm eff} = T/X$ can be considered a thermodynamic temperature. Future research will show what is the true meaning of these violation factors in KCMs of the coarsening type.

FDT violations in the glassy regime of KCMs are not simply described within a thermodynamic IS formalism, the Kob–Andersen model perhaps being an exception. In fact, the blocked states in the 1,1-SFM and the East model generate identical configurational entropies [70] albeit they show very different dynamics (diffusive and cooperative respectively). The applicability of thermodynamic non-equilibrium concepts to models with trivial equilibrium thermodynamics remains an open question.

8. QFDT: the experimental evidence

Any valuable physical theory must be successfully challenged by experiments. Traditionally, the most direct way to experimentally access FDT violations is through noise measurements. In the frequency domain the FDT (60) corresponds to the Nyquist formula that relates the power spectrum of an observable to the imaginary part of its susceptibility. With the same notation we used in sections 2 and 3 we can define the power spectrum $S_{A,B}(\omega)$ and the complex susceptibility $\chi_{A,B}(\omega)$,

$$S_{A,B}(\omega) = \frac{1}{\pi}\int_{-\infty}^{\infty} C_{A,B}(t)\exp(\mathrm{i}\omega t)\,\mathrm{d}t \tag{275}$$

$$\chi_{A,B}(\omega) = \frac{\delta\langle \hat{A}(\omega)\rangle}{\delta B(\omega)} \tag{276}$$

where $\hat{A}(\omega)$ (and analogously B) is given by

$$\hat{A}(\omega) = \int_{-\infty}^{\infty} A(t) \exp(\mathrm{i}\omega t)\, \mathrm{d}t. \tag{277}$$

If $\chi_{A,B}(\omega) = \chi'_{A,B}(\omega) + \mathrm{i}\chi''_{A,B}(\omega)$ the Nyquist formula (133) reads [295]

$$S_{A,B}(\omega) = \frac{2k_B T}{\pi} \frac{\chi''_{A,B}(\omega)}{\omega}. \tag{278}$$

The power spectrum can be experimentally measured considering the case where the external perturbation couples to the measured observable $A = B$. In the experimental protocol, the time evolution of the observable $A(t)$ and the out-of-phase susceptibility $\chi''_{A,B}(\omega)$ are recorded. The power spectrum is given by $S_A(\omega) \propto \langle |\hat{A}(\omega)|^2 \rangle$. This allows us to verify the Nyquist relation (278). Typical noise experiments are the observation of electric voltage fluctuations or the motion of a Brownian particle. Other measurements included sample to sample fluctuations of the resistivity in small samples [335, 336]. Observations of magnetic noise were successfully undertaken in spin glasses [337–339], more than ten years ago, and despite the extremely low noise signal characteristic of magnetic systems. Globally, these experiments show that, within the accessible window of frequencies and times, no systematic FDT violations are observed. The out-of-phase susceptibility $\chi''(\omega)$ associated with $\chi(\omega)$ is practically frequency independent and the power spectrum shows the characteristic $1/f$ behaviour. The negative result of these experiments points out one of the most important difficulties encountered in these types of experiments. As they cover the frequency range 10^{-2}–10^{2} Hertz, these frequencies are much larger than the inverse of the aging time, therefore only the locally equilibrated regime $\omega t \gg 1$ is explored. Only seldom is the 'slow' regime $\omega t \sim 1$, where FDT violations are expected, measured. Very recently, direct measurements of FDT violations in the time domain have been reported for insulating spin glasses [340]. FDT violations have been measured beyond the quasi-stationary regime and experimental FD plots have been found to be consistent with results obtained by numerical simulations in spin-glass models (see section 7.2.1). However, the value of the effective temperature obtained in these experiments is much larger than the annealing temperature at which the system is equilibrated before the quenching takes place, casting doubts on the meaning of the effective temperature as a thermodynamic temperature in these experiments. Moreover, these measurements reveal that, within the experimentally accessible time window, FD curves $\chi(C)$ (103) are time dependent and quite far from the expected asymptotic curve. This may explain previously reported discrepancies among FD plots obtained by analysing the magnetization data of several spin-glass systems [341]. These indirect measurements of FDT violations do not show any clear evidence of a universal curve $\chi(C)$ and suggest that experimental measurements are quite far from the asymptotic regime. Experimental FD plots are shown in figure 37.

In structural glasses recent measurements also show the existence of FDT violations, however the physical interpretation of these experiments is still unclear. Voltage noise measurements [342] in an electric resonant circuit formed by a capacitor containing glycerol and an inductance show that the Nyquist formula (278) is violated depending on the waiting time and the frequency. By defining the effective temperature $T_{\mathrm{eff}}(\omega, t_w)$ as in (133) (i.e. the temperature that satisfies the Nyquist formula (278)) experiments reveal that the capacitance ages and FDT violations appear also in the range $\omega t_w \gg 1$. This seems to be in contradiction with previous old experimental results in spin glasses. The origin of this discrepancy is presently unclear. Other recent experiments by Ciliberto and co-workers [343, 344] on Laponite, a synthetic clay of charged particles that have the shape of a disc, show strong FD violations. If let evolve inside water, Laponite generates a colloid glass consisting of a packed

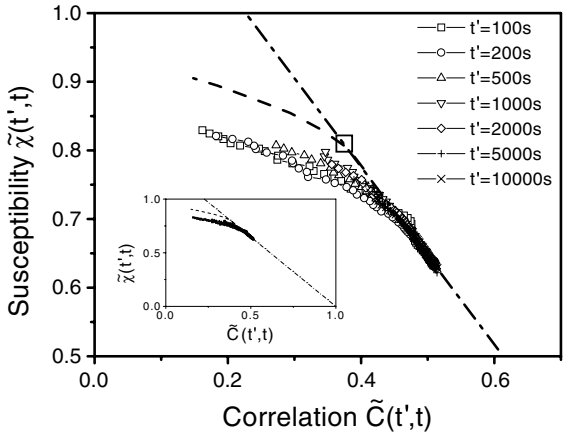

Figure 37. FD plot obtained by measuring voltage autocorrelations and relaxation susceptibility in the insulating spin glass $CdCr_{1.7}In_{0.3}S_4$ quenched from $T = 1.2T_g$ down to $T = 0.8T_g$ ($T_g = 16.2$ K). Effective temperatures are around 30 K and much larger than the annealing temperature 19.4 K. From [340].

irregular structure of discs due to the complex pattern of quadrupolar interactions. It is found that the value of the effective temperature $T_{\rm eff}(\omega, t_w)$, for low enough frequencies, is up to three or four orders of magnitude larger than the bath temperature. Although this has been interpreted as evidence for coarsening dynamics (where $T_{\rm eff} \to \infty$) a conclusive explanation of the origin of these high values is still unknown. One interesting aspect of these experiments is the scaling behaviour $\omega t^{1/2}$ observed in the power spectrum, indicative that FDT violations persist even in the regime $\omega t_w \gg 1$, in agreement with the previous results on glycerol. Contrary to what would be expected, noise measurements in a rheological experiment for Laponite do not detect significant FDT violations.

Experiments that successfully clearly demonstrate the existence of effective temperatures related to FDT violations are certainly needed. This preliminary account of results shows that much work has still to be done in aging, driven or granular systems to provide a safe ground for many of these ideas.

9. Conclusions

In this review we have presented an overview on what is now an active area of research, i.e. the study of FDT violations in glassy systems. Glassy systems are widespread in nature and found in many different areas covering physics, chemistry or biology. These are non-equilibrium systems which are either in a non-stationary slowly relaxing aging state or in a weakly driven stationary state. Equilibrium systems are often described by a set of intensive parameters such as temperature, pressure or density. In a similar way, in glassy systems an important role is played by the waiting time (aging systems) or the intensity of the driving force and/or its frequency (driven systems). These parameters describe how far from equilibrium the system is. In fact, it is becoming steadily clear that a thermodynamic description of glassy systems can be partially rescued. In this description the glassy regime can be rationalized by using some of the concepts of equilibrium statistical physics such as the existence of a modified version of the FDT, the so-called quasi-FDT (QFDT).

Associated with the existence of the QFDT there is the concept of effective temperature. Rather than being a useful parameter to describe the behaviour of non-equilibrium systems, the

effective temperature has a deeper physical meaning. It could be the vestige of the existence of some dynamical measure underlying the non-equilibrium regime. However, we do not know how to prove the existence of the QFDT from first principles in the same way we do not know how to prove the Boltzmann equal probability hypothesis in equilibrium theory. Therefore, establishing the existence of this dynamical measure is somehow equivalent to assuming the existence of a QFDT. Then the crucial point is what are the specific predictions, that can be experimentally tested, one can derive from the existence of a QFDT. The measurement of the effective temperature itself appears as the most direct way of challenging the QFDT. However, direct measurements of this non-equilibrium temperature appear quite difficult, results are still very preliminary and much progress is yet to be done to reach convincing and clear evidence.

The study of several families of models, as described in this review, appears to be a very fruitful source of inspiration for new concepts and ideas that could be eventually exported to different classes of problems. However this path is not free of challenges and ambiguities. Indeed, what are natural concepts for some families of models appear to be quite artificial in other families. As an example, key concepts in a thermodynamic formulation of the glassy state are the existence of an effective temperature associated with the configurational entropy or complexity, in the same way the bath temperature is associated with the Boltzmann entropy in equilibrium theory. However, what appears to be an interesting quantity describing glassy systems with two timescales cannot be easily translated into systems with many timescales. Furthermore, what appears to be a meaningful quantity for models having complex thermodynamics (such as spin-glass models) appears to be meaningless in models described by a trivial Hamiltonian (such as kinetically constrained models).

From the point of view of theoretical studies, our understanding of the existence of a QFDT also appears quite problematic. Most of the solutions we have described in this review are only valid in the case of mean-field interactions, however their validity beyond that limit remains speculative. The use of numerical simulations has aided in bridging the gap. It is quite interesting that most of the results predicted in mean-field models are qualitatively also observed in short-range systems. This tendency to rationalize the behaviour of real systems within a mean-field scenario, i.e. far beyond their natural domain of applicability, has become quite standard in the study of glassy systems. The description of the equilibrium properties of spin-glass systems has for many years followed a similar route. Although the knowledge we can gain from numerical simulations in glassy systems is always quite qualitative (either due to the limited range of timescales or to the inherent simplicity of the simulated model) the accumulated evidence, as reported throughout this review, points towards the emergence of a QFDT in the non-equilibrium regime of glassy systems, reminiscent of how the Boltzmann measure emerges in equilibrium systems. The same conclusion holds for the Edwards measure in granular media.

What will be the future in the research of FDT violations? Although modelling promises to offer new ideas and will clarify our understanding we feel that more progress is certainly needed in basic theory and experiment. In theory we need to understand the origin of the existence of a QFDT right from the microscopics. Cooperative processes in glasses involve a few tens of atoms and occur along nanometric length scales. How to link the microscopic activated processes to the emergence of macroscopic properties (such as the effective temperature) is a real challenge. In this context, it appears quite interesting to pursue the investigation of the so-called fluctuation theorems recently proposed to quantify transient violations of the second law of thermodynamics. From the experimental side the current accumulated knowledge is still too poor and more experiments are certainly needed for this field of research to grow. A future line of progress is the use of nanotechnology devices to make noise measurements over

spatially localized regions of nanometric size. These devices could be used as a microscope to measure activated processes occurring on small length scales.

Certainly we will see upcoming developments in this exciting area of research. A continuous exchange of ideas among theory, simulation and experiments is highly desirable and certainly needed to improve our current understanding in this field.

Acknowledgments

We are grateful to all our collaborators, much of whose work has been described in this review, including L L Bonilla, J P Bouchaud, S Ciuchi, B Coluzzi, L F Cugliandolo, K Dawson, S Franz, A Garriga, J Hertz, H Horner, J Kurchan, L Leuzzi, E Marinari, U Marini Bettolo, M Mezard, Th M Nieuwenhuizen, F G Padilla, I Pagonabarraga, G Parisi, M Picco, A Puglisi, F Ricci-Tersenghi, F Rao, M Rubí, A Rocco, G Ruocco, M Sales, D Sherrington, F Sciortino, M Sellitto, P Sollich, H-J Sommers, H Sompolinsky and P Tartaglia. We are also indebted to many other colleagues for enlightening discussions on many of the topics covered in this review. We are particularly grateful to P Sollich for useful comments and suggestions for improvement. FR has been supported by the Spanish Ministerio de Ciencia y Tecnología Grant BFM2001-3525, Generalitat de Catalunya and Acciones-Integradas Italia–España (HI2000-0087).

References

[1] Struik L C E 1978 *Physical Aging in Amorphous Polymers and Other Materials* (Amsterdam: Elsevier)
[2] Tool A Q 1946 Relation between inelastic deformability and thermal expansion of glass in its annealing range *Acta Mech.* **29** 240–53
[3] Cugliandolo L F 2002 Dynamics of glassy systems *Preprint* cond-mat/0210312
[4] Jackle J 1986 Models of the glass transition *Rep. Prog. Phys.* **49** 171–231
[5] Angell C A 1988 The glass transition: an assessment of current thinking *Nucl. Phys.* B **5A** 69–80
[6] Ediger M D, Angell C A and Nagel S R 1996 Supercooled liquids and glasses *J. Phys. Chem.* **100** 13200 –12
[7] De Benedetti P G 1996 *Metastable Liquids: Concepts and Principles* (Princeton, NJ: Princeton University Press)
[8] Wolynes P G 1997 Entropy crises in glasses and random heteropolymers *J. Res. Natl Inst. Stand. Tech.* **102** 187–94
[9] Di Marzio E A 1995 The entropy theory of glass formation after 40 years *Comput. Mater. Sci.* **4** 317–24
[10] Gotze W and Sjogren L 1992 Relaxation processes in supercooled liquids *Rep. Prog. Phys.* **55** 241–376
[11] Gotze W 1999 Recent tests of the mode-coupling theory for glassy dynamics *J. Phys.: Condens. Matter* **11** A1–A45
[12] Kob W 1999 Computer simulations of supercooled liquids and glasses *J. Phys.: Condens. Matter* **11** R85
[13] Young A P (ed) 1998 *Spin Glasses and Random Fields* (Singapore: World Scientific)
[14] Bouchaud J-P, Cugliandolo L F, Kurchan J and Mezard M 1996 Mode-coupling approximations, glass theory and disordered systems *Physica* A **226** 243–73
[15] Ritort F and Sollich P 2002 Glassy dynamics of kinetically constrained models *Preprint* cond-mat/0210382
[16] Bouchaud J-P 2002 Granular media: some ideas from statistical physics *Preprint* cond-mat/0211196
[17] Rubi J M and Perez-Vicente C J (ed) 1997 *Proc. Sitges Conference, 1996: Complex Behaviour of Glassy Systems* (Berlin: Springer)
[18] Franz S, Glotzer S C and Sastry S (ed) 1999 *Proc. Trieste Workshop Unifying Concepts in Glassy Physics. J. Phys.: Condens. Matter* **29** 6295–682
[19] Sollich P and Ritort F (ed) 2002 *Proc. Barcelona Workshop on Glassy Dynamics in Kinetically Constrained Models: J. Phys.: Condens. Matter* **7** 1381–696
[20] Ma S-K 1985 *Statistical Mechanics* (Singapore: World Scientific)
[21] Callen H B 1985 *Thermodynamics and Introduction to Thermostatistics* (New York: Wiley)
[22] Beck C and Schloegel F 1993 *Thermodynamics of Chaotic Systems: An Introduction (Cambridge Nonlinear Science Series)* (Cambridge: Cambridge University Press)
[23] Onsager L 1931 Reciprocal relations in irreversible processes: I *Phys. Rev.* **37** 405–26

[24] Onsager L 1931 Reciprocal relations in irreversible processes: II *Phys. Rev.* **38** 2265–79
[25] Plischke M and Bergensen B 1994 *Equilibrium Statistical Physics* (Singapore: World Scientific)
[26] Risken H 1996 *The Fokker–Planck Equation: Methods of Solution and Applications* (Berlin: Springer)
[27] Parisi G 1998 *Statistical Field Theory* (Reading, MA: Addison-Wesley)
[28] Zinn-Justin J 1996 *Quantum Field Theory and Critical Phenomena (International Series of Monographs on Physics vol 92)* (Oxford: Clarendon)
[29] Gantmacher F R 1959 *The Theory of Matrices* (New York: Chelsea)
[30] Miller R S and MacPhail R A 1997 Ultraslow nonequilibrium dynamics in supercooled glycerol by stimulated brillouin gain spectroscopy *J. Chem. Phys.* **106** 3393–401
[31] Padilla F G and Ritort F 1997 Langevin dynamics of the Lebowitz–Percus model *J. Phys. A: Math. Gen.* **30** 7089–114
[32] Horner H 1984 Dynamic mean field theory of the sk-spin glass: I. Regularization by bond dynamics *Z. Phys.* B **57** 29–37
[33] Cugliandolo L F and Kurchan J 1995 Weak ergodicity breaking in mean-field spin-glass models *Phil. Mag.* B **71** 501–14
[34] Franz S and Mezard M 1994 On mean-field glassy dynamics out of equilibrium *Physica* A **210** 48–72
[35] Mezard M, Parisi G and Virasoro M A 1987 *Spin-Glass Theory and Beyond* (Singapore: World Scientific)
[36] Crisanti A and Ritort F 2002 Inherent structures, configurational entropy and slow glassy dynamics *J. Phys.: Condens. Matter* **14** 1381–95
[37] Palmer R G 1982 Broken ergodicity *Adv. Phys.* **31** 669–735
[38] Brawer S A 1984 Theory of relaxation in viscous liquids and glasses *J. Chem. Phys.* **81** 954–75
[39] Dyre J C 1987 Master-equation approach to the glass transition *Phys. Rev. Lett.* **58** 792–5
[40] Bouchaud J-P 1992 Weak ergodicity breaking and aging in disordered systems *J. Physique* I **2** 1705–13
[41] Coniglio A and Nicodemi M 2001 A statistical mechanics approach to the inherent states of granular media *Physica* A **296** 451–9
[42] Kirkpatrick T R and Wolynes P G 1987 Stable and metastable states in mean-field Potts and structural glasses *Phys. Rev.* B **36** 8552–64
[43] Kirkpatrick T R and Thirumalai D 1987 Dynamics of the structural glass transition and the p-spin-interaction spin-glass model *Phys. Rev. Lett.* **58** 2091–4
[44] Kirkpatrick T R and Thirumalai D 1987 p-spin-interaction spin-glass models: connections with the structural glass problem *Phys. Rev.* B **36** 5388–97
[45] Kauzmann W 1948 *Chem. Rev.* **43** 219
[46] Franz S and Virasoro M A 2000 Quasi equilibirum interpretation of aging dynamics *J. Phys. A: Math. Gen.* **33** 891–905
[47] Biroli G and Kurchan J 2001 Metastable states in glassy systems *Phys. Rev.* E **64** 016101
[48] Mezard M, Parisi G and Virasoro M A 1985 Random free energies in spin glasses *J. Physique Lett.* **46** L217–22
[49] Nieuwenhuizen Th M 1998 Thermodynamic description of a dynamical glassy transition *J. Phys. A: Math. Gen.* **31** L201–7
[50] Crisanti A and Ritort F 2002 A glass transition scenario based on heterogeneities and entropy barriers *Phil. Mag.* B **82** 143–9
[51] Crisanti A and Ritort F 2001 A real-space description of the glass transition based on heterogeneities and entropy barriers *Preprint* cond-mat/0102104
[52] Cugliandolo L F and Kurchan J 1993 Analytical solution of the off-equilibrium dynamics of a long-range spin-glass model *Phys. Rev. Lett.* **71** 173–6
[53] Cugliandolo L F and Kurchan J 1994 On the out-of-equilibrium relaxation of the Sherrington–Kirkpatrick model *J. Phys. A: Math. Gen.* **27** 5749–72
[54] Fielding S M and Sollich P 2002 Observable dependence of fluctuation–dissipation relations and effective temperatures *Phys. Rev. Lett.* **88** 050603
[55] Sollich P, Fielding S and Mayer P 2002 Fluctuation–dissipation relations and effective temperatures in simple non-mean field systems *J. Phys.: Condens. Matter* **14** 1683–96
[56] Goldstein M 1969 Viscous liquids and the glass transition: a potential energy barrier picture *J. Phys. Chem.* **51** 3728–39
[57] Stillinger F H and Weber T A 1982 Hidden structure in liquids *Phys. Rev.* A **25** 978–89
[58] Stillinger F H and Weber T A 1984 Packing structures and transitions in liquids and solids *Science* **225** 983–9
[59] Stillinger F H 1995 Statistical-mechanics of metastable matter—superheated and stretched liquids *Phys. Rev.* E **52** 4685–90
[60] Heuer A 1997 Properties of a glass-forming system as derived from its potential energy landscape *Phys. Rev. Lett.* **78** 4051–4

[61] Buchner S and Heuer A 1999 Potential energy landscape of a model glass former: thermodynamics anharmonicities, and finite size effects *Phys. Rev.* E **60** 6507–18
[62] Sastry S, Debenedetti P G, Stillinger F H, Schroder T B, Dyre J C and Glotzer S C 1999 Potential energy landscape signatures of slow dynamics in glass forming liquids *Physica* A **270** 301–8
[63] Schroder T B, Sastry S, Dyre J C and Glotzer S C 2000 Crossover to potential energy landscape dominated dynamics in a model glass-forming liquid *J. Chem. Phys.* **112** 9834–40
[64] Angelani L, Di Leonardo R, Ruocco G, Scala A and Sciortino F 2000 Saddles in the energy landscape probed by supercooled liquids *Phys. Rev. Lett.* **85** 5356–9
[65] Crisanti A and Ritort F 2000 Potential energy landscape of finite-size mean-field models for glasses *Europhys. Lett.* **51** 147
[66] Crisanti A and Ritort F 2000 Activated processes and inherent structure dynamics of finite-size mean-field models for glasses *Europhys. Lett.* **52** 640
[67] Crisanti A and Ritort F 2000 Equilibrium and ageing dynamics of simple models for glasses *J. Phys.: Condens. Matter* **12** 6413–22
[68] Crisanti A and Ritort F 2001 Configurational entropy and the one-step rsb scenario in glasses *Disordered and Complex Systems (AIP Conference Proceedings vol 553)* ed A C C Coolen, L P Hughston, P Sollich and R F Streater (New York: AIP)
[69] Biroli G and Monasson R 2000 From inherent structures to pure states: some simple remarks and examples *Europhys. Lett.* **50** 155–61
[70] Crisanti A, Ritort F, Rocco A and Sellitto M 2000 Inherent structures and nonequilibrium dynamics of one-dimensional constrained kinetic models: a comparison study *J. Chem. Phys.* **113** 10615–34
[71] Thouless D J, Anderson P W and Palmer R G 1977 Solution of 'solvable model of a spin glass' *Phil. Mag.* **35** 593–601
[72] Bray A J and Moore M A 1980 Metastable states in spin glasses *J. Phys. C: Solid State Phys.* **13** L469–76
[73] Crisanti A and Sommers H-J 1995 Thouless–Anderson–Palmer approach to the spherical *p*-spin spin glass model *J. Physique* **5** 805–13
[74] Parisi G and Potters M 1995 Mean-field equations for spin models with orthogonal interaction matrices *J. Phys. A: Math. Gen.* **28** 5267–85
[75] Parisi G and Potters M 1995 On the number of metastable states in spin glasses *Europhys. Lett.* **32** 13–7
[76] Cavagna A, Giardina I and Parisi G 1998 Stationary points of the Thouless–Anderson–Palmer free energy *Phys. Rev.* B **57** 11251–7
[77] Monasson R 1995 Structural glass transition and the entropy of the metastable states *Phys. Rev. Lett.* **75** 2847–50
[78] Mezard M 1999 How to compute the thermodynamics of a glass using a cloned liquid *Physica* A **265** 352
[79] Mezard M and Parisi G 1999 Thermodynamics of glasses: a first principles computation *Phys. Rev. Lett.* **82** 747–50
[80] Mezard M and Parisi G 1999 A first-principle computation of the thermodynamics of glasses *J. Chem. Phys.* **111** 1076–95
[81] Coluzzi B, Parisi G and Verrocchio P 2000 Thermodynamical liquid-glass transition in a Lennard-Jones binary mixture *Phys. Rev. Lett.* **84** 306–9
[82] Coluzzi B, Parisi G and Verrocchio P 2000 Lennard-Jones binary mixture: a thermodynamical approach to glass transition *J. Chem. Phys.* **112** 2933
[83] De Santis E, Parisi G and Ritort F 1995 On the static and dynamical transition in the mean-field Potts glass *J. Phys. A: Math. Gen.* **28** 3025–41
[84] Ritort F 1996 Classical and quantum behaviour in mean-field glassy systems *Complex Behavior in Glassy Systems* ed C J Perez-Vicente and M Rubi (Berlin: Springer)
[85] Franz S and Parisi G 1995 Recipes for metastable states in spin glasses *J. Physique* I **5** 1401–15
[86] Cardenas M, Franz S and Parisi G 1998 Glass transition and effective potential in the hypernetted chain approximation *J. Phys. A: Math. Gen.* **31** L163–9
[87] Cardenas M, Franz S and Parisi G 1999 Constrained Boltzmann–Gibbs measures and effective potential for glasses in hypernetted chain approximation and numerical simulations *J. Chem. Phys.* **110** 1726–34
[88] Speedy R J 1993 The entropy of a glass *Mol. Phys.* **80** 1105–20
[89] Speedy R J 2001 Estimates of the configurational entropy of a liquid *J. Phys. Chem.* B **105** 11737–42
[90] Speedy R J 2001 Configurational entropy and diffusion in a hard disc fluid *J. Chem. Phys.* **114** 9069–74
[91] Sciortino F, Kob W and Tartaglia P 1999 Inherent structure entropy of supercooled liquids *Phys. Rev. Lett.* **83** 3214–7
[92] Mossa S, La Nave E, Stanley H E, Donati C, Sciortino F and Tartaglia P 2002 Dynamics and configurational entropy in the Lewis–Wahnström model for supercooled orthoterphenyl *Phys. Rev.* E **65** 041205
[93] Crisanti A and Ritort F 2002 unpublished

[94] Sastry S 1999 The relationship between fragility, configurational entropy and the potential energy landscape of glass-forming liquids *Nature* **409** 164–7
[95] Coluzzi B, Marinari E, Parisi G and Rieger H 2000 On the energy minima of the Sherrington–Kirkpatrick model *J. Phys. A: Math. Gen.* **33** 3851–62
[96] Coluzzi B, Crisanti A, Marinari E, Ritort F and Rocco A 2003 A new method to compute the configurational entropy in spin glasses *Eur. Phys. J.* B at press
[97] Hohenberg P and Shraiman B 1989 Chaotic behaviour of an extended system *Physica* D **37** 109–15
[98] Hodge I M 1987 *Macromolecules* **20** 2897
[99] Hodge I M 1994 Enthalpy relaxation and recovery in amorphous materials *J. Non-Cryst. Solids* **169** 211–66
[100] Cugliandolo L F, Kurchan J and Peliti L 1997 Energy flow, partial equilibration, and effective temperatures in systems with slow dynamics *Phys. Rev.* E **55** 3898–914
[101] Cugliandolo L F and Kurchan J 2000 Frontiers in magnetism *J. Phys. Soc. Japan* **69** 247
[102] Cugliandolo L F and Kurchan J 1999 Thermal properties of slow dynamics *Physica* A **263** 242–51
[103] Garriga A and Ritort F 2001 Validity of the zero-thermodynamic law in off-equilibrium coupled harmonic oscillators *Eur. Phys. J.* B **20** 105–22
[104] Cugliandolo L F, Dean D S and Kurchan J 1997 Fluctuation–dissipation theorems and entropy production in relaxational systems *Phys. Rev. Lett.* **79** 2168–71
[105] Garriga A and Ritort F 2001 Heat transfer and Fourier's law in off-equilibrium systems *Eur. Phys. J.* B **21** 115–20
[106] Exartier R and Peliti L 2000 Measuring effective temperatures in out-of-equilibrium driven systems *Eur. Phys. J.* B **16** 119–26
[107] Nieuwenhuizen Th M 1998 Thermodynamics of the glassy state: effective temperature as an additional parameter *Phys. Rev. Lett.* **80** 5580–3
[108] Nieuwenhuizen Th M 2000 Thermodynamic picture of the glassy state gained from exactly solvable models *Phys. Rev.* E **61** 267–92
[109] Nieuwenhuizen Th M 1997 Ehrenfest relations at the glass transition: solution to an old paradox *Phys. Rev. Lett.* **79** 1317–20
[110] Edwards S F 1898 Theory of powders *Physica* A **157** 1080–90
[111] Edwards S F and Oakeshott R B S 1989 Theory of powders *Physica* A **157** 1080–90
[112] Mehta A and Edwards S F 1989 Statistical mechanics of powder mixtures *Physica* A **157** 1091–100
[113] Edwards S F 1990 The flow of powders and of liquids of high viscosity *J. Phys.: Condens. Matter* **2** 63–9
[114] Mehta A and Edwards S F 1990 A phenomenological approach to relaxation in powders *Physica* A **168** 714–22
[115] Monasson R and Pouliquen O 1997 Entropy of particle packings: an illustration on a toy model *Physica* A **236** 395–410
[116] Berg J, Franz S and Sellitto M 2002 Testing the Edwards hypothesis in spin systems under tapping dynamics *Eur. Phys. J.* B **26** 349
[117] Berthier L, Barrat J-L and Kurchan J 2001 Dynamic ultrametricity in spin glasses *Phys. Rev.* E **63** 016105
[118] Coniglio A, Fierro A and Nicodemi M 2001 Applications of the statistical mechanics of inherent states to granular media *Physica* A **302** 193–201
[119] Kurchan J 2002 Emergence of macroscopic temperatures in systems that are not thermodynamical macroscopically: towards a thermodynamical description of slow granular rheology *J. Phys.: Condens. Matter* **12** 6611–17
[120] Kirkpatrick T R and Wolynes P G 1987 Connections between some kinetic and equilibrium theories of the glass transition *Phys. Rev.* A **35** 3072–80
[121] Leutheusser E 1984 Dynamical model of the liquid–glass transition *Phys. Rev.* A **29** 2765–73
[122] Bengtzelius U, Goetze W and Sjolander A 1984 Dynamics of supercooled liquids and the glass transition *J. Phys. C: Solid State Phys.* **17** 5915–34
[123] Goetze W 1991 Aspect of structural glass transitions *Liquids, Freezing and Glass Transition* ed D Levesque, J P Hansen and J Zinn-Justin (Amsterdam: North-Holland)
[124] Gross D J, Kanter I and Sopolinsky H 1985 Mean-field theory of the Potts glass *Phys. Rev. Lett.* **55** 304–7
[125] Goldbardt P and Sherrington D 1985 Replica theory of the uniaxial quadrupolar glass *J. Phys. C: Solid State Phys.* **18** 1923–40
[126] Derrida B 1981 Random-energy model: an exactly solvable model of disordered systems *Phys. Rev.* B 2613–26
[127] Gross D J and Mezard M 1984 The simplest spin glass *Nucl. Phys.* B **240** 431–52
[128] Gardner E 1985 Spin glasses with p-spin interactions *Nucl. Phys.* B 747–65
[129] Sherrington D and Kirkpatrick A 1975 Solvable model of a spin-glass *Phys. Rev. Lett.* **35** 1792–6
[130] Kirkpatrick S and Sherrington D 1978 Infinite-ranged models of spin-glasses *Phys. Rev.* B **17** 4384–403
[131] Crisanti A and Sommers H-J 1992 The spherical *p*-spin interaction spin glass model: the statics *Z. Phys.* B **87** 341–54

[132] Crisanti A, Horner H and Sommers H-J 1993 The spherical *p*-spin interaction spin glass model: the dynamics *Z. Phys.* B **92** 257–71
[133] Hohenberg P C and Halperin B I 1977 Theory of dynamic critical phenomena *Rev. Mod. Phys.* **49** 435–79
[134] Sompolinsky H and Zippelius A 1982 Relaxational dynamics of the Edwards–Anderson model and the mean-field theory of spin-glasses *Phys. Rev.* B **25** 6860–75
[135] Parisi G 1983 Order parameter for spin-glasses *Phys. Rev. Lett.* **50** 1946–8
[136] Kurchan J, Parisi G and Virasoro M A 1993 Barriers and metastable states as saddle points in the replica approach *J. Physique* I **3** 1819–38
[137] Franz S and Parisi G 1997 Phase diagram of coupled glassy systems: a mean-field study *Phys. Rev. Lett.* **79** 2486–9
[138] Cavagna A, Giardina I and Parisi G 1997 An investigation of the hidden structure of states in a mean-field spin-glass model *J. Phys. A: Math. Gen.* **30** 7021–38
[139] Barrat A, Franz S and Parisi G 1997 Temperature evolution and bifurcations of metastable states in mean-field spin glasses, with connections with structural glasses *J. Phys. A: Math. Gen.* **30** 5593–612
[140] Cavagna A, Giardina I and Parisi G 1997 Structure of metastable states in spin glasses by means of a three replica potential *J. Phys. A: Math. Gen.* **30** 4449–66
[141] Sompolinsky H 1981 Time-dependent order parameters in spin-glasses *Phys. Rev. Lett.* **47** 935–8
[142] Horner H 1986 Dynamic mean-field theory of a slowly cooled spin glass *Europhys. Lett.* **2** 487–91
[143] Ioffe L B 1988 Quasiequilibrium states of spin glasses *Phys. Rev.* B **38** 5181–3
[144] Cugliandolo L F and Le Doussal P 1996 Large time nonequilibrium dynamics of a particle in a random potential *Phys. Rev.* E **53** 1525–52
[145] Nieuwenhuizen Th M 1995 Exactly solvable model of a quantum spin glass *Phys. Rev. Lett.* **74** 4289–92
[146] Hertz J A, Sherrington D and Nieuwenhuizen Th M 1999 Competition between glassiness and order in a multispin glass *Phys. Rev.* E **60** R2460–R2463
[147] Ciuchi S and Crisanti A 2000 Different scenarios for critical glassy dynamics *Europhys. Lett.* **49** 754–60
[148] Crisanti A, Hertz J, Nieuwenhuizen Th M and Sherrington D 2003 Static and dynamical direct and TAP approaches to the p-spin model with a ferromagnetic bias, unpublished
[149] Ciuchi S and De Pasquale F 1988 Nonlinear relaxation and ergodicity breakdown in random anisotropy spin glasses *Nucl. Phys.* B **300** 31–60
[150] Cugliandolo L F and Dean D S 1995 Full dynamical solution for a spherical spin-glass model *J. Phys. A: Math. Gen.* **28** 4213–34
[151] Cugliandolo L F and Dean D S 1995 On the dynamics of a spherical spin-glass in a magnetic field *J. Phys. A: Math. Gen.* **28** L453–9
[152] Campellone M, Parisi G and Ranieri P 1998 Dynamical fluctuations in an exactly solvable model of spin glasses *J. Phys. A: Math. Gen.* **31** 1893–900
[153] Zippold W, Kuhn R and Horner H 2000 Non-equilibrium dynamics of simple spherical spin models *Eur. Phys. J.* B **13** 531–7
[154] Ciuchi S, De Pasquale F and Monachesi P 1990 Relaxation phenomena in two interacting spin lattices *J. Phys.: Condens. Matter* **2** 4921–34
[155] Kinzelbach H and Horner H 1993 Dynamics of manifolds in random media: II. Long range correlations in the disordered medium *J. Physique* I **3** 1901–19
[156] Sompolinsky H and Zippelius A 1981 Dynamic theory of the spin-glass phase *Phys. Rev. Lett.* **47** 359–62
[157] Sommers H-J and Fisher K H 1985 Dynamic scaling for spin glasses near the De Almedia–Thouless line *Z. Phys.* B **58** 125–31
[158] Sommers H-J 1983 On the dynamic mean field theory of spin glasses *Z. Phys.* B **50** 97–105
[159] Baldassarri A, Cugliandolo L F, Kurchan J and Parisi G 1995 On the out-of-equilibrium order parameter in long-range spin-glasses *J. Phys. A: Math. Gen.* **28** 1831–45
[160] Franz S, Mezard M, Parisi G and Peliti L 1998 Measuring equilibrium properties in aging systems *Phys. Rev. Lett.* **81** 1758–61
[161] Franz S, Mezard M, Parisi G and Peliti L 1999 The response of glassy systems to random perturbations: a bridge between equilibrium and off-equilibrium *J. Stat. Phys.* **97** 459–88
[162] Blatter G, Feigel'man M V, Geshkenbein V B, Larkin A L and Vinokur V M 1994 Vortices in high-temperature superconductors *Rev. Mod. Phys.* **66** 1125–388
[163] Nattermann T and Rujan P 1989 Random field and other systems dominated by disorder fluctuations *Int. J. Mod. Phys.* B **3** 1597–654
[164] Cule D and Shapir Y 1995 Glassy roughness of a crystalline surface upon a disordered substrate *Phys. Rev. Lett.* **74** 114–7
[165] Nieuwenhuizen Th M 1997 Solvable glassy system: static versus dynamical transition *Phys. Rev. Lett.* **78** 3491–4

[166] Cugliandolo L F, Kurchan J and Le Doussal P 1996 Large time out-of-equilibrium dynamics of a manifold in a random potential *Phys. Rev. Lett.* **76** 2390–3
[167] Engel A 1993 Replica symmetry breaking in zero dimension *Nucl. Phys.* B **410** 617–46
[168] Yoshino H 1998 Aging effects of an elastic string diffusing in a disordered media *Phys. Rev. Lett.* **81** 1493–6
[169] Pitard E and Shakhnovich E I 2001 Mode-coupling theory for heteropolymers *Phys. Rev.* E **63** 041501/1–14
[170] Cugliandolo L F, Kurchan J and Parisi G 1994 Off equilibrium dynamics and aging in unfrustrated systems *J. Physique* I **4** 1641–56
[171] Corberi F, Nicodemi M, Piccioni M and Coniglio A 1999 Off-equilibrium dynamics in a singular diffusion model *Phys. Rev. Lett.* **83** 5054–7
[172] Corberi F, Nicodemi M, Piccioni M and Coniglio A 2001 Slow dynamics and aging in a constrained diffusion model *Phys. Rev.* E **63** 031106
[173] Barrat A and Mezard M 1995 Phase space diffusion and low temperature aging *J. Physique* I **5** 941–7
[174] Derrida B 1980 Random-energy model: limit of a family of disordered models *Phys. Rev. Lett.* **45** 79–82
[175] Derrida B 1981 Random-energy model: an exactly solvable model of disordered systems *Phys. Rev.* B **24** 2613–26
[176] Monthus C and Bouchaud J-P 1996 Models of traps and glass phenomenology *J. Phys. A: Math. Gen.* **29** 3847–69
[177] Bouchaud J-P, Comtet A and Monthus C 1995 On a dynamical model of glasses *J. Physique* **5** 1521–6
[178] Bouchaud J-P and Dean D S 1995 Aging on Parisi's tree *J. Physique* I **5** 265
[179] Bertin E and Bouchaud J-P 2002 Dynamical ultrametricity in the critical trap model *J. Phys. A: Math. Gen.* **35** 3039–51
[180] Odagaki T 1995 Glass transition singularities *Phys. Rev. Lett.* **75** 3701–4
[181] Ritort F 2003 Universal dependence of the fluctuation–dissipation ratio on the transition rates in trap models *Preprint* cond-mat/0303445
[182] Lippiello E and Zannetti M 2000 Fluctuation–dissipation ratio in the one-dimensional kinetic Ising model *Phys. Rev.* E **61** 3369–74
[183] Sollich P, Lequeux F, Hebraud P and Cates M 1997 Rheology of soft glassy materials *Phys. Rev. Lett.* **70** 2020
[184] Sollich P 1998 Rheological constitutive equation for a model of soft glassy materials *Phys. Rev.* E **58** 738–59
[185] Fielding S M and Sollich P 2003 Equivalence of driven and ageing fluctuation–dissipation relation in the trap model *Phys. Rev.* E **67** 011101
[186] Kurchan J and Laloux L 1996 Phase space geometry and slow dynamics *J. Phys. A: Math. Gen.* **29** 1929–48
[187] Leuzzi L and Ritort F 2002 Disordered backgammon model *Phys. Rev.* E **65** 56125
[188] Garriga A 2002 The zeroth law in structural glasses: an example *J. Phys.: Condens. Matter* **14** 1581–8
[189] Bonilla L L, Padilla F G, Parisi G and Ritort F 1996 Analytical solution of the Monte Carlo dynamics of a simple spin-glass model *Europhys. Lett.* **34** 159–64
[190] Bonilla L L, Padilla F G, Parisi G and Ritort F 1996 Closure of the Monte Carlo dynamical equations in the spherical Sherrington–Kirkpatrick model *Phys. Rev.* B **54** 4170–82
[191] Bonilla L L, Padilla F G and Ritort F 1998 Aging in the linear harmonic oscillator *Physica* A **250** 315–26
[192] Leuzzi L and Nieuwenhuizen Th M 2001 Inherent structures in models for fragile and strong glass *Phys. Rev.* E **64** 066125
[193] Leuzzi L and Nieuwenhuizen Th M 2001 Effective temperatures in an exactly solvable model for a fragile glass *Phys. Rev.* E **64** 011508
[194] Leuzzi L and Nieuwenhuizen Th M 2002 Exactly solvable model glass with a facilitated dynamics *J. Phys.: Condens. Matter* **14** 1637
[195] Ritort F 1995 Glassiness in a model without energy barriers *Phys. Rev. Lett.* **75** 1190–3
[196] Godreche C, Bouchaud J-P and Mezard M 1995 Entropy barriers and slow relaxation in some random walk models *J. Phys. A: Math. Gen.* **28** L603–11
[197] Arora D, Bhatia D P and Prasad M A 1999 Exact solutions of some urn models of relaxation in glassy dynamics *Phys. Rev.* E **60** 145–8
[198] Lipowski A 1997 Absorption time in certain urn models *J. Phys. A: Math. Gen.* **30** L91–4
[199] Franz S and Ritort F 1995 Dynamical solution of a model without energy barriers *Europhys. Lett.* **31** 507–12
[200] Franz S and Ritort F 1996 Glassy mean-field dynamics of the backgammon model *J. Stat. Phys.* **85** 131–50
[201] Godreche C and Luck J M 1996 Long-time regime and scaling of correlations in a simple model with glassy behaviour *J. Phys. A: Math. Gen.* **29** 1915–28
[202] Franz S and Ritort F 1997 Relaxation processes and entropic traps in the backgammon model *J. Phys. A: Math. Gen.* **30** L359–L365
[203] Prados A, Brey J J and Sanchezrey B 1997 Glassy behaviour in a simple model with entropy barriers *Phys. Rev.* B **55** 6343–55

[204] Godreche C and Luck J M 1999 Correlation and response in the backgammon model: the Ehrenfest legacy *J. Phys. A: Math. Gen.* **32** 6033–54
[205] Godreche C and Luck J M 2000 Response of non-equilibrium systems at criticality: ferromagnetic models in dimension two and above *J. Phys. A: Math. Gen.* **33** 9141–64
[206] Garriga A, Pagonabarraga I and Ritort F 2003 in preparation
[207] Godreche C and Luck J M 2001 Nonequilibrium dynamics of the zeta urn model *Eur. Phys. J.* B **23** 473–86
[208] Godreche C and Luck J M 2002 Nonequilibrium dynamics of urn models *J. Phys.: Condens. Matter* **14** 1601–15
[209] Glauber R J 1963 Time-dependent statistics of the Ising model *J. Math. Phys.* **4** 294–307
[210] Bray A J 1989 Upper and lower bounds on dynamic correlations in the Griffiths phase *J. Phys. A: Math. Gen.* **22** L81–5
[211] Prados A, Brey J J and Sanchezrey B 1997 Aging in the one-dimensional Ising model with Glauber dynamics *Europhys. Lett.* **40** 13–8
[212] Godreche C and Luck J M 2000 Response of non-equilibrium systems at criticality: exact results for the Glauber–Ising chain *J. Phys. A: Math. Gen.* **33** 1151–70
[213] Godreche C and Luck J M 2002 Nonequilibrium critical dynamics of ferromagnetic spin systems *J. Phys.: Condens. Matter* **14** 1589–99
[214] Corberi F, Lippiello E and Zannetti M 2002 Slow relaxation in the large-n model for phase ordering *Phys. Rev.* E **65** 046136–11
[215] Garrahan J P, Mayer P M, Berthier L and Sollich P 2003 Fluctuation–dissipation relations in the non-equilibrium dynamics of Ising models *Preprint* cond-mat/0301493
[216] Henkel M, Pleimling M, Godreche C and Luck J M 2001 Aging, phase ordering, and conformal invariance *Phys. Rev. Lett.* **87** 265701
[217] Corberi F, Lippiello E and Zannetti M 2001 Interface fluctuations, bulk fluctuations, and dimensionality in the off-equilibrium response of coarsening systems *Phys. Rev.* E **63** 061506
[218] Calabrese P and Gambassi A 2002 Aging in ferromagnetic systems at criticality near four dimensions *Phys. Rev.* E **65** 066120
[219] Calabrese P and Gambassi A 2002 Two-loop critical fluctuation–dissipation ratio for the relaxational dynamics of the o(n) Landau–Ginzburg Hamiltonian *Phys. Rev.* E **66** 066101
[220] Berthier L, Holsworth P C W and Sellitto M 2001 Nonequilibrium critical dynamics of the two-dimensional xy model *J. Phys. A: Math. Gen.* **34** 1805–24
[221] Bernu B, Hansen J P, Hiwatari Y and Pastore G 1987 Soft-sphere model for the glass transition in binary alloys: pair structure and self-diffusion *Phys. Rev.* A **36** 4891–903
[222] Barrat J-L, Roux J N and Hansen J P 1990 Diffusion, viscosity and structural slowing down in soft sphere alloys near the kinetic glass transition *Chem. Phys.* **149** 197–208
[223] Hansen J P and Yip S 1995 Molecular dynamics investigations of slow relaxations in supercooled liquids *Transp. Theory Stat. Phys.* **24** 1149–78
[224] Parisi G 1997 Short-time aging in binary glasses *J. Phys. A: Math. Gen.* **30** L765–70
[225] Parisi G 1997 Off-equilibrium fluctuation–dissipation relation in fragile glasses *Phys. Rev. Lett.* **79** 3660–3
[226] Parisi G 1997 Numerical indications for the existence of a thermodynamic transition in binary glasses *J. Phys. A: Math. Gen.* **30** 8523–39
[227] Di Leonardo R, Angelani L, Parisi G and Ruocco G 2000 Off-equilibrium effective temperature in monatomic Lennard-Jones glass *Phys. Rev. Lett.* **84** 6054–7
[228] Angelani L, Di Leonardo R, Parisi G and Ruocco G 2001 Topological description of the aging dynamics in simple glasses *Phys. Rev. Lett.* **87** 055502/1–4
[229] Kob W and Andersen H C 1994 Scaling behaviour in the beta-relaxation regime of a supercooled Lennard-Jones mixture: *Phys. Rev. Lett.* **73** 1376–9
[230] Kob W and Andersen H C 1995 Testing mode-coupling theory for a supercooled binary Lennard-Jones mixture: I. The van hove correlation function *Phys. Rev.* E **51** 4626–41
[231] Kob W and Andersen H C 1995 Testing mode-coupling theory for a supercooled binary Lennard-Jones mixture: II. Intermediate scattering function and dynamic susceptibility *Phys. Rev.* E **52** 4134–53
[232] Gleim T, Kob W and Binder K 1998 How does the relaxation of a supercooled liquid depend on its microscopic dynamics? *Phys. Rev. Lett.* **81** 4404–7
[233] Barrat J-L and Kob W 1999 Aging and the fluctuation dissipation ratio in a Lennard-Jones fluid *J. Phys. A: Math. Gen.* **11** A247–52
[234] Barrat J-L and Kob W 1999 Fluctuation–dissipation ratio in an aging Lennard-Jones glass *Europhys. Lett.* **46** 637–42
[235] Kob W and Barrat J-L 2000 Fluctuations, response and aging dynamics in a simple glass-forming liquid out of equilibrium *Eur. Phys. J.* B **13** 319

[236] Angelani L, Parisi G, Ruocco G and Viliani G 1998 Connected network of minima as a model glass: long time dynamics *Phys. Rev. Lett.* **81** 4648
[237] Angelani L, Parisi G, Ruocco G and Viliani G 2000 Potential energy landscape and long-time dynamics in a simple model glass *Phys. Rev.* E **61** 1681–91
[238] Sciortino F and Tartaglia P 2001 Extension of the fluctuation–dissipation theorem to the physical aging of a model glass-forming liquid *Phys. Rev. Lett.* **86** 107–10
[239] Brangian C, Kob W and Binder K 2001 Finite-size scaling at the dynamical transition of the mean-field 10-state Potts glass *Europhys. Lett.* **53** 756–61
[240] Brangian C, Kob W and Binder K 2002 Statics and dynamics of the ten-state mean-field Potts glass model: a Monte Carlo study *J. Phys. A: Math. Gen.* **35** 191–216
[241] Marinari E, Giorgio G and Ritrot F 1994 Replica field theory for deterministic models: II. A non-random spin glass with glassy behaviour *J. Phys. A: Math. Gen.* **27** 7647–68
[242] Barrat A and Franz S 1998 Basins of attraction of metastable states of the spherical p-spin model *J. Phys. A: Math. Gen.* **31** L119–27
[243] Rao F, Crisanti A and Ritort F 2003 Frequency-domain study of relaxation in a spin glass model for the structural glass transition *Europhys. Lett.* at press
[244] Kob W, Sciortino F and Tartaglia P 2000 Aging as dynamics in configuration space *Europhys. Lett.* **49** 590
[245] Marinari E, Parisi G and Ruiz-Lorenzo J J 1997 Numerical simulations of spin glass systems *Spin Glasses and Random Fields* ed A P Young (Singapore: World Scientific)
[246] Andersson J-O, Mattson J and Svedlindh P 1992 Monte Carlo studies of Ising spin-glass systems: aging behaviour and crossover between equilibrium and nonequilibrium dynamics *Phys. Rev.* B **46** 8297–304
[247] Franz S and Rieger H 1995 Fluctuation–dissipation ratio in three-dimensional spin glasses *J. Stat. Phys.* **79** 749–58
[248] Cugliandolo L F, Kurchan J and Ritort F 1994 Evidence of aging in spin-glass mean-field models *Phys. Rev.* B **49** 6331–4
[249] Marinari E, Parisi G, Ricci-Tersenghi F and Ruiz-Lorenzo J J 1998 Violation of the fluctuation–dissipation theorem in finite-dimensional spin glasses *J. Phys. A: Math. Gen.* **31** 2611–20
[250] Parisi G, Ricci-Tersenghi F and Ruiz-Lorenzo J J 1999 Generalized off-equilibrium fluctuation–dissipation relations in random Ising systems *Eur. Phys. J.* B **11** 317–25
[251] Parisi G, Ricci-Tersenghi F and Ruiz-Lorenzo J J 1998 Dynamics of the four-dimensional spin glass in a magnetic field *Phys. Rev.* B **57** 13617–23
[252] Parisi G, Ricci-Tersenghi F and Ruiz-Lorenzo J J 1999 Universality in the off-equilibrium critical dynamics of the three-dimensional diluted Ising model *Phys. Rev.* E **60** 5198–201
[253] Marinari E, Parisi G, Ricci-Tersenghi F and Ruiz-Lorenzo J J 2000 Off-equilibrium dynamics at very low temperatures in three-dimensional spin glasses *J. Phys. A: Math. Gen.* **33** 2373–82
[254] Picco M, Ricci-Tersenghi F and Ritort F 2001 Aging effects and dynamic scaling in the 3D Edwards–Anderson spin glasses: a comparison with experiments *Eur. Phys. J.* B **21** 211–7
[255] Parisi G and Toulouse G 1980 A simple hypothesis for the spin glass phase of the infinite-ranged sk model *J. Physique Lett.* **41** L361–4
[256] Vannimenus J, Toulouse G and Parisi G 1981 Study of a simple hypothesis for the mean-field theory of spin-glasses *J. Physique* **42** 565–71
[257] Alvarez D, Franz S and Ritort F 1996 Fragile-glass behaviour of a short-range p-spin model *Phys. Rev.* B **54** 9756–64
[258] Marinari E, Naitza C, Parisi G, Picco M, Ritort F and Zuliani F 1998 A general method to determine replica symmetry breaking transitions *Phys. Rev. Lett.* **81** 1698–702
[259] Franz S and Parisi G 1999 Critical properties of a three dimensional p-spin model *Eur. Phys. J.* B **8** 417–22
[260] Campellone M, Coluzzi B and Parisi G 1998 Numerical study of a short-range p-spin glass model in three dimensions *Phys. Rev.* B **58** 12081–9
[261] Parisi G, Picco M and Ritort F 1999 Continuous phase transition in a model without time-reversal symmetry *Phys. Rev.* E **60** 58–68
[262] Barrat A and Berthier L 2001 Real-space application of the mean-field description of spin-glass dynamics *Phys. Rev. Lett.* **87** 087204
[263] Castillo H E, Chamon C, Cugliandolo L F and Kennett M P 2002 Heterogeneous aging in spin glasses *Phys. Rev. Lett.* **88** 237201–4
[264] Nicodemi M and Coniglio A 1997 The glassy transition of the frustrated Ising lattice gas *J. Phys. A: Math. Gen.* **30** L187–L194
[265] Stariolo D A and Arenzon J J 1999 Off-equilibrium dynamics of the frustrated Ising lattice gas *Phys. Rev.* E **59** R4762–R4765

[266] Arenzon J J, Ricci-Tersenghi F and Stariolo D A 2000 Dynamics of the frustrated Ising lattice gas *Phys. Rev.* E **62** 5978–85
[267] Crisanti A and Leuzzi L 2002 First order phase transition and phase coexistence in a spin-glass model *Phys. Rev. Lett.* **89** 237204
[268] Bray A J 1994 Theory of phase ordering kinetics *Adv. Phys.* **43** 357
[269] Fisher D S and Huse D A 1988 Nonequilibrium dynamics of spin glasses *Phys. Rev.* B **38** 373–85
[270] Fisher D S 1997 Dynamics and domain walls: Is the landscape paradigm instructive? *Physica* D **107** 204–17
[271] Kivelson D and Tarjus G 1998 The Kauzmann paradox interpreted via the theory of frustration-limited-domains *J. Chem. Phys.* **109** 5481–6
[272] Barrat A 1998 Monte Carlo simulations of the violation of the fluctuation–dissipation theorem in domain growth processes *Phys. Rev.* E **57** 3629–32
[273] Berthier L, Barrat J-L and Kurchan J 1999 Response function of coarsening systems *Eur. Phys. J.* B **11** 635–41
[274] Stariolo D A and Cannas S A 1999 Violation of the fluctuation–dissipation theorem in a two-dimensional Ising model with dipolar interactions *Phys. Rev.* B **60** 3013–6
[275] Kivelson D, Kivelson S A, Zhao X, Nussinov Z and Gilles T 1995 A thermodynamic theory of supercooled liquids *Physica* A **219** 27–38
[276] Pryadko L P, Kivelson S and Hone D W 1998 Instability of charge ordered states in doped antiferromagnets *Phys. Rev. Lett.* **80** 5651–4
[277] Sampaio L C, de Albuquerque M P and de Menezes F S 1996 Magnetic relaxation and formation of magnetic domains in ultrathin films with perpendicular anisotropy *Phys. Rev.* B **54** 6465–72
[278] MacIsaac A B, Whitehead J P, Robinson M C and De Bell K 1995 Striped phases in two-dimensional dipolar ferromagnets *Phys. Rev.* B **51** 16033–45
[279] Ricci-Tersenghi F and Ritort F 2000 Absence of ageing in the remanent magnetization in Migdal–Kadanoff spin glasses *J. Phys. A: Math. Gen.* **33** 3727–34
[280] Lebowitz J L and Percus J K 1966 Mean spherical model for lattice gases with extended hard cores and continuum fluids *Phys. Rev.* **144** 251–8
[281] Kosterlitz J M, Thouless D J and Jones R C 1976 Spherical model of a spin-glass *Phys. Rev. Lett.* **36** 1217–20
[282] Cannas A, Stariolo D A and Tamarit F A 2001 Dynamics of ferromagnetic spherical spin models with power law interactions: exact solution *Physica* A **294** 362–74
[283] Parisi G 1986 Asymmetric neural networks and the process of learning *J. Phys. A: Math. Gen.* **19** L675–80
[284] Crisanti A and Sompolinsky H 1987 Dynamics of spin system with random asymmetric bonds: Langevin dynamics and a spherical model *Phys. Rev.* A **36** 4922–39
[285] Crisanti A and Sompolinsky H 1988 Dynamics of spin system with random asymmetric bonds: Ising spins and Glauber dynamics *Phys. Rev.* A **37** 4865–74
[286] Cugliandolo L F, Kurchan J, Le Doussal P and Peliti L 1997 Glassy behaviour in disordered systems with nonrelaxational dynamics *Phys. Rev. Lett.* **78** 350–3
[287] Berthier L, Barrat J-L and Kurchan J 2000 A two-time-scale, two-temperature scenario for non-linear rheology *Phys. Rev.* E **61** 5464–72
[288] Berthier L and Barrat J-L 2002 Shearing a glassy material: numerical tests of non-equilibirum mode-coupling approaches and experimental proposals *Phys. Rev. Lett.* **89** 095702
[289] Berthier L and Barrat J-L 2002 Non-equilibrium dynamics and fluctuation–dissipation relation in a sheared fluid *J. Chem. Phys.* **116** 6228–42
[290] Barrat J-L and Berthier L 2001 Fluctuation–dissipation relation in a sheared fluid *Phys. Rev.* E **63** 012503
[291] Angelani L, Ruocco G, Sciortino F, Tartaglia P and Zamponi F 2002 Crossover between equilibrium and shear-controlled dynamics in sheared liquids *Phys. Rev.* E **66** 061505
[292] Larson R G 1999 *The Structure and Rheology of Complex Fluids* (New York: Oxford University Press)
[293] Bedeaux D and Rubi J M 2002 Nonequilibrium thermodynamics of colloids *Physica* A **305** 360–70
[294] Jou D, Casas-Vazquez J and Lebon G 1999 Extended irreversible thermodynamics revisited (1988-98) *Rep. Prog. Phys.* **62** 1035–142
[295] de Groot S R and Mazur P 1984 *Non-Equilibrium Thermodynamics* (New York: Dover)
[296] Corberi F, Gonnella G, Lippiello E and Zannetti M 2002 Correlation functions and fluctuation–dissipation relation in driven mixtures: an exactly solvable model *Preprint* cond-mat/0210464
[297] Berthier L, Cugliandolo L F and Iguain J L 2001 Glassy systems under time-dependent driving forces: Application to slow granular rheology *Phys. Rev.* E **63** 051302/1–15
[298] Kolton A B, Exartier R, Cugliandolo L F, Dominguez D and Gronbech-Jensen N 2002 Effective temperature in driven vortex lattices with random pinning *Preprint* cond-mat/0206042
[299] Horner H 1996 Drift, creep and pinning of a particle in a correlated random potential *Z. Phys.* B **100** 243–58
[300] Thalmann F 1998 Activated drift motion of a classical particle with a dynamical pinning effect *Eur. Phys. J.* B **3** 497–505

[301] Kob W and Andersen H C 1993 Kinetic lattice-gas model of cage effects in high-density liquids and a test of mode-coupling theory of the ideal-glass transition *Phys. Rev.* E **48** 4364–77
[302] Kurchan J, Peliti L and Sellitto M 1997 Aging in lattice-gas models with constrained dynamics *Europhys. Lett.* **39** 365–70
[303] Sellitto M and Arenzon J J 2000 Free-volume kinetic models of granular matter *Phys. Rev.* E **62** 7793–6
[304] Sellitto M 1998 Fluctuation–dissipation ratio in lattice-gas models with kinetic constraints *Acta Mech.* **4** 135–8
[305] Barrat A, Kurchan J, Loreto V and Sellitto M 2001 Edwards' measures: a thermodynamic construction for dense granular media and glasses *Phys. Rev.* E **63** 051301
[306] Barrat A, Kurchan J, Loreto V and Sellitto M 2000 Edwards' measures for powders and glasses *Phys. Rev. Lett.* **85** 5034–7
[307] Barrat A, Colizza V and Loreto V 2002 Fluctuation–dissipation ratio for compacting granular media *Phys. Rev.* E **66** 011310
[308] Caglioti E, Loreto V, Herrmann H J and Nicodemi M 1997 A 'tetris-like' model for the compaction of dry granular media *Phys. Rev. Lett.* **79** 1575–8
[309] Nicodemi M 1999 Dynamical response functions in models of vibrated granular media *Phys. Rev. Lett.* **82** 3734–7
[310] Edwards S F and Grinev D V 1998 Statistical mechanics of vibration-induced compaction of powders *Phys. Rev.* E **58** 4758–62
[311] Edwards S F and Grinev D V 1999 Compactivity and transmission of stress in granular materials *Chaos* **82** 5397–400
[312] Lefevre A and Dean D S 2001 Tapping thermodynamics of the one-dimensional Ising model *J. Phys. A: Math. Gen.* **34** L213–20
[313] Maakse H A and Kurchan J 2002 Testing the thermodynamic approach to granular matter with a numerical model of a decisive experiment *Nature* **415** 614–7
[314] Levin Y, Arenzon J J and Sellitto M 2001 Aging dynamics and density relaxation in kinetic lattice gases under gravity *Europhys. Lett.* **55** 767–73
[315] Sellitto M 2001 Effective temperature of an aging powder *Phys. Rev.* E **63** 060301(R)
[316] Sellitto M 2002 Effective temperature and compactivity of a lattice-gas under gravity *Phys. Rev.* E **66** 042101
[317] Lefevre A 2002 Edwards measure and the steady state regime of a model with kinetic constraints under tapping *J. Phys. A: Math. Gen.* **35** 9037
[318] Franz S, Mulet R and Parisi G 2002 Kob–Andersen model: a nonstandard mechanism for the glassy transition *Phys. Rev.* E **65** 021506
[319] Fredrickson G H and Andersen H C 1984 Kinetic Ising-model of the glass-transition *Phys. Rev. Lett.* **53** 1244–7
[320] Fredrickson G H and Andersen H C 1985 Facilitated kinetic Ising-models and the glass-transition *J. Chem. Phys.* **83** 5822–31
[321] Kob W and Andersen H C 1993 Relaxation dynamics in a lattice gas: a test of the mode-coupling theory of the ideal glass transition *Phys. Rev.* E **47** 3281–302
[322] Peliti L and Sellitto M 1998 Aging in a simple model of a structural glass *J. Physique* **8** 49–56
[323] Davison L and Sherrington D 2000 Glassy behaviour in a simple topological model *J. Phys. A: Math. Gen.* **33** 8615–25
[324] Davison L, Sherrington D, Garrahan J P and Buhot A 2001 Glassy behaviour in a 3-state spin model *J. Phys. A: Math. Gen.* **34** 5147–82
[325] Lipowski A and Johnston D 2000 Metastability in a four-spin Ising model *J. Phys. A: Math. Gen.* **33** 4451–60
[326] Lipowski A and Johnston D 2000 Cooling-rate effects in a model of glasses *Phys. Rev.* E **61** 6375–82
[327] Buhot A and Garrahan J P 2002 Fluctuation–dissipation relations in the activated regime of simple strong-glass models *Phys. Rev. Lett.* **88** 225702
[328] Jackle J and Eisinger S 1991 A hierarchically constrained kinetic Ising-model *Z. Phys.* B **84** 115–24
[329] Reiter J, Mauch F and Jackle J 1992 Blocking transitions in lattice spin models with directed kinetic constraints *Physica* A **184** 458–76
[330] Buhot A and Garrahan J P 2001 Crossover from fragile to strong glassy behaviour in kinetically constrained systems *Phys. Rev.* E **6402** 1505
[331] Corberi F, de Candia A, Lippiello E and Zannetti M 2002 Off equilibrium response function in the one dimensional random field Ising model *Phys. Rev.* E **65** 046114
[332] Crisanti A, Ritort F, Rocco A and Sellitto M 2002 Is the Stillinger and Weber decomposition relevant for coarsening models? *J. Phys.: Condens. Matter* **14** 1523–38
[333] Newman M E J and Moore C 1999 Glassy dynamics and aging in an exactly solvable spin model *Phys. Rev.* E **60** 5068–72
[334] Garrahan J P and Newman M E J 2000 Glassiness and constrained dynamics of a short-range nondisordered spin model *Phys. Rev.* E **62** 7670–8

[335] Alers G B, Weissmann M B and Israeloff N E 1992 Mesoscopic tests for thermally chaotic states in a CuMn spin glass *Phys. Rev.* B **46** 507–9
[336] Weissman M B 1993 What is a spin glass? A glimpse via mesoscopic noise *Rev. Mod. Phys.* **65** 829–39
[337] Alba M, Hammann J, Ocio M, Refregier P and Bouchiat H 1987 Spin-glass dynamics from magnetic noise, relaxation, and susceptibility measurements *J. Appl. Phys.* **61** 3683–8
[338] Refregier P and Ocio M 1987 Measurement of spontaneous magnetic fluctuations *Rev. Phys. Appl.* **22** 367–74
[339] Bouchiat H 1990 Experimental studies of the spin glass dynamics: towards a better understanding of the spatial correlations in the spin glass phase? *Physica* A **163** 284–90
[340] Herisson D and Ocio M 2002 Fluctuation–dissipation ratio of a spin glass in the aging regime *Phys. Rev. Lett.* **88** 257202
[341] Cugliandolo L F, Grempel D R, Kurchan J and Vincent E 1999 A search for fluctuation–dissipation theorem violations in spin-glasses from susceptibility data *Europhys. Lett.* **48** 699–705
[342] Grigera T S and Israeloff N E 1999 Observation of fluctuation–dissipation-theorem violations in a structural glass *Phys. Rev. Lett.* **83** 5038
[343] Bellon L, Ciliberto S and Laroche C 2001 Violation of the fluctuation–dissipation relation during the formation of a colloidal glass *Europhys. Lett.* **53** 511–17
[344] Bellon L and Ciliberto S 2002 Experimental study of the fluctuation–dissipation-relation during an aging process *Preprint* cond-mat/0201224